Manual of Petroleum Measurement Standards Chapter 19.2

Evaporative Loss From Floating-Roof Tanks

THIRD EDITION, OCTOBER 2012

energy API®

AMERICAN PETROLEUM INSTITUTE

Manual of Petroleum Measurement Standards Chapter 19.2

Evaporative Loss From Floating-Roof Tanks

Measurement Coordination

THIRD EDITION, OCTOBER 2012

energy API
AMERICAN PETROLEUM INSTITUTE

Special Notes

API publications necessarily address problems of a general nature. With respect to particular circumstances, local, state, and federal laws and regulations should be reviewed.

Neither API nor any of API's employees, subcontractors, consultants, committees, or other assignees make any warranty or representation, either express or implied, with respect to the accuracy, completeness, or usefulness of the information contained herein, or assume any liability or responsibility for any use, or the results of such use, of any information or process disclosed in this publication. Neither API nor any of API's employees, subcontractors, consultants, or other assignees represent that use of this publication would not infringe upon privately owned rights.

API publications may be used by anyone desiring to do so. Every effort has been made by the Institute to assure the accuracy and reliability of the data contained in them; however, the Institute makes no representation, warranty, or guarantee in connection with this publication and hereby expressly disclaims any liability or responsibility for loss or damage resulting from its use or for the violation of any authorities having jurisdiction with which this publication may conflict.

API publications are published to facilitate the broad availability of proven, sound engineering and operating practices. These publications are not intended to obviate the need for applying sound engineering judgment regarding when and where these publications should be utilized. The formulation and publication of API publications is not intended in any way to inhibit anyone from using any other practices.

Any manufacturer marking equipment or materials in conformance with the marking requirements of an API standard is solely responsible for complying with all the applicable requirements of that standard. API does not represent, warrant, or guarantee that such products do in fact conform to the applicable API standard.

Users of this standard should not rely exclusively on the information contained in this document. Sound business, scientific, engineering, and safety judgment should be used in employing the information contained herein.

Foreword

Nothing contained in any API publication is to be construed as granting any right, by implication or otherwise, for the manufacture, sale, or use of any method, apparatus, or product covered by letters patent. Neither should anything contained in the publication be construed as insuring anyone against liability for infringement of letters patent.

Shall: As used in a standard, “shall” denotes a minimum requirement in order to conform to the specification.

Should: As used in a standard, “should” denotes a recommendation or that which is advised but not required in order to conform to the specification.

This document was produced under API standardization procedures that ensure appropriate notification and participation in the developmental process and is designated as an API standard. Questions concerning the interpretation of the content of this publication or comments and questions concerning the procedures under which this publication was developed should be directed in writing to the Director of Standards, American Petroleum Institute, 1220 L Street, NW, Washington, DC 20005. Requests for permission to reproduce or translate all or any part of the material published herein should also be addressed to the director.

Generally, API standards are reviewed and revised, reaffirmed, or withdrawn at least every five years. A one-time extension of up to two years may be added to this review cycle. Status of the publication can be ascertained from the API Standards Department, telephone (202) 682-8000. A catalog of API publications and materials is published annually by API, 1220 L Street, NW, Washington, DC 20005.

Suggested revisions are invited and should be submitted to the Standards Department, API, 1220 L Street, NW, Washington, DC 20005, standards@api.org.

Summary of Changes to API MPMS Chapters 19.1, 19.2 and 19.4

The third edition of API Manual of Petroleum Measurement Standards (*MPMS*) Chapter 19.4 was published following a revision that was carried out concurrently with revisions to Chapter 19.1, published as the fourth edition, and Chapter 19.2, published as the third edition. Primary changes are:

1) Consolidation of common material in Chapter 19.4. Material that had previously been included in both Chapters 19.1 and 19.2 has been moved to Chapter 19.4. Chapter 19.4, which was previously *Recommended Practice for Speciation of Evaporative Losses*, now has the title *Evaporative Loss Reference Information and Speciation Methodology.* This Chapter had already contained reference information on the properties of chemicals and typical petroleum liquids, and this information has now been removed from Chapters 19.1 and 19.2. In addition, meteorological data have been moved from Chapters 19.1 and 19.2 to Chapter 19.4. In the revised documents:

   a) Meteorological data are found in Chapter 19.4,

   b) Calculation of storage tank temperatures is found in Chapters 19.1 and 19.2 (in that fixed-roof tanks involve calculation of the vapor space temperature in order to determine vapor density, whereas this step is not involved in estimating emissions from floating-roof tanks), and

   c) Calculation of true vapor pressure is found in Chapter 19.4 (in that this is now calculated in the same manner for both fixed- and floating-roof tanks).

2) Reconciliation of nomenclature. Chapters 19.1 and 19.2 previously had different nomenclature for the same variables. These revisions adopt a common set of symbols for both chapters.

3) Reorganization of the formats. In addition to common material having been removed from Chapters 19.1 and 19.2, the remaining text has been edited to remove unnecessarily verbose or repetitive language. The summary tables were deemed redundant, and have been deleted.

4) Appendices. Appendices have been redesignated as annexes.

5) SI units. An annex has been added to each chapter to address SI units.

Chapter 19.2, third edition

In addition to common reference material being deleted from Chapter 19.2, the following changes have been made:

1) Reference to API Technical Reports. References to API TR 2567 (floating roof landings), API TR 2568 (cleaning storage tanks), and API TR 2569 (closed vent IFRTs) have been added.

2) Terminology. The following terminology has been revised:

   a) "Covered floating-roof tank (CFRT)" has been changed to "domed EFRT."

   b) "Standing storage loss" has been changed to "standing loss."

   c) "Withdrawal loss" has been changed to "working loss."

   d) "Solar insolation" has been changed to "insolation."

3) True vapor pressure from liquid surface temperature. The temperature used for calculation of the true vapor pressure has been changed from the liquid bulk temperature to the liquid surface temperature for floating-roof tanks, using the same method to calculate liquid surface temperature as has been used for fixed-roof tanks. This

brings the API methodology into line with the EPA methodology published in AP-42 at the time of publication of this 3rd Edition of the API standard.

4) Ladder/Guidepole Combination. An equipment description and factors for ladder/guidepole combinations have been added.

5) Effective Throughput. An expression has been added for the sum of changes in liquid level, designated ΣH_Q, for calculating effective throughput.

Contents

Contents

Chapter 19.2—Evaporative Loss From Floating-Roof Tanks

1 Scope

This standard contains methodologies for estimating the total evaporative losses of hydrocarbons from external floating-roof tanks (EFRTs), freely vented internal floating-roof tanks (IFRTs), and domed external floating-roof tanks (domed EFRTs).

The methodologies provide loss estimates for general equipment types based on laboratory, test-tank, and field-tank data.

Types of floating roofs, rim-seal systems, and deck fittings are described for information only.

The equations estimate average annual losses from floating-roof tanks for various types of tank construction, floating-roof construction, rim-seal systems, and deck fittings, as well as for various liquid stocks, stock vapor pressures, tank sizes, and wind speeds (EFRTs).

The equations were developed for:

a) stocks with a true vapor pressure greater than approximately 0.1 psia,

b) average wind speeds ranging from 0 miles per hour (mph) to 15 mph (EFRTs), and

c) tank diameters greater than 20 ft.

The estimation techniques become more approximate when these conditions are not met.

When this standard is used to estimate losses from non-freely vented (closed vent) internal or domed external floating-roof tanks (tanks vented only through a pressure-vacuum relief vent, blanketed with an inert gas, vented to a vapor processing unit, or otherwise restricted from being freely vented), refer to the methodology in API TR 2569[7].

The equations are not intended to be used in the following applications.

a) To estimate losses from unstable or boiling stocks (i.e. stocks with a true vapor pressure greater than the atmospheric pressure at the tank location) or from petroleum liquids or petrochemicals for which the vapor pressure is not known or cannot readily be predicted.

b) To estimate losses from tanks in which the materials used in the rim seal, deck fittings, or deck seams have either deteriorated or been significantly permeated by the stored stock.

c) To estimate losses from storage tanks which do not have a floating roof.

d) To estimate losses from landing floating roofs (API TR 2567[8] addresses this).

e) To estimate losses from cleaning storage tanks (API TR 2568[9] addresses this).

The estimation procedures were developed to provide estimates of typical losses from floating-roof tanks that are properly maintained and in normal working condition. Losses from poorly maintained tanks can be greater. Because the loss equations are based on equipment conditions that represent a large population of tanks, a loss estimate for a group of floating-roof tanks will be more accurate than a loss estimate for an individual tank. The estimation can be improved by using detailed field information, including climatic data and operational data for the appropriate time period.

Evaporative-loss considerations are not the only criteria for equipment selection. Many other factors not addressed in this standard, such as tank operation, maintenance, and safety, are important in designing and selecting tank equipment for a given application.

2 Normative References

The following referenced documents are indispensable for the application of this document. For dated references, only the edition cited applies. For undated references, the latest edition of the referenced document (including any amendments) applies.

API *Manual of Petroleum Measurement Standards (MPMS) Ch.* 19.4, *Evaporative Loss Reference Information and Speciation Methodology*, 3rd Edition, 2012.

3 Symbols

Symbol	Description	Units	See Section
A_{fi}	liquid surface area within type i deck fitting	in^2	4.2.2.3
C_L	clingage factor	bbl/1000 ft^2	4.3.3
D	tank diameter	ft	4.2.2, 4.3.1
D_C	effective column diameter	ft	4.3.6
F_d	total deck-seam loss factor	lb-mole/yr	4.2.2.4
F_f	total deck-fitting loss factor	lb-mole/yr	4.2.2.3
F_r	total rim-seal loss factor	lb-mole/yr	4.2.2.2
ΣH_Q	annual sum of the decreases in liquid level	ft/yr	4.3.2
i	fitting type number (1, 2, …, k)	dimensionless	4.2.2.3
I	average daily total insolation on a horizontal surface	Btu/(ft^2 day)	4.2.3.2
k	total number of different types of deck fittings	dimensionless	4.2.2.3
K_C	product factor	dimensionless	4.2.3.4
K_d	deck-seam loss per unit seam length factor	lb-mole/ft-yr	4.2.2.4
K_{fai}	zero-wind-speed loss factor for type i deck fitting	lb-mole/yr	4.2.2.3 and Table 2
K_{fbi}	wind-dependent loss factor for type i deck fitting	lb-mole/mph^m-yr	4.2.2.3 and Table 2
K_{fi}	loss factor for type $\underline{i}$ deck fitting	lb-mole/yr	4.2.2.3
K_r	rim-seal loss per unit length factor	lb-mole/ft-yr	4.2.2.2
K_{ra}	zero-wind-speed rim-seal loss factor	lb-mole/ft-yr	4.2.2.2 and Table 1
K_{rb}	wind-dependent rim-seal loss factor	lb-mole/mph^n-ft-yr	4.2.2.2 and Table 1
K_v	fitting wind-speed correction factor	dimensionless	4.2.2.3
l	length of a deck panel	ft	4.2.2.4 and Table 6
L_S	standing loss	lb/yr	4.2
L_{seam}	total length of deck seams	ft	4.2.2.4
L_T	total loss	lb/yr	4.1
L_W	working loss	lb/yr	4.3
m_i	wind-dependent loss exponent for type i deck fitting	dimensionless	4.2.2.3 and Table 2
M_V	average molecular weight of stock vapor	lb/lb-mole	4.2.3.3
n	wind-dependent rim-seal loss exponent	dimensionless	4.2.2.2 and Table 1
N_{fah}	number of access hatches	dimensionless	4.2.2.3 and Table 2
N_{fc}	number of fixed-roof support columns	dimensionless	4.2.2.3, and Tables 2 & 3, 4.3.5
N_{fdd}	number of deck drains	dimensionless	4.2.2.3, and Tables 2 & 4
N_{fdl}	number of deck legs	dimensionless	4.2.2.3, and Tables 2 & 5
N_{fgf}	number of gauge floats (automatic gauge)	dimensionless	4.2.2.3 and Table 2

Symbol	Description	Units	See Section
N_{fi}	number of type i deck fittings	dimensionless	4.2.2.3
N_{fl}	number of vertical ladders	dimensionless	4.2.2.3 and Table 2
N_{flg}	number of ladder/guidepole combinations	dimensionless	4.2.2.3 and Table 2
N_{frv}	number of rim vents	dimensionless	4.2.2.3 and Table 2
N_{fsgp}	number of slotted (perforated) guidepoles	dimensionless	4.2.2.3 and Table 2
N_{fsp}	number of gauge hatch/sample ports	dimensionless	4.2.2.3 and Table 2
N_{fugp}	number of unslotted (unperforated) guidepoles	dimensionless	4.2.2.3 and Table 2
N_{fvb}	number of vacuum breakers	dimensionless	4.2.2.3, and Tables 2 & 4
P^*	vapor pressure function	dimensionless	4.2.3.2
P_A	average atmospheric pressure at the tank site	psia	4.2.3.2
P_{VA}	stock true vapor pressure at the daily average liquid surface temperature	psia	4.2.3.2
Q	annual stock throughput	bbl/yr	4.3.2
Q_N	net stock throughput associated with decreasing the liquid level in the tank	bbl/yr	4.3.2
S_d	deck-seam length factor	ft/ft^2	4.2.2.4 and Table 6
T_{AA}	average daily ambient temperature	°R	4.2.3.2
T_{AN}	average daily minimum ambient temperature	°R	4.2.3.2
T_{AX}	average daily maximum ambient temperature	°R	4.2.3.2
T_B	average liquid bulk temperature	°R	4.2.3.2
T_{MAX}	average daily maximum ambient temperature	°F	4.2.3.2
T_{MIN}	average daily minimum ambient temperature	°F	4.2.3.2
T_{LA}	average liquid surface temperature	°R	4.2.3.2
V	average ambient wind speed at the tank site	mi/hr	4.2.2.2, 4.2.2.3
w	width of deck sheet or panel	ft	4.2.2.4 and Table 6
W_L	average stock liquid density at 60 °F	lb/gal	4.3.4
α	tank surface solar absorptance	dimensionless	4.2.3.2

4 Procedure for Estimating Loss

4.1 General

The total loss L_T is the sum of the standing loss L_S and the working loss L_W:

$$L_T = L_S + L_W \tag{1}$$

4.2 Standing Loss L_S

4.2.1 Overview

Standing loss pertains to evaporative loss of stock liquid from beneath the floating roof while it is floating. The standing loss L_S can be estimated as follows:

$$L_S = (F_r + F_f + F_d)\, P^*\, M_V\, K_C \tag{2}$$

where

F_r is the total rim-seal loss factor, in pound-moles per year,

F_f is the total deck-fitting loss factor, in pound-moles per year,

F_d is the total deck-seam loss factor, in pound-moles per year,

$P*$ is the vapor pressure function, dimensionless,

M_V is the average molecular weight of stock vapor, in pounds per pound-mole,

K_C is the product factor, dimensionless.

The loss factors F_r, F_f, and F_d pertain to the design of the tank and floating roof, and are designated equipment-related factors. The loss factors $P*$, M_V, and K_C pertain to the characteristics of the stored stock liquid, and are designated stock-related factors. While the equipment-related factors are expressed in units of pound-moles per year, they have to be multiplied by the dimensionless stock-related factors $P*$ and K_C to determine actual pound-moles per year of evaporative loss for a given liquid product. To convert the actual pound-moles per year to pounds per year, multiply by the molecular weight of the product in its vapor phase, M_V, with molecular weight having units of pounds per pound-mole.

4.2.2 Equipment-Related Factors

4.2.2.1 General

The equipment-related factors F_r, F_f, and F_d in the standing loss equation are dependent only on the characteristics of the tank and floating roof, and are independent of the stored stock liquid.

4.2.2.2 Rim-Seal Loss Factor F_r

The rim seal loss factor F_r can be estimated as follows:

$$F_r = K_r D \tag{3}$$

where

K_r is the rim seal loss per unit length factor (lb-mole/ft-yr),

D is the tank diameter (ft).

The rim seal loss factor K_r can be estimated as follows:

$$K_r = K_{ra} + K_{rb} V^n \tag{4}$$

where

K_{ra} is the zero-wind-speed rim-seal loss factor (lb-mole/ft-yr); see Table 1,

K_{rb} is the wind-dependent rim-seal loss factor (lb-mole/(mi/hr)^n-ft-yr); see Table 1,

V is the average ambient wind speed at the tank site (mi/hr),

n is the wind-dependent rim-seal loss exponent; see Table 1.

Table 1—Rim-Seal Loss Factors

Tank Construction and Rim-seal System	Average-fitting Seals: Zero-wind Speed Loss Factor K_{ra} (lb-mol/ft-yr)	Average-fitting Seals: Wind-dependent Loss Factor K_{rb} [lb-mol/(mph)^n-ft-yr]	Average-fitting Seals: Wind-dependent Loss Exponent n (dimensionless)	Average-fitting Seals: Rim-seal Loss Factor K_r (lb-mol/ft-yr) 0 (mph)	5 (mph)	10 (mph)	15 (mph)	Tight-fitting[a] Seals: Zero-wind Speed Loss Factor K_{ra} (lb-mol/ft-yr)	Tight-fitting[a] Seals: Wind-dependent Loss Factor K_{rb} [lb-mol/(mph)^n-ft-yr]	Tight-fitting[a] Seals: Wind-dependent Loss Factor n (dimensionless)	Tight-fitting[a] Seals: Rim-seal Loss Factor K_r (lb-mol/ft-yr) 0 (mph)	5 (mph)	10 (mph)	15 (mph)
Welded Tanks														
Mechanical-shoe seal														
Primary only	5.8 [b,c]	0.3 [c]	2.1 [c]	5.8	15	44	94	1.5	0.4	1.9	1.5	10	33	70
Shoe-mounted secondary	1.6	0.3	1.6	1.6	5.5	14	24	1.0	0.4	1.5	1.0	5.5	14	24
Rim-mounted secondary	0.6	0.4	1.0	0.6	2.6	4.6	6.6	0.4	0.4	1.0	0.4	2.4	4.4	6.4
Liquid-mounted seal														
Primary only	1.6	0.3	1.5	1.6	5.0	11	19	1.0	0.08	1.8	1.0	2.4	6.0	11
Weather shield	0.7	0.3	1.2	0.7	2.8	5.5	8.4	0.4	0.2	1.3	0.4	2.0	4.4	7.2
Rim-mounted secondary	0.3	0.6	0.3	0.3	1.3	1.5	1.7	0.2	0.4	0.4	0.2	1.0	1.2	1.4
Vapor-mounted seal														
Primary only	6.7 [d]	0.2	3.0	6.7	32	210	680	5.6	0.2	2.4	5.6	15	56	139
Weather shield	3.3	0.1	3.0	3.3	16	100	340	2.8	0.1	2.3	2.8	6.9	23	54
Rim-mounted secondary	2.2	0.003	4.3	2.2	5.2	62	340	2.2	0.02	2.6	2.2	3.5	10	25
Riveted Tanks														
Mechanical-shoe seal														
Primary only	10.8	0.4	2.0	11	21	51	100	[e]	[e]	[e]				
Shoe-mounted secondary	9.2	0.2	1.9	9.2	14	25	44	[e]	[e]	[e]				
Rim-mounted secondary	1.1	0.3	1.5	1.1	4.5	11	19	[e]	[e]	[e]				

Notes:

[a] "Tight-fitting" means that the floating roof is maintained with no gaps more than $^1/_8$ in. wide between the rim seal and the tank shell.

[b] When no specific information is available, a welded tank with an average-fitting mechanical-shoe primary seal only can be assumed to represent the most common or typical construction and rim-seal system in use on domed EFRTs.

[c] When no specific information is available, a welded tank with an average-fitting mechanical-shoe primary seal only can be assumed to represent the most common or typical construction and rim-seal system in use on EFRTs.

[d] When no specific information is available, a welded tank with an average-fitting vapor-mounted primary seal only can be assumed to represent the most common or typical construction and rim-seal system in use on IFRTs.

[e] No evaporative-loss information is available for riveted tanks with consistently tight-fitting rim-seal systems.

The rim-seal loss factors may only be used for ambient wind speeds from 0 mph to 15 mph. If the average ambient wind speed V at the tank site is not available, wind-speed data from the nearest local weather station or values from API *MPMS* Ch. 19.4, 3rd Edition, Table 1 may be used as an approximation. For IFRTs and domed EFRTs, ambient wind speed is not a significant parameter and the value of V is set equal to zero. The equation then becomes:

$$K_r = K_{ra} \quad (5)$$

Rim-seal systems are described in 6.1.3. The loss factors for average-fitting seals are applicable for typical rim-seal conditions and should be used except when a rim-seal system is known to be consistently tight-fitting (that is, when there are no gaps more than $^1/_8$ in. wide between the rim seal and the tank shell), in which case the loss factors for tight-fitting seals are applicable. If the rim seal fit is unknown, use factors for average fitting seals.

4.2.2.3 Deck-Fitting Loss Factor F_f

The deck-fitting loss factor F_f can be estimated as follows:

$$F_f = N_{f1}K_{f1} + N_{f2}K_{f2} + \ldots + N_{fk}K_{fk} \quad (6)$$

where

N_{fi} is the number of type i deck fittings. If N_{fi} is unknown, determine N_{fi} from Table 2,

i is the fitting type number 1, 2, …, k,

k is the total number of different types of deck fittings,

K_{fi} is the loss factor for type i deck fitting (lb-mole/yr) (see Table 2).

The deck fitting loss factor K_{fi} can be estimated as follows:

$$K_{fi} = K_{fai} + K_{fbi}\left(K_v V\right)^{m_i} \quad (7)$$

where

K_{fai} is the zero-wind-speed loss factor for type i deck fitting (lb-mole/yr); see Table 2,

K_{fbi} is the wind-dependent loss factor for type i deck fitting (lb-mole/(mi/hr)^m-yr); see Table 2,

K_v is the fitting wind-speed correction factor, given a value of 0.7,

V is the average ambient wind speed at the tank site (mi/hr),

m_i is the wind-dependent loss exponent for type i deck fitting (dimensionless); see Table 2.

The deck-fitting loss factors may only be used for ambient wind speeds from 0 mph to 15 mph. If the average ambient wind speed V at the tank site is not available, wind-speed data from the nearest local weather station or values from API *MPMS* Ch. 19.4, 3rd Edition, Table 1 may be used as an approximation. For IFRTs and domed EFRTs, ambient wind speed is not a significant parameter and the value of V is set equal to zero. The equation then becomes:

$$K_{fi} = K_{fai} \quad (8)$$

The most common types of deck fittings are listed in Table 2, along with loss factors for various types of construction details. These common deck fittings are described in 6.1.4. For deck-fitting configurations that are not listed in Table 2, loss factors may be estimated at the zero miles-per-hour wind speed condition (IFRTs and domed EFRTs) from the following:

$$K_{fai} = 0.27(A_{fi})^{0.86} \tag{9}$$

where

A_{fi} is the liquid surface area within type i deck fitting (square inches), which is the area inside the deck fitting well or leg sleeve, less any area occupied by an obstruction in the deck-fitting well or leg sleeve (such as a fixed-roof support column, unslotted guidepole, guidepole float, or deck support leg).

The coefficient, 0.27, has units of pound-moles per (square inch)$^{0.86}$-year, and the exponent, 0.86, is dimensionless.

Equation (9) is only applicable when the distance from the liquid surface to the top of the deck-fitting well or leg sleeve is 12 in. or greater. Shorter deck-fitting wells or leg sleeves can result in higher loss rates. There are no similar algorithms available for estimating loss factors for shorter deck-fitting wells or leg sleeves.

Equation (9) is for an uncontrolled deck fitting. Effective deck-fitting controls would be expected to result in lower loss factors than would be estimated by this equation, but there are no algorithms available for estimating the effectiveness of deck-fitting controls.

Equation (9) is for the zero miles-per-hour wind speed condition. There are no algorithms available for estimating loss factors at non-zero wind speeds (EFRTs).

Table 2—Deck-Fitting Loss Factors

Table 2A—Other-than-guidepole deck fittings

Deck-fitting Type and Construction Details	Zero-wind Speed Loss Factor K_{fa} (lb-mol/yr)	Wind-dependent Loss Factor K_{fb} [lb-mol/(mph)^m•yr]	Wind-dependent Loss Exponent m (dimensionless)	Typical Number of Deck Fittings N_f (dimensionless)	Deck-fitting Loss Factor K_f (lb-mol/yr) 0 (mph)	5 (mph)	10 (mph)	15 (mph)
Access hatches				N_{fah} = 1				
Unbolted cover, ungasketed	36	5.9	1.2		36	63	97	140
Unbolted cover, gasketed	31	5.2	1.3		31	58	96	140
Bolted cover, gasketed	1.6	0.0	0.0		1.6	1.6	1.6	1.6
Fixed-roof support columns				N_{fc}: note a, Table 3				
Round pipe, ungasketed sliding cover	31				31			
Round pipe, gasketed sliding cover	25				25			
Round pipe, flexible fabric sleeve seal	10				10			
Built-up column, ungasketed sliding cover	51				51			
Built-up column, gasketed sliding cover	33				33			
Gauge floats (automatic gauge)				N_{fgf} = 1				
Unbolted cover, ungasketed	14	5.4	1.1		14	35	60	86
Unbolted cover, gasketed	4.3	17	0.38		4.3	32	40	46
Bolted cover, gasketed	2.8	0.0	0.0		2.8	2.8	2.8	2.8
Gauge hatch/sample ports				N_{fsp} = 1				
Weighted mechanical actuation, ungasketed	2.3	0.0	0.0		2.3	2.3	2.3	2.3
Weighted mechanical actuation, gasketed	0.47	0.02	0.97		0.5	0.5	0.6	0.7
Slit fabric seal (10 % open area)	12	[b]	[b]		12			
Vacuum breakers				N_{fvb}: note c, Table 4				
Weighted mechanical actuation, ungasketed	7.8	0.01	4.0		7.8	9.3	32	130
Weighted mechanical actuation, gasketed	6.2	1.2	0.94		6.2	10	14	17
Deck drains (opening which drains directly into the product)				N_{fdd}: note d, Table 4				
3-in. diameter, open	1.5	0.21	1.7		1.5	3.3	7.2	13
3-in. diameter (10 % open area)	1.8	0.14	1.1		1.8	2.4	3.0	3.7
1-in. diameter	1.2	[b]	[b]		1.2			
Deck legs				N_{fdl}: notes e & f, Table 5				
Adjustable (API 650, Appendix H type)	7.9	[b]	[b]		7.9			
Adjustable (API 650, Appendix C-type, double-deck roofs and center area of pontoon roofs)								
Ungasketed, no sock	0.82	0.53	0.14		0.8	1.5	1.5	1.6
Gasketed, no sock	0.53	0.11	0.13		0.5	0.7	0.7	0.7
With sock, no gasket	0.49	0.16	0.14		0.5	0.7	0.7	0.7
Adjustable (API 650, Appendix C-type, pontoon area of pontoon roofs)								
Ungasketed, no sock	2.0	0.37	0.91		2	3.2	4.2	5.1
Gasketed, no sock	1.3	0.08	0.65		1.3	1.5	1.6	1.7
With sock, no gasket	1.2	0.14	0.65		1.2	1.5	1.7	1.8
Fixed	0.0	0.0	0.0		0	0	0	0
Rim vents				N_{frv} = 1, note h				
Weighted mechanical actuation, ungasketed	0.68	1.8	1.0		0.7	7.0	13	20
Weighted mechanical actuation, gasketed	0.71	0.10	1.0		0.7	1.1	1.4	1.8

Table 2A—Other-than-guidepole deck fittings

Deck-fitting Type and Construction Details	Zero-wind Speed Loss Factor K_{fa} (lb-mol/yr)	Wind-dependent Loss Factor K_{fb} [lb-mol/(mph)^m•yr]	Wind-dependent Loss Exponent m (dimensionless)	Typical Number of Deck Fittings N_f (dimensionless)	Deck-fitting Loss Factor K_f (lb-mol/yr) 0 (mph)	5 (mph)	10 (mph)	15 (mph)
Ladders				N_{fl} = 0, note i				
Sliding cover, ungasketed	98	b	b		98			
Sliding cover, gasketed	56	b	b		56			
Ladder/guidepole combinations				N_{flg} = 0, note g				
Sliding cover, ungasketed	98	b	b		98			
Ladder sleeve with ungasketed sliding cover	65	b	b		65			
Ladder sleeve with gasketed sliding cover	60	b	b		60			

Table 2B—Guidepoles [j]

Unslotted (Unperforated) Guidepoles:				Zero-wind Speed Loss Factor	Wind-dependent Loss Factor	Wind-dependent Loss Exponent	Deck-fitting Loss Factor K_f (lb-mol/yr)			
Well Gasket (YES/NO)	Float with Wiper [k] (YES/NO)	Pole Wiper [p] (YES/NO)	Pole Sleeve (YES/NO)	K_{fa} (lb-mol/yr)	K_{fb} [lb-mol/(mph)^m•yr]	m (dimensionless)	0 (mph)	5 (mph)	10 (mph)	15 (mph)
NO	NO	NO	NO	31	150	1.4	31	900	2300	4100
YES	NO	NO	NO	25	13	2.2	25	230	970	2300
NO	NO	NO	YES	25	2.2	2.1	25	56	160	330
YES	NO	NO	YES	8.6	12	0.81	9	42	67	89
YES	NO	YES	NO	14	3.7	0.78	14	24	31	37
Slotted (Perforated) Guidepoles:				Zero-wind Speed Loss Factor	Wind-dependent Loss Factor	Wind-dependent Loss Exponent	Deck-fitting Loss Factor K_f (lb-mol/yr)			
Well Gasket (YES/NO)	Float with Wiper (YES/NO)	Pole Wiper [p] (YES/NO)	Pole Sleeve (YES/NO)	K_{fa} (lb-mol/yr)	K_{fb} [lb-mol/(mph)^m•yr]	m (dimensionless)	0 (mph)	5 (mph)	10 (mph)	15 (mph)
YES or NO [m]	NO	NO	NO	43	270	1.4	43	1600	4200	7300
YES or NO [m]	YES [l]	NO	NO	31	36	2.0	31	470	1800	4000
YES [n]	NO	YES	NO	41	48	1.4	41	320	770	1300
YES [n]	NO	NO	YES	11	46	1.4	11	280	710	1200
YES [n]	YES [l]	YES	NO	21	7.9	1.8	21	100	280	570
YES [n]	NO	YES	YES	8.3	4.4	1.6	8	41	110	200
YES [n]	YES [o]	YES	YES	11	9.9	0.89	11	41	67	91

Notes:

[a] Columns are not used on tanks with self-supporting fixed roofs (typical of domed EFRTs), or on tanks without fixed roofs (EFRTs).

[b] This feature is not typically used on API 650, Appendix C decks, and no information is available for wind-dependent evaporative loss from this fitting construction (EFRTs).

[c] The number of vacuum breakers on API 650, Appendix H decks (IFRTs) can be assumed to be:

$N_{fvb} = 1$

[d] The number of deck drains on API 650, Appendix H decks (IFRTs) can be assumed to be:

$N_{fdd} = 0$, for welded decks.

$N_{fdd} = D^2/125$ for bolted decks, where D = tank diameter (ft).

[e] The number of deck legs on API 650, Appendix H decks (IFRTs) can be assumed to be:

$N_{fdl} = (5 + D/10 + D^2/600)$, where D = tank diameter (ft).

[f] The deck legs tested for API 650, Appendix H decks (IFRTs) had 12-in. tall leg sleeves. The deck legs tested for API 650, Appendix C decks (EFRTs and domed EFRTs) had 30-in. tall leg sleeves for the pontoon area of pontoon roofs, and 48-in. tall leg sleeves for double-deck roofs and for the center area of pontoon roofs.

[g] Ladder/guidepole combinations that penetrate the deck are not typically used on open-top tanks with API 650, Appendix C decks (EFRTs).

[h] Rim vents are used only with some mechanical-shoe primary seals.

[i] Vertical ladders that penetrate the deck are not typically used on open-top tanks with API 650, Appendix C decks (EFRTs). The number of ladders on API 650, Appendix H decks (IFRTs) can be assumed to be:

$N_{fl} = 1$

[j] The quantity and type of guidepole should be confirmed for a given tank, rather than applying a default assumption.

[k] Floats are not used in unslotted guidepoles.

[l] Float wiper positioned at an elevation 1 in. above the sliding cover. No further reductions in emissions were achieved by positioning the float wiper at the same elevation as the sliding cover.

[m] Limited data do not support differentiation for the presence or absence of well gaskets for these construction details.

[n] No evaporative-loss information is currently available for these construction details without well gaskets.

[o] Tests were conducted with the float wiper at the same elevation as, 1 in. above, and 5 in. below the sliding cover. The data do not support differentiating between float wiper elevations when a float is used with a pole sleeve.

[p] Tests were conducted with the pole wiper at the same elevation as and 6 in. above the sliding cover. The data do not support differentiating between pole wiper elevations.

Table 3—Typical Number of Columns N_{fc} for Tanks with Column-Supported Roofs

Tank Diameter Range D (ft)		Typical Number of Columns
$< D$	$D \leq$	N_{fc}
0	85	1
85	100	6
100	120	7
120	135	8
135	150	9
150	170	16
170	190	19
190	220	22
220	235	31
235	270	37
270	275	43
275	290	49
290	330	61
330	360	71
360	400	81

NOTE This table was derived from a survey of users and manufacturers. The actual number of columns in a particular tank can vary greatly depending on tank age, fixed-roof construction, roof design loads, and manufacturing preferences. There are no columns on tanks with self-supporting fixed roofs (typical of domed EFRTs) or on tanks without fixed roofs (EFRTs). This table should not supersede actual tank data.

Table 4—Typical Number of Vacuum-Breakers N_{fvb} and Deck Drains N_{fdd} for API 650 Appendix C Decks (EFRTs and Domed EFRTs)

Tank Diameter D (ft) (note b)	Number of Vacuum Breakers N_{fvb}		Number of Deck Drains N_{fdd}	
	Single-Deck Pontoon Roof	Double-Deck Roof	Single-Deck Pontoon Roof	Double-Deck Roof
50	1	1	0	1
100	1	1	0	1
150	2	2	0	2
200	3	2	0	3
250	4	3	0	5
300	5	3	0	7
350	6	4	0	–
400	7	4	0	–

Notes:

a. This table was derived from a survey of users and manufacturers. The actual number of vacuum breakers can vary greatly depending on throughput and manufacturing preferences. The actual number of deck drains can vary greatly depending on the design rainfall and manufacturing preferences. For tanks greater than 300 ft in diameter, actual tank data or the manufacturer’s recommendations may be needed for the number of deck drains. This table should not supersede actual tank data.

b. If the tank diameter is between the diameters listed, the closest diameter listed should be used. If the tank diameter is midway between the diameters listed, the next larger diameter should be used.

Table 5—Typical Number of Deck Legs N_{fdl} for API 650 Appendix C Floating Roofs

Tank Diameter D (ft) (note b)	Single-Deck Pontoon Floating Roof		Double-Deck Floating Roof
	N_{fdl} in pontoon area	N_{fdl} in center (single-deck) area	N_{fdl}
30	4	2	6
40	4	4	7
50	6	6	8
60	9	7	10
70	13	9	13
80	15	10	16
90	16	12	20
100	17	16	25
110	18	20	29
120	19	24	34
130	20	28	40
140	21	33	46
150	23	38	52
160	26	42	58
170	27	49	66
180	28	56	74
190	29	62	82
200	30	69	90
210	31	77	98
220	32	83	107
230	33	92	115
240	34	101	127
250	35	109	138
260	36	118	149
270	36	128	162
280	37	138	173
290	38	148	186
300	38	156	200
310	39	168	213
320	39	179	226
330	40	190	240
340	41	202	255
350	42	213	270
360	44	226	285
370	45	238	300
380	46	252	315
390	47	266	330
400	48	281	345

Notes:
a. This table was derived from a survey of users and manufacturers. The actual number of deck legs can vary greatly depending on the tank age, floating roof construction, roof design loads, and manufacturing preferences. This table should not supersede actual tank data.
b. If the tank diameter is between the diameters listed, the closest diameter listed should be used. If the tank diameter is midway between the diameters listed, the next larger diameter should be used.

4.2.2.4 Deck-Seam Loss Factor F_d

Deck-seam loss factors only apply to API 650, Appendix H decks (IFRTs) that are of bolted construction. The deck-seam loss factor F_d can be estimated as follows:

For EFRTs,

$$F_d = 0 \tag{10}$$

For IFRTs,

$$F_d = K_d\, S_d\, D^2 \tag{11}$$

where

K_d is the deck-seam loss per unit seam length factor (lb-mole/ft-yr),

S_d is the deck-seam length factor (ft/ft^2),

D is the tank diameter (ft).

The deck-seam loss per unit seam length factor K_d can be estimated as follows:

K_d = 0 for a welded deck,

= 0.34 for a bolted deck.

If the deck construction is unknown, K_d = 0 for tanks with self-supporting roofs and K_d = 0.34 for tanks with column-supported fixed roofs.

The deck-seam length factor S_d can be estimated as follows:

$$S_d = L_{seam}/(\pi D^2/4) \tag{12}$$

where L_{seam} is the total length of deck seams (ft).

If L_{seam} is unknown, determine S_d using Table 6. If the deck construction is unknown, S_d = 0.20.

This calculation is based on the assumption that losses from deck seams occur continuously or from discrete, localized points that are distributed along the entire length of the seam. This assumption may be more applicable to some seam designs than others, but it is judged to be the most reasonable and conservative (potentially over-estimating loss) for determining general deck-seam loss factors. Deck seam losses from specific designs can vary significantly and can originate from joints or seam details that are not proportional to the total seam length.

No information is available for other deck types (for example, adhesively-joined seams).

4.2.3 Stock-Related Factors

4.2.3.1 General

The stock-related factors P^*, M_V, and K_C in the standing loss equation pertain to the properties of the stored stock liquid at the actual storage conditions. As such, these factors depend upon the location of the tank site and the physical characteristics of the tank, as well as the properties of the stored stock liquid.

Table 6—Deck-Seam Length Factors S_d

Deck Construction	S_d (ft/ft^2)
Continuous sheet construction, $S_d = 1/w$, where w = width of deck sheet or panel (ft)	
5 ft wide sheets	0.20
6 ft wide sheets	0.17
7 ft wide sheets	0.14
Panel Construction, $S_d = (l + w)/(l \times w)$, where l = length of a deck panel (ft)	
5 × 7.5 ft rectangular panels	0.33
5 × 12 ft rectangular panels	0.28

4.2.3.2 Vapor Pressure Function P^*

The vapor pressure function P^* can be estimated as follows:

$$P^* = \frac{P_{VA} / P_A}{\left\{1 + \left[1 - \left(P_{VA} / P_A\right)\right]^{0.5}\right\}^2} \tag{13}$$

where

P_{VA} is the stock true vapor pressure (psia) at the average liquid surface temperature T_{LA}. Use API *MPMS* Ch. 19.4, 3rd Edition, Section 4.2 to determine vapor pressure at a given temperature.

P_A is the average atmospheric pressure (psia) at the tank site. If P_A is unknown, use 14.7 psia.

The average liquid surface temperature T_{LA} (°R) may be determined (in order of decreasing accuracy) from measurements, from API *MPMS* Ch. 19.4, 3rd Edition, Appendix I, or from the following equation:

$$T_{LA} = 0.44T_{AA} + 0.56T_B + 0.0079\alpha I \tag{14}$$

where

T_{AA} is the average daily ambient temperature (°R),

T_B is the average liquid bulk temperature (°R),

α is the tank surface solar absorptance (dimensionless) (see API *MPMS* Ch. 19.4, 3rd Edition, Section 4.8),

I is the average daily total insolation on a horizontal surface (Btu/(ft^2 day)) (see API *MPMS* Ch. 19.4, 3rd Edition, Table 1).

The constants 0.44 and 0.56 are dimensionless. The constant 0.0079 has units of degrees Rankine square-foot day per British thermal unit.

The average daily ambient temperature T_{AA} can be estimated as follows:

$$T_{AA} = (T_{AX} + T_{AN})/2 \tag{15}$$

where

$$T_{AX} = T_{MAX} + 459.67 \tag{16}$$

T_{MAX} is the average daily maximum ambient temperature (°F), obtained from weather records or from historical averages given in API *MPMS* Ch. 19.4, 3rd Edition, Table 1,

$$T_{AN} = T_{MIN} + 459.67 \tag{17}$$

T_{MIN} is the average daily minimum ambient temperature (°F), obtained from weather records or from historical averages given in API *MPMS* Ch. 19.4, 3rd Edition, Table 1.

The constant 459.67 converts degrees Fahrenheit to degrees Rankine.

The average liquid bulk temperature T_B may be determined (in order of decreasing accuracy) from measurements, from API *MPMS* Ch. 19.4, 3rd Edition, Appendix I, or from the following equation:

$$T_B = T_{AA} + (6\alpha - 1) \tag{18}$$

The constants 6 and 1 have units of degrees Rankine.

4.2.3.3 Stock Vapor Molecular Weight M_V

For selected petroleum liquids (multicomponent stocks), the stock vapor molecular weight M_V is given in API *MPMS* Ch. 19.4, 3rd Edition, Table 2. For single component stocks, the stock vapor molecular weight M_V is equal to the molecular weight of the stock liquid. Molecular weights of selected petrochemicals are given in API *MPMS* Ch. 19.4, 3rd Edition, Table 3.

4.2.3.4 Product Factor K_C

The product factor accounts for the effect of different stocks on standing loss. The product factor K_C is:

K_C = 0.4 for crude oil stocks, except if the true vapor pressure of the crude oil is determined by the HOST method, K_C = 1.0 (see API *MPMS* Ch. 19.4, 3rd Edition, Appendix E),

K_C = 1.0 for refined petroleum stocks,

K_C = 1.0 for single component petrochemical stocks.

4.3 Working Loss L_W

4.3.1 Overview

Working, or withdrawal, loss pertains to the evaporation of stock liquid that clings to the tank shell (and any fixed-roof support columns) while the stock is withdrawn (i.e. while the liquid level is decreased). The working loss L_W can be estimated as follows:

$$L_W = \frac{0.943 Q_N C_L W_L}{D}\left(1 + \frac{N_{fc} D_C}{D}\right) \tag{19}$$

where

Q_N is the net stock throughput associated with decreasing the liquid level in the tank (bbl/yr),

C_L is the clingage factor (bbl/1000 ft^2),

W_L is the average stock liquid density at 60°F (lb/gal),

N_{fc} is the number of fixed-roof support columns (dimensionless),

D_C is the effective column diameter (ft),

D is the tank diameter (ft).

The constant 0.943 has units of thousand cubic foot-gallons per barrel^2.

4.3.2 Net Stock Throughput Q_N

The net stock throughput Q_N is:

$$Q_N = 0.1781\ (\Sigma H_Q)\ (\pi\ D^2/4) \tag{20}$$

where ΣH_Q = annual sum of the decreases in liquid level (ft/yr).

The constant 0.1781 has units of barrels per cubic foot.

Q_N is the stock throughput associated with decreasing the liquid level in the tank. If Q_N is unknown, use the stock throughput Q for Q_N. Note that Q overestimates Q_N if product is pumped into and out of the tank simultaneously.

4.3.3 Clingage Factor C_L

The clingage factor C_L is given in Table 7.

Table 7—Clingage Factors C_L for Steel Tanks (bbl/1000 ft^2)

	Shell Condition		
Product Stored	**light rust**	**dense rust**	**gunite lining**
gasoline	0.0015	0.0075	0.15
single-component stocks	0.0015	0.0075	0.15
crude oil	0.0060	0.030	0.60

4.3.4 Stock Liquid Density W_L

For selected petroleum liquids (multicomponent stocks), the stock liquid density W_L is given in API *MPMS* Ch. 19.4, 3rd Edition, Table 2. The stock liquid density W_L of selected petrochemicals (single component stocks) is given in API *MPMS* Ch. 19.4, 3rd Edition, Table 3.

4.3.5 Number of Fixed-Roof Support Columns N_{fc}

If the number of fixed-roof support columns N_{fc} is unknown, N_{fc} may be determined from Table 3. Only tanks with column-supported fixed roofs have columns (typical of IFRTs). Tanks with self-supporting fixed roofs (typical of domed EFRTs) and tanks without fixed roofs (EFRTs) do not have fixed-roof support columns.

4.3.6 Effective Column Diameter D_C

The effective column diameter D_C is:

$$D_C = (\text{column perimeter in ft})/\pi \tag{21}$$

Table 8—Effective Column Diameter D_C for Typical Column Construction

Column description	Effective Column Diameter D_C (ft)
9 in. × 7 in. built up column	1.1
8” pipe	0.7
Unknown	1.0

5 Sample Problems

5.1 General

The total evaporative loss is the sum of the standing loss and the working loss.

Sample problems are provided which illustrate the procedure for estimating evaporative loss. An EFRT problem is given in 5.2, an IFRT problem in 5.3, and a domed EFRT problem in 5.4. Estimated emissions are expressed to two significant figures, in that greater precision cannot be supported due to limitations in the precision of the empirically-derived emission factors.

5.2 EFRT Sample Problem

5.2.1 Overview

Estimate the total annual evaporative loss, in pounds per year, given the following information.

A welded EFRT in good condition has the following characteristics:

a) a diameter of 100 ft;

b) a shell painted an aluminum color, with a specular (shiny) finish in average condition;

c) a pontoon (single-deck) floating roof;

d) a mechanical-shoe primary seal, with no secondary seal;

e) an unslotted guidepole with no controls (that is, no well gasket, pole wiper, or pole sleeve);

f) construction details for all other deck fittings are as indicated in the calculations below.

The motor gasoline stored in the tank has the following characteristics (no vapor or liquid composition is given):

a) a Reid vapor pressure of 10 psi,

b) a stock liquid density of 6.1 lb/gal,

c) an average net throughput of 1.5 million bbl/yr.

The ambient conditions are as follows:

a) an average annual ambient temperature of 60 °F,

b) an atmospheric pressure of 14.7 psia,

c) an average annual ambient wind speed of 10 mph,

d) an average daily total insolation on a horizontal surface of 1300 Btu/(ft^2 day).

5.2.2 EFRT Standing Loss

Estimate the standing loss from Equation (2):

$$L_S = (F_r + F_f + F_d)\, P^*\, M_V\, K_C \tag{2}$$

The variables in Equation (2) can be determined as follows:

Total Rim-Seal Loss Factor

$$F_r = K_r D \quad (3)$$

= 4400 lb-mol/yr [from Equation (3) for an average-fitting primary only mechanical-shoe seal, with V = 10 mph].

where

K_r = 5.8 + (0.3)(10)$^{2.1}$,

= 44 (lb-mol/ft-yr) [for a welded tank with a mechanical-shoe primary seal, from Equation (4) and Table 1, or directly from Table 1],

D = 100 ft (given).

Total Deck-Fitting Loss Factor

$$F_f = N_{f1}K_{f1} + N_{f2}K_{f2} + \ldots + N_{fk}K_{fk} \quad (6)$$

= 2500 lb-mol/yr [from Equation (6), with V = 10 mph].

where

$N_{fah}K_{fah}$ = (1)[(1.6) + (0)(0.7 × 10)^{0}]

= 1.6 lb-mol/yr [for bolted, gasketed access hatches, from Equation (7) and Table 2, or directly from Table 2].

$N_{fc}K_{fc}$ = (not used on EFRTs)

= 0 lb-mol/yr (for fixed-roof support columns).

$N_{fgf}K_{fgf}$ = (1)[(14) + (5.4)(0.7 × 10)$^{1.1}$]

= 60 lb-mol/yr [for unbolted, ungasketed gauge floats, from Equation (7) and Table 2, or directly from Table 2].

$N_{fsp}K_{fsp}$ = (1)[(0.47) + (0.02)(0.7 × 10)$^{0.97}$]

= 0.6 lb-mol/yr [for gasketed gauge hatch/sample ports, from Equation (7) and Table 2, or directly from Table 2].

$N_{fvb}K_{fvb}$ = (1)[(6.2) + (1.2)(0.7 × 10)$^{0.94}$]

= 14 lb-mol/yr [for gasketed vacuum breakers, K_{fvb}, from Equation (7) and Table 2, or directly from Table 2, N_{fvb} from Table 4].

$N_{fdd}K_{fdd}$ = (not typically used on pontoon (single-deck) floating roofs)

= 0 lb-mol/yr [for open deck drains].

$N_{fdl}K_{fdl}$ = (17) [(2.0) + (0.37) (0.7 × 10)$^{0.91}$] + (16) [(0.82) + (0.53) (0.7 × 10)$^{0.14}$]

= 95 lb-mol/yr [for deck legs, K_{fdl} from Equation (7) and Table 2, or directly from Table 2, N_{fdl} from Table 5].

$N_{frv}K_{frv}$ = (1)[(0.71) + (0.10)(0.7 × 10)$^{1.0}$]

= 1.4 lb-mol/yr [for gasketed rim vents, from Equation (7) and Table 2, or directly from Table 2].

$N_{fl}K_{fl}$ = (not typically used on EFRTs)

= 0 lb-mol/yr (for vertical ladders).

$N_{fugp}K_{fugp}$ = (1)[(31) + (150)(0.7 × 10)$^{1.4}$]

= 2300 lb-mol/yr [for unslotted guidepoles with no well gasket, pole wiper or pole sleeve, from Equation (7) and Table 2, or directly from Table 2].

$N_{fsgp}K_{fsgp}$ = (not present in this example)

= 0 lb-mol/yr (for slotted guide-poles).

Total Deck-Seam Loss Factor

$$F_d = K_d\, S_d\, D^2 \tag{11}$$

= (0.0)(0.0)(100)^2

= 0 lb-mol/yr [from Equation (11) for a welded deck].

Vapor Pressure Function

$$P^* = \frac{P_{VA}/P_A}{\left\{1+\left[1-\left(P_{VA}/P_A\right)\right]^{0.5}\right\}^2} \tag{13}$$

$$P^* = \frac{5.8/14.7}{\left\{1+\left[1-\left(5.8/14.7\right)\right]^{0.5}\right\}^2}$$

= 0.125 [for P = 5.8 psia, from Equation (13)].

where

T_{AA} = 60 °F [given];

$$T_{LA} = 0.44T_{AA} + 0.56T_B + 0.0079\alpha I \tag{14}$$

= 65.4 °F [from Equation (14), with T_B = 61.6 °F];

T_B = 61.6 °F [from Equation (18), with T_{AA} = 60 °F, α = 0.44];

α = 0.44 [for aluminum specular paint in average condition, from API *MPMS* Ch. 19.4, 3rd Edition, Table 7];

I = 1300 Btu/(ft^2 day) [given];

RVP = Reid vapor pressure;

= 10 psi [given];

P_{VA} = 5.8 psia [for gasoline with RVP = 10 psi and T_{LA} = 65.4 °F, from API *MPMS* Ch. 19.4, 3rd Edition, Section 4.2];

P_A = 14.7 psia [given].

Vapor Molecular Weight

M_V = 66 lb/lb-mol [for gasoline, from API *MPMS* Ch. 19.4, 3rd Edition, Table 2].

Product Factor

K_C = 1.0 [for refined stocks, from 4.2.3.4].

<u>EFRT Standing Loss</u>

To estimate the standing loss in pounds per year, substitute the values above into Equation (2):

L_S = [4400 + 2500 + 0] (0.125) (66) (1.0)

= 57,000 lb/yr

5.2.3 EFRT Working Loss

Estimate the working loss from Equation (19):

$$L_W = \frac{0.943 Q_N\, C_L\, W_L}{D}\left(1 + \frac{N_{fc}\, D_C}{D}\right) \tag{19}$$

The variables in Equation (19) can be determined as follows:

Q = 1.5 × 10^6 bbl/yr (given);

C_L = 0.0015 bbl/1000 ft^2 (for gasoline in a lightly rusted tank, from Table 7);

W_L = 6.1 lb/gal (given);

D = 100 ft (given);

N_{fc} = 0

To estimate the working loss in pounds per year, substitute the values above into Equation (19):

$$L_W = \left[\frac{(0.943)\left(1.5\times10^6\right)(0.0015)(6.1)}{100}\right]\left[1 + \frac{(0)}{100}\right]$$

= 130 lb/yr

5.2.4 EFRT Total Loss

Estimate the total loss from Equation (1):

$$L_T = L_S + L_W \tag{1}$$

= 57,000 + 130

= 57,000 lb/yr

In this EFRT sample problem, the contribution of the working loss is relatively insignificant. Estimated emissions are expressed to two significant figures, in that greater precision cannot be supported due to limitations in the precision of the empirically-derived emission factors.

5.3 IFRT Sample Problem

5.3.1 Overview

Estimate the total annual evaporative loss, in pounds per year, given the following information.

A welded shell, IFRT in good condition has the following characteristics:

a) a diameter of 100 ft,

b) built-up fixed-roof support columns,

c) a shell painted an aluminum color, with a specular (shiny) finish in average condition,

d) a noncontact aluminum floating roof,

e) a wiper-type primary seal, with no secondary seal,

f) bolted deck seams,

g) construction details for deck fittings are as indicated in the calculations below.

The motor gasoline stored in the tank has the following characteristics (no vapor or liquid composition is given):

a) a Reid vapor pressure of 10 psi,

b) a stock liquid density of 6.1 lb/gal,

c) an average net throughput of 1.5 million bbl/yr.

The ambient conditions are as follows:

a) an average annual ambient temperature of 60 °F,

b) an atmospheric pressure of 14.7 psia

c) an average daily total insolation on a horizontal surface of 1300 Btu/(ft^2 day).

5.3.2 IFRT Standing Loss

Estimate the standing loss from Equation (2):

$$L_S = (F_r + F_f + F_d)\, P^*\, M_V\, K_C \tag{2}$$

The variables in Equation (2) can be determined as follows.

Total Rim-Seal Loss Factor

$$F_r = K_r\, D \tag{3}$$

$= 670$ lb-mol/yr [from Equation (3) for an average-fitting primary only vapor-mounted seal].

where

$K_r = 6.7$ (lb-mol/ft-yr) [for an average-fitting primary only vapor-mounted seal, from Equation (5) and Table 1, or directly from Table 1];

$D = 100$ ft (given).

Total Deck-Fitting Loss Factor

$$F_f = N_{f1}K_{f1} + N_{f2}K_{f2} + \ldots + N_{fk}K_{fk} \tag{6}$$

= 820 lb-mol/yr [from Equation (6)].

where

$N_{fah}K_{fah}$ = (1)(36)

= 36 lb-mol/yr [for unbolted cover, ungasketed access hatches, from Equation (8) and Table 2],

$N_{fc}K_{fc}$ = (6)(51)

= 310 lb-mol/yr [for built-up columns, ungasketed sliding covers, from Equation (8) and Table 2 and Table 3],

$N_{fgf}K_{fgf}$ = (1)(14)

= 14 lb-mol/yr [for unbolted, ungasketed gauge floats, from Equation (8) and Table 2],

$N_{fsp}K_{fsp}$ = (1)(12)

= 12 lb-mol/yr [for gauge hatch/sample ports with slit fabric seals, from Equation (8) and Table 2],

$N_{fvb}K_{fvb}$ = (1)(6.2)

= 6.2 lb-mol/yr [for gasketed vacuum breakers, from Equation (8) and Table 2],

$N_{fdd}K_{fdd}$ = (80)(1.2)

= 96 lb-mol/yr [for 1-in. deck drains, from Equation (8) and Table 2],

$N_{fdl}K_{fdl}$ = (32)(7.9)

= 250 lb-mol/yr [for adjustable deck legs, from Equation (8) and Table 2],

$N_{frv}K_{frv}$ = (not used with vapor-mounted rim seals)

= 0 lb-mol/yr (for rim vents),

$N_{fl}K_{fl}$ = (1)(98)

= 98 lb-mol/yr [for vertical ladders, sliding ungasketed cover, from Equation (8) and Table 2],

$N_{fugp}K_{fugp}$ = (not present in this example)

= 0 lb-mol/yr (for unslotted guidepoles),

$N_{fsgp}K_{fsgp}$ = (not present in this example)

= 0 lb-mol/yr (for slotted guidepoles).

Total Deck-Seam Loss Factor

$$F_d = K_d\, S_d\, D^2 \tag{11}$$

$= (0.34)(0.20)(100)^2$

= 680 lb-mol/yr [from Equation (11) and Table 6 for a bolted noncontact deck with 5-ft wide sheets].

Vapor Pressure Function

$$P^* = \frac{P_{VA} / P_A}{\left\{1 + \left[1 - \left(P_{VA} / P_A\right)\right]^{0.5}\right\}^2} \tag{13}$$

$$P^* = \frac{5.8/14.7}{\left\{1 + \left[1 - \left(5.8/14.7\right)\right]^{0.5}\right\}^2}$$

= 0.125 [for P = 5.8 psia, from Equation (13)].

where

T_{AA} = 60 °F [given];

T_{LA} = 0.44T_{AA} + 0.56T_B + 0.0079αI (14)

= 65.4 °F [from Equation (14), with T_B = 61.6 °F];

T_B = 61.6 °F [from Equation (18), with T_{AA} = 60 °F, α = 0.44];

α = 0.44 [for aluminum specular paint in average condition, from API *MPMS* Ch. 19.4, 3rd Edition, Table 7];

I = 1300 Btu/(ft^2 day) [given];

RVP = Reid vapor pressure;

= 10 psi [given];

P_{VA} = 5.8 psia [for gasoline with RVP = 10 psi and T_{LA} = 65.4 °F, from API *MPMS* Ch. 19.4, 3rd Edition, Section 4.2];

P_A = 14.7 psia [given].

Vapor Molecular Weight

M_V = 66 lb/lb-mol [for gasoline, from API *MPMS* Ch. 19.4, 3rd Edition, Table 2].

Product Factor

K_C = 1.0 [for refined stocks, from 4.2.3.4].

IFRT Standing Loss

To estimate the standing loss in pounds per year, substitute the values above into Equation (2):

L_S = [670 + 820 + 680] (0.125) (66) (1.0)

= 18,000 lb/yr

5.3.3 IFRT Working Loss

Estimate the working loss from Equation (19):

$$L_W = \frac{0.943 Q_N C_L W_L}{D}\left(1 + \frac{N_{fc} D_C}{D}\right) \tag{19}$$

The variables in Equation (19) can be determined as follows:

Q = 1.5 × 10^6 bbl/yr (given);

C_L = 0.0015 bbl/1000 ft^2 (for gasoline in a lightly rusted tank, from Table 7);

W_L = 6.1 lb/gal (given);

D = 100 ft (given);

N_{fc} = 6 (from Table 3 for a 100-ft tank);

D_C = 1.1 ft (for typical built-up columns).

To estimate the working loss in pounds per year, substitute the values above into Equation (19):

$$L_W = \left[\frac{(0.943)\left(1.5\times10^6\right)(0.0015)(6.1)}{100}\right]\left[1+\frac{6(1.1)}{100}\right]$$

= 140 lb/yr.

5.3.4 IFRT Total Loss

Estimate the total loss from Equation (1):

$$L_T = L_S + L_W \qquad (1)$$

= 18,000 + 140

= 18,000 lb/yr

In this IFRT sample problem, the contribution of the working loss is relatively insignificant. Estimated emissions are expressed to two significant figures, in that greater precision cannot be supported due to limitations in the precision of the empirically-derived emission factors.

5.4 Domed EFRT Sample Problem

5.4.1 Overview

Estimate the total annual evaporative loss, in pounds per year, given the following information.

A welded shell, domed EFRT in good condition has the following characteristics:

a) a diameter of 100 ft;

b) a shell painted an aluminum color, with a specular (shiny) finish in average condition;

c) a pontoon (single-deck) floating roof (originally built in accordance with API 650, Appendix C[3]);

d) a mechanical-shoe primary seal, with no secondary seal;

e) an unslotted guidepole with no controls (e.g. no well gasket, pole wiper, or pole sleeve);

f) construction details for all other deck-fittings are as indicated in the calculations below;

g) a self-supporting aluminum dome roof.

The motor gasoline stored in the tank has the following characteristics (no vapor or liquid composition is given):

a) a Reid vapor pressure of 10 psi,

b) a stock liquid density of 6.1 lb/gal,

c) an average net throughput of 1.5 million bbl/yr.

The ambient conditions are as follows:

a) an average annual ambient temperature of 60 °F;

b) an atmospheric pressure of 14.7 psia

c) an average daily total insolation on a horizontal surface of 1300 Btu/(ft^2 day).

5.4.2 Domed EFRT Standing Loss

Estimate the standing loss from Equation (2):

$$L_S = (F_r + F_f + F_d)\, P^*\, M_V\, K_C \tag{2}$$

The variables in Equation (2) can be determined as follows.

Total Rim-Seal Loss Factor

$$F_r = K_r\, D \tag{3}$$

= 580 lb-mol/yr [from Equation (3) for an average-fitting primary only mechanical-shoe seal, with $V = 0$ mph].

where

K_r = 5.8 (lb-mol/ft-yr) [for a welded tank with a mechanical-shoe primary seal, from Equation (5) and Table 1, or directly from Table 1];

D = 100 ft (given).

Total Deck-Fitting Loss Factor

$$F_f = N_{f1}K_{f1} + N_{f2}K_{f2} + \ldots + N_{fk}K_{fk} \tag{6}$$

= 100 lb-mol/yr [from Equation (6), with $V = 0$ mph].

where

$N_{fah}K_{fah}$ = (1)(1.6)

= 1.6 lb-mol/yr [for bolted, gasketed access hatches, from Equation (8) and Table 2];

$N_{fc}K_{fc}$ = (not used on self-supporting fixed roofs)

= 0 lb-mol/yr (for fixed-roof support columns);

$N_{fgf}K_{fgf}$ = (1)(14)

= 14 lb-mol/yr [for unbolted, ungasketed gauge floats, from Equation (8) and Table 2];

$N_{fsp}K_{fsp}$ = (1)(0.47)

= 0.47 lb-mol/yr [for gasketed gauge hatch/sample ports, from Equation (8) and Table 2];

$N_{fvb}K_{fvb}$ = (1)(6.2)

= 6.2 lb-mol/yr [for gasketed vacuum breakers, from Equation (8) and Table 2 and Table 4];

$N_{fdd}K_{fdd}$ = (not typically used on pontoon (single-deck) floating roofs)

= 0 lb-mol/yr [for open deck drains];

$N_{fdl}K_{fdl}$ = (17) (2.0) + (16) (0.82)

= 47 lb-mol/yr [for deck legs, from Equation (8) and Table 2 and Table 5];

$N_{frv}K_{frv}$ = (1)(0.71)

= 0.71 lb-mol/yr [for gasketed rim vents, from Equation (8) and Table 2];

$N_{fl}K_{fl}$ = (not present in this example)

= 0 lb-mol/yr (for vertical ladders);

$N_{fugp}K_{fugp}$ = (1)(31)

= 31 lb-mol/yr [for unslotted guidepoles with no well gasket, pole wiper or pole sleeve, from Equation (8) and Table 2];

$N_{fsgp}K_{fsgp}$ = (not present in this example)

= 0 lb-mol/yr (for slotted guidepoles).

Total Deck-Seam Loss Factor

$$F_d = K_d\, S_d\, D^2 \tag{11}$$

$$= (0.0)(0.0)(100)^2$$

= 0 lb-mol/yr [from Equation (11) for a welded deck].

Vapor Pressure Function

$$P^* = \frac{P_{VA}/P_A}{\left\{1+\left[1-\left(P_{VA}/P_A\right)\right]^{0.5}\right\}^2} \tag{13}$$

$$P^* = \frac{5.8/14.7}{\left\{1+\left[1-\left(5.8/14.7\right)\right]^{0.5}\right\}^2}$$

= 0.125 [for P = 5.8 psia, from Equation (13)].

where

T_{AA} = 60 °F [given];

$$T_{LA} = 0.44T_{AA} + 0.56T_B + 0.0079\alpha I \tag{14}$$

= 65.4 °F [from Equation (14), with T_B = 61.6 °F];

T_B = 61.6 °F [from Equation (18), with T_{AA} = 60 °F, α = 0.44];

α = 0.44 [for aluminum specular paint in average condition, from API *MPMS* Ch. 19.4, 3rd Edition, Table 7];

I = 1300 Btu/(ft^2 day) [given];

RVP = Reid vapor pressure;

= 10 psi [given];

P_{VA} = 5.8 psia [for gasoline with RVP = 10 psi and T_{LA} = 65.4 °F, from API *MPMS* Ch. 19.4, 3rd Edition, Section 4.2];

P_A = 14.7 psia [given].

Vapor Molecular Weight

M_V = 66 lb/lb-mol [for gasoline, from API *MPMS* Ch. 19.4, 3rd Edition, Table 2].

Product Factor

K_C = 1.0 [for refined stocks, from 4.2.3.4].

<u>Domed EFRT Standing Loss</u>

To estimate the standing loss in pounds per year, substitute the values above into Equation (2):

L_S = [580 + 100 + 0] (0.125) (66) (1.0)

= 5600 lb/yr

5.4.3 Domed EFRT Working Loss

Estimate the working loss from Equation (19):

$$L_W = \frac{0.943 Q_N C_L W_L}{D}\left(1 + \frac{N_{fc} D_C}{D}\right) \tag{19}$$

The variables in Equation (19) can be determined as follows:

Q = 1.5 × 10^6 bbl/yr (given);

C_L = 0.0015 bbl/1000 ft^2 (for gasoline in a lightly rusted tank, from Table 7);

W_L = 6.1 lb/gal (given);

D = 100 ft (given);

N_{fc} = 0

To estimate the working loss in pounds per year, substitute the values above into Equation (19):

$$L_W = \left[\frac{(0.943)\left(1.5\times 10^6\right)(0.0015)(6.1)}{100}\right]\left[1+\frac{(0)}{100}\right]$$

$= 130$ lb/yr

5.4.4 Domed EFRT Total Loss

Estimate the total loss from Equation (1):

$$L_T = L_S + L_W \tag{1}$$

$= 5600 + 130$

$= 5700$ lb/yr

Estimated emissions are expressed to two significant figures, in that greater precision cannot be supported due to limitations in the precision of the empirically-derived emission factors.

6 Equipment Descriptions

6.1 Components

6.1.1 General

This section describes the evaporative-loss-related construction features of floating-roof tanks. These are vessels that have a vertical cylindrical shell and a roof that floats on the surface of the stock liquid. They can also have a fixed roof attached to the top of the shell.

The basic components of the floating roof include:

a) a floating deck;

b) an annular rim seal attached to the perimeter of the floating deck; and

c) fittings that penetrate the floating deck for some functional purpose.

General types of these components, which are available in a range of commercial designs, are described in this section. Included in these descriptions are comments on the potential for evaporative loss, as well as some design and operational characteristics. Other factors, such as tank maintenance and safety, are important in designing and selecting tank equipment but are outside the scope of this publication.

6.1.2 Floating Decks

Floating decks reduce evaporative stock loss by covering the liquid surface, thereby minimizing the liquid surface exposed to evaporation. The floating deck may be in contact with the liquid surface or may confine a layer of saturated vapor under the deck supported on floats above the liquid (IFRTs). The loss of vapor otherwise displaced from fixed-roof tanks by filling and breathing is virtually eliminated[6]. Evaporative loss does occur during standing storage through the annular rim space, deck fittings, and in some cases, deck seams (IFRTs).

Floating decks are used in volatile stock service for stocks with a true vapor pressure at storage conditions below atmospheric pressure (that is, nonboiling). They are available in virtually all commercial tank sizes, from about 20 ft to 400 ft in diameter. Modified designs have been installed in tanks down to 8 ft in diameter. Methods and materials have been developed to properly seal the annular rim space, which is located between the tank shell and the rim of the deck, and to seal around the fittings that penetrate the floating deck.

Floating decks are typically constructed by joining sheets or panels of deck material in the field. This may be accomplished by a mechanical means, such as by bolting or by welding. Decks with bolted seams are typically made of aluminum. Bolted deck seams are described in 6.1.5.2 and 6.1.5.3. Welded decks are typically made of steel plates, but may be constructed of other materials. Welded deck seams are described in 6.1.5.4.

Floating decks are sometimes characterized by the location of the deck relative to the stock liquid surface. A deck that is supported above the stock liquid surface by buoyant structures is referred to as a noncontact deck. A deck that floats directly on the stock liquid surface is referred to as a contact deck. Steel decks are typically of contact design, whereas nonferrous materials such as aluminum are used in both noncontact and contact designs.

API 650[3] has two appendices for the design of floating roofs. Decks of sufficiently heavy construction to support environmental loadings, such as rainfall, are designed in accordance with API 650, Appendix C. Decks that are intended for use only in tanks that also have a fixed roof at the top of the shell tend to be of lighter construction, in that the fixed roof protects the floating deck from exposure to the elements. These decks are designed in accordance with API 650, Appendix H.

Tanks that have the heavier floating deck, and which do not have a fixed roof, are designated EFRTs. Tanks that have the lighter floating deck protected by a fixed roof are designated IFRTs[10]. Tanks that have a floating deck of the heavier external floating roof type, but which also have a fixed roof, are designated domed EFRTs.

The types of floating decks commonly used in EFRTs are described in 6.2.1 (see Figure 1 and Figure 2). The types of floating decks commonly used for IFRTs are described in 6.2.2 (see Figure 3). Domed EFRTs, described in 6.2.3, have the same types of floating decks as those used in EFRTs (see Figure 4).

6.1.3 Rim Seals

6.1.3.1 General

All types of floating roofs have an annular space between the perimeter or rim of the deck and the shell of the tank to permit travel of the floating roof within the tank. A rim-seal system is used to control evaporative loss from the rim space. Effective rim-seal systems close the rim space, accommodate irregularities between the floating roof and the tank shell, and help to center the roof, yet permit normal roof movement.

A rim-seal system can consist of one or two separate seals:

a) the primary seal and

b) the secondary seal, which is mounted above the primary seal.

Three basic types of primary seals are currently in widespread use:

a) vapor mounted,

b) liquid mounted, and

c) mechanical shoe.

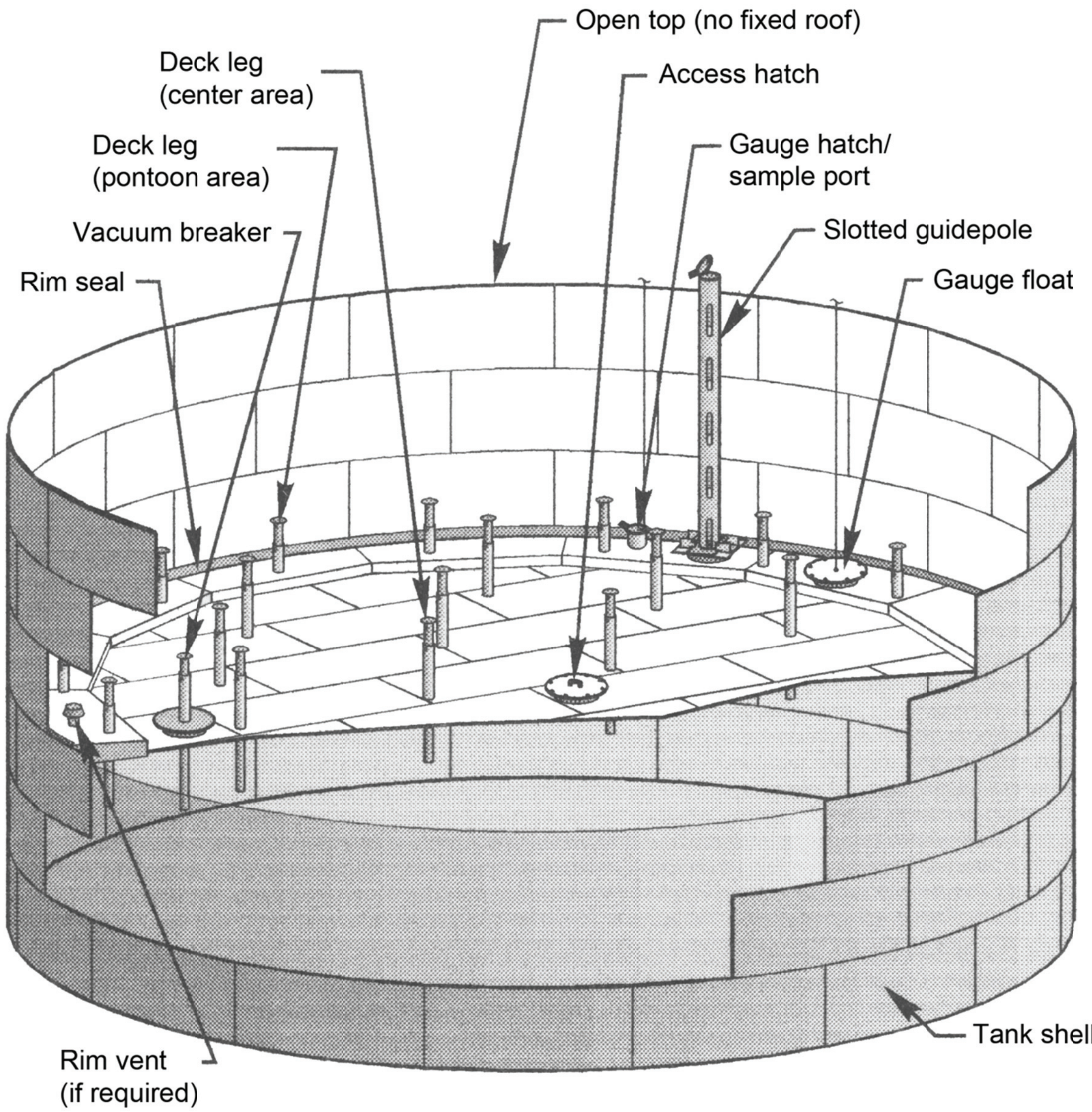

NOTE Details shown do not necessarily represent the most common or typical features in use.

Figure 1—EFRT with Pontoon Floating Roof[12]

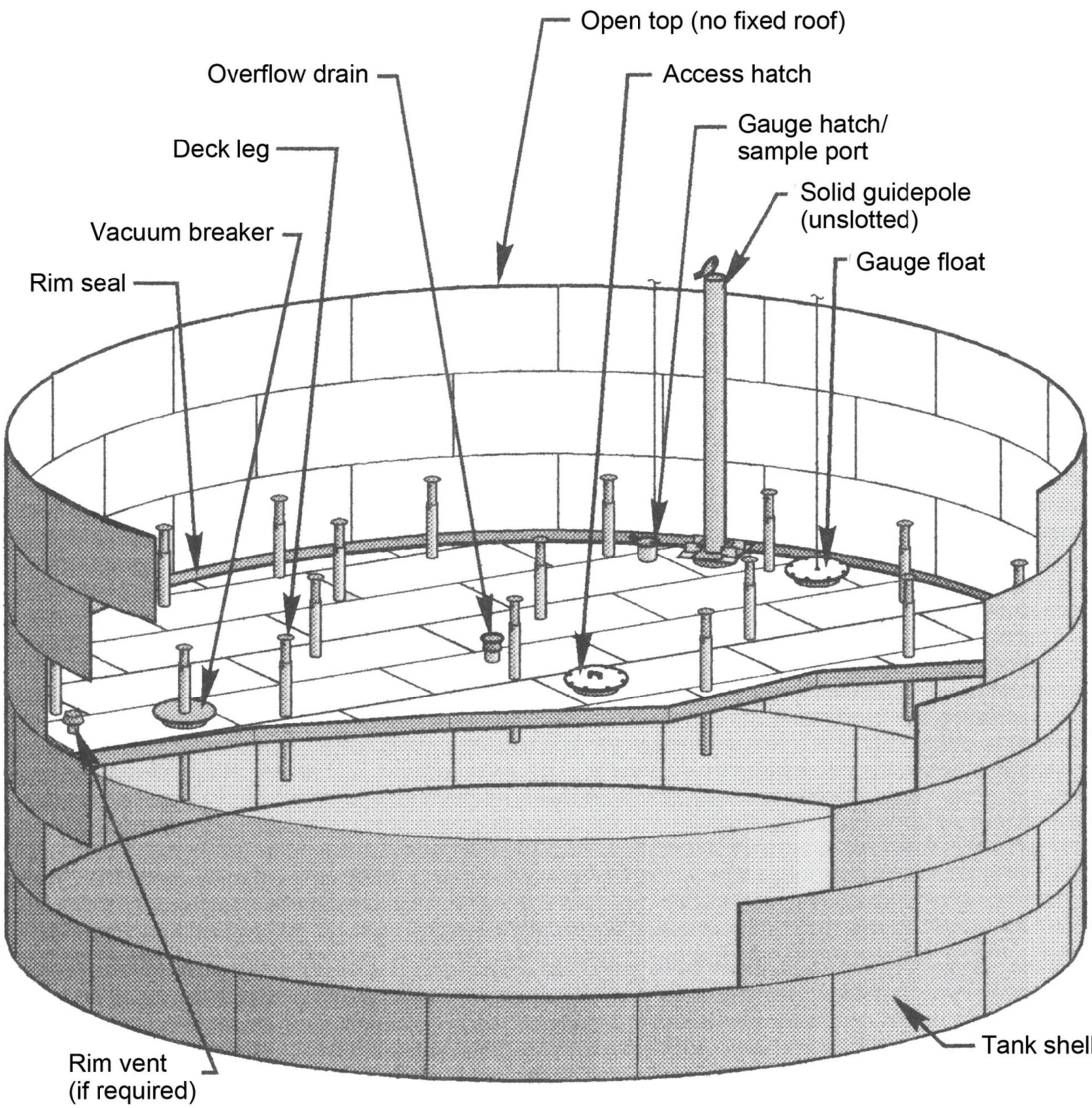

NOTE Details shown do not necessarily represent the most common or typical features in use.

Figure 2—EFRT with Double-deck Floating Roof[12]

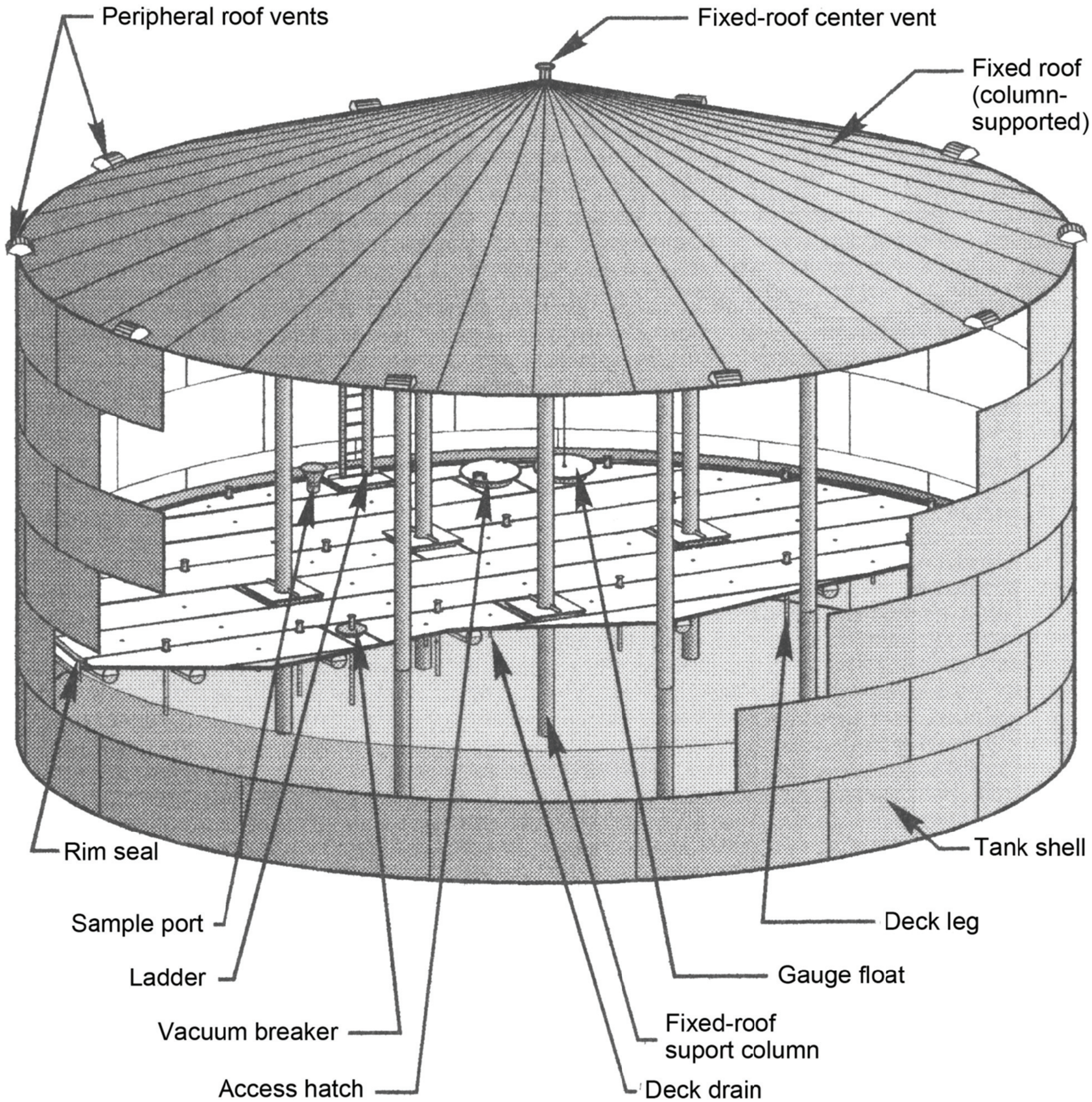

NOTE Details shown do not necessarily represent the most common or typical features in use.

Figure 3—IFRT with Noncontact Deck[12]

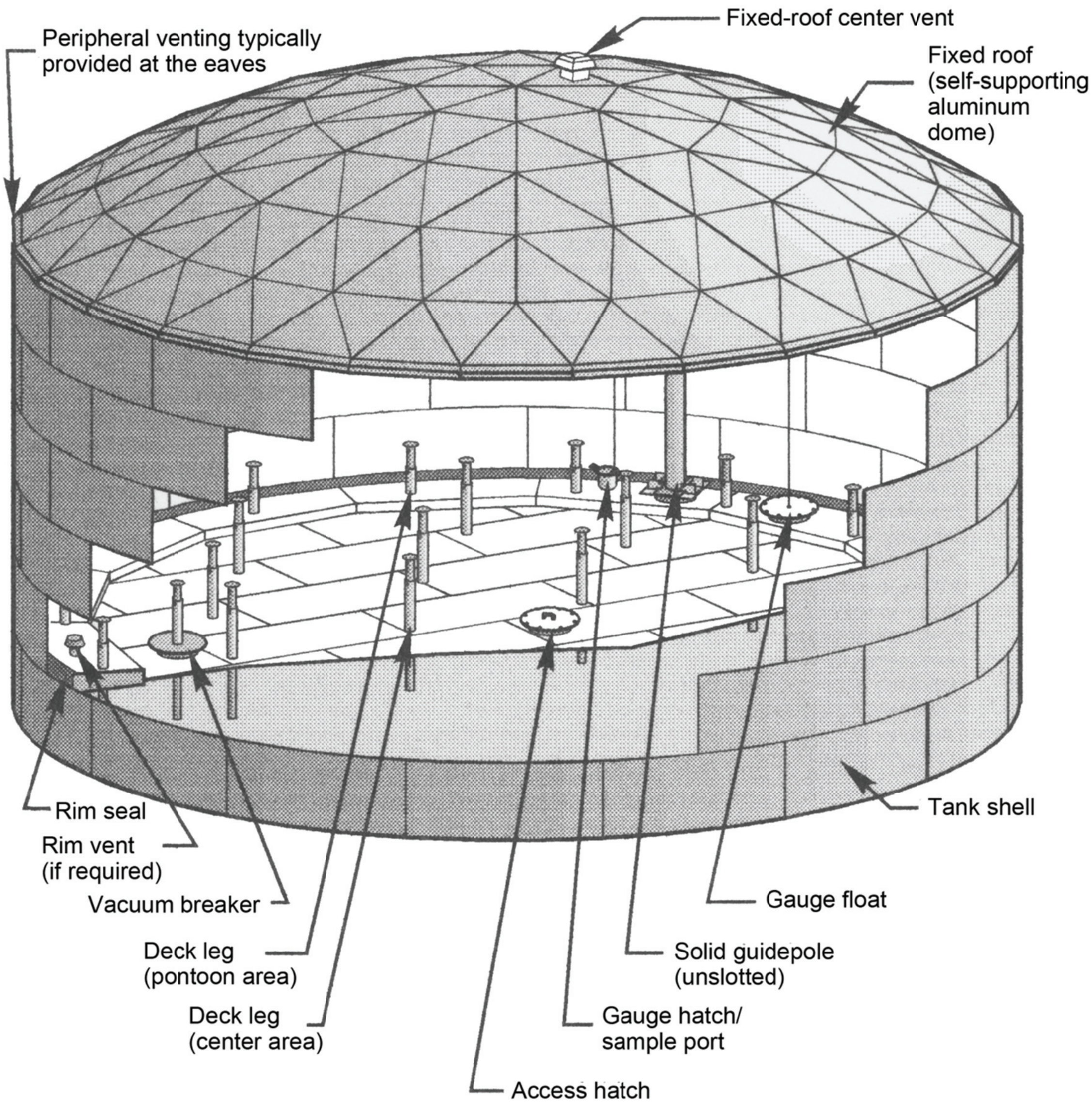

NOTE Details shown do not necessarily represent the most common or typical features in use.

Figure 4—Domed EFRT[12]

Vapor-mounted and liquid-mounted primary seals are both typically made of nonmetallic materials and are differentiated from each other by the location of the rim seal relative to the stock liquid surface. Rim seals mounted on the floating deck such that a vapor space exists between the stock liquid and the bottom of the rim seal are referred to as vapor mounted. If the bottom of the rim seal touches the liquid, it is referred to as a liquid-mounted seal. Mechanical-shoe seals are a different type of construction altogether, being made primarily of metallic materials.

Two basic configurations of secondary seals are currently in widespread use: shoe-mounted and rim-mounted. In addition, some external floating-roof rim-seal systems include a weather shield. Other types of primary and secondary seals have been or are being developed, but these rim seals are not currently in widespread use. A number of specific types of rim seals and weather shields, which represent most of the rim-seal systems currently in use, are described below.

Proper attention should be given to the selection of the materials used in the construction of rim-seal systems because of the potential for chemical incompatibility with the stored product.

6.1.3.2 Vapor-Mounted Primary Seals

Vapor-mounted primary seals include resilient-filled seals positioned sufficiently above the liquid surface (see Figure 5) so as to not be in contact with it, and flexible-wiper seals.

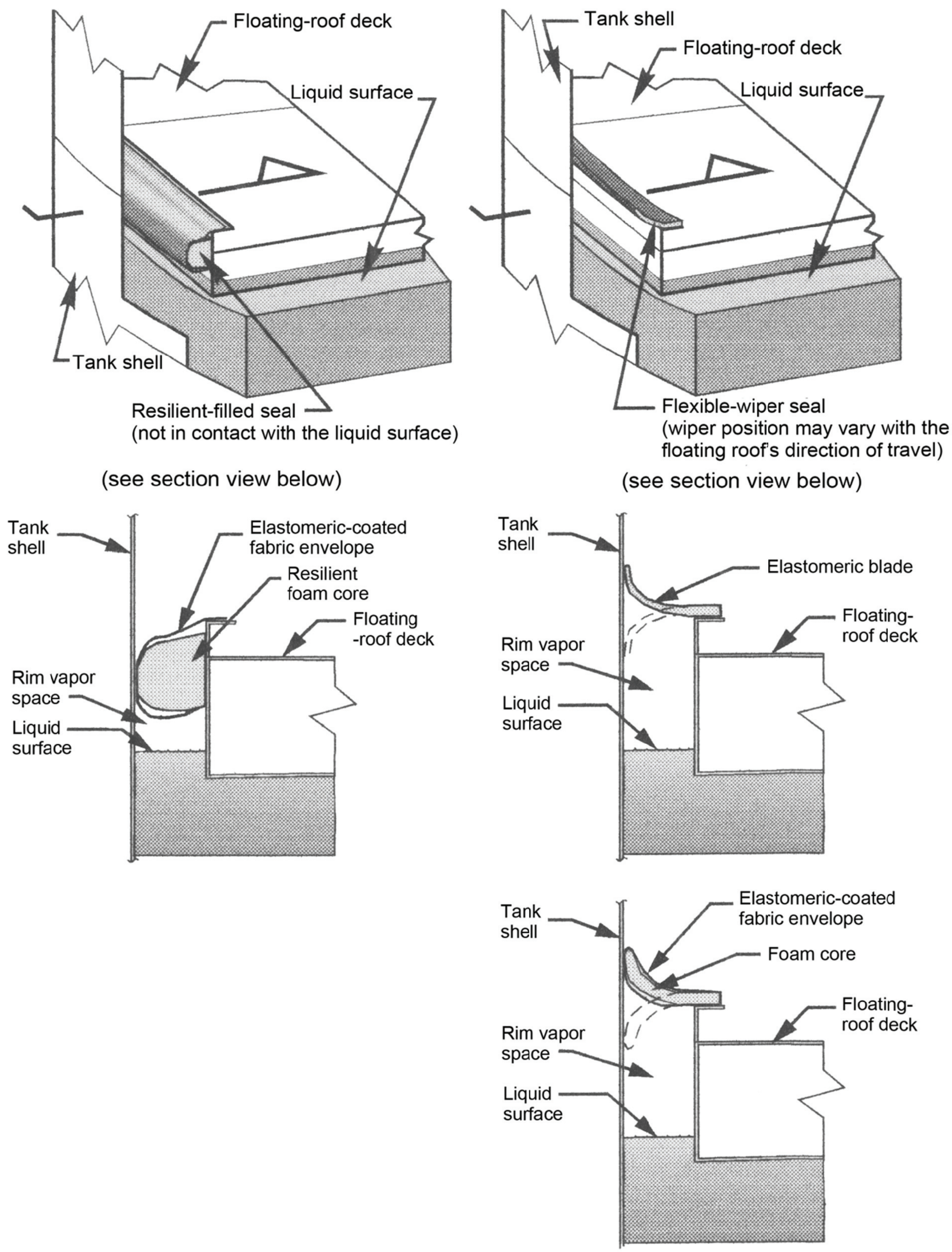

Figure 5—Vapor-mounted Primary Seals[12]

Resilient-filled seals work on the principle of expansion and compression of a resilient material to maintain contact with the tank shell while accommodating varying annular rim space widths. These seals typically consist of a core of open-cell foam enclosed in an elastomer-coated fabric envelope. The resiliency of the foam core pushes the fabric into contact with the tank shell. Polyurethane-coated nylon fabric and polyurethane foam are common materials. Reinforced polytetrafluoroethylene (PTFE) and fluorocarbon fabrics are also available. The foam core provides the flexibility and support while the fabric envelope provides the vapor barrier and wear surface.

Vapor-mounted primary seals are attached to the deck perimeter and extend around the circumference of the deck. For evaporative-loss control, it is important that the attachment of the seal to the deck and the radial seal joints are essentially vapor-tight and that the seal be generally in contact with the tank shell.

Flexible-wiper seals consist of an annular blade of flexible material attached to the deck perimeter, spanning the annular rim space and contacting the tank shell. The mounting is such that the blade is flexed and its elasticity provides a sealing pressure against the tank shell. For evaporative-loss control, it is important that the attachment of the seal to the deck and the radial seal joints be essentially vapor-tight; the seal extend around the circumference; the blade be generally in contact with the tank shell; and the edge of the seal not extend into the liquid during upward travel of the deck.

Two types of flexible wipers are commonly used. One type consists of a cellular, elastomeric material tapered in cross section with the thicker portion at the mounting. Synthetic rubber is a commonly used material; urethane and cellular plastic are also available.

A second type of flexible wiper uses an open-cell foam core enclosed in an elastomer-coated fabric envelope. This type of flexible-wiper seal uses materials of construction similar to a resilient-filled seal, but is configured so as to act in flexure rather than in compression.

6.1.3.3 Liquid-Mounted Primary Seals

When resilient-filled seals are mounted in a position that results in the bottom of the seal touching the liquid surface, they are considered liquid-mounted primary seals (see Figure 6). The fabric envelope of a liquid-mounted seal may be filled with a resilient foam, similar to that used in a vapor-mounted seal, or may be filled with a liquid.

Liquid-mounted primary seals are attached to the deck perimeter and extend around the circumference of the deck. For evaporative-loss control, it is important that the attachment of the seal to the deck and the radial seal joints are essentially vapor-tight and that the seal be generally in contact with the tank shell.

As with all seals that rely on a fabric envelope as the sliding contact with the tank shell, liquid-mounted seals are subject to being torn by rivet heads or weld burrs on the tank shell. Furthermore, coated fabrics in contact with hydrocarbon products, especially those with high aromatic content, have in some cases experienced reduced life or required increased maintenance. Recent advances in synthetic compounding have resulted in fabrics with increased compatibility with hydrocarbon products. Seal manufacturers can recommend the most suitable envelope fabric for particular applications.

Most vapor- and liquid-mounted seals are designed to accommodate a normal variation of ±4 in. in a nominal 8-in.-wide rim space. Different details are available for tanks with large diameters or with rim spaces wider than 8 in.

6.1.3.4 Mechanical-Shoe Primary Seals

The identifying characteristic of a mechanical-shoe seal is that it uses a light-gauge metallic band as the sliding contact with the shell of the tank (see Figure 7). The band is formed as a series of sheets (shoes) that are joined together to form a ring and are held against the tank shell by a mechanical device. The joints may be bolted, riveted, or sliding and may incorporate a gasket. While details vary by manufacturer, the shoes are normally 3 ft to 5 ft in height and thus provide a potentially large contact area with the tank shell. Expansion and contraction of the ring is provided for as the ring passes over shell irregularities or rivets.

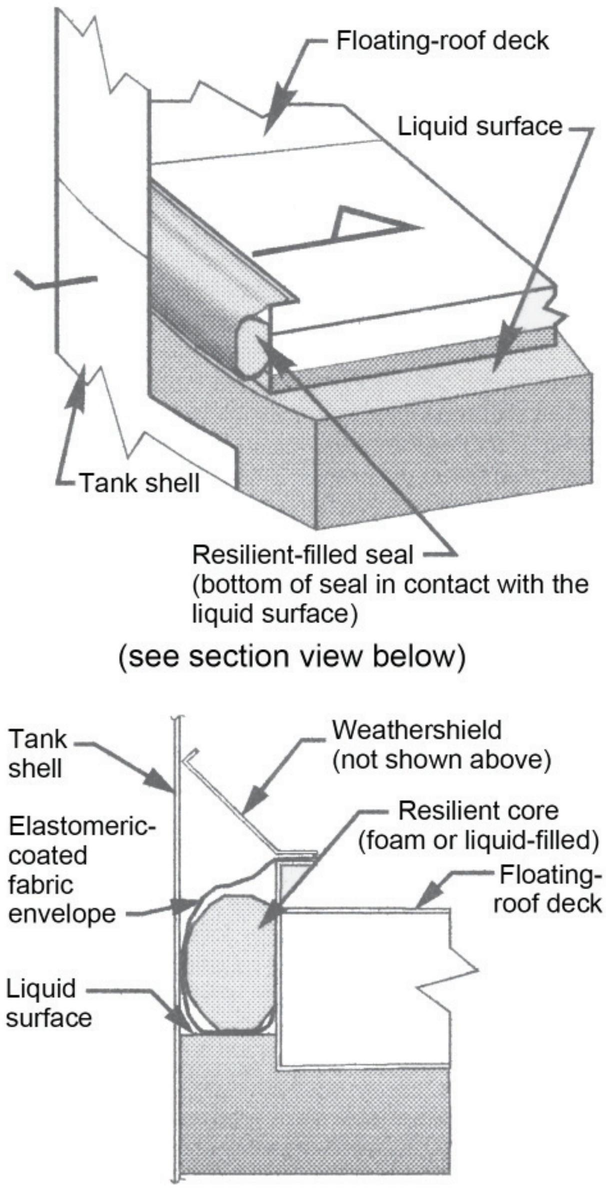

Figure 6—Liquid-mounted Primary Seals[12]

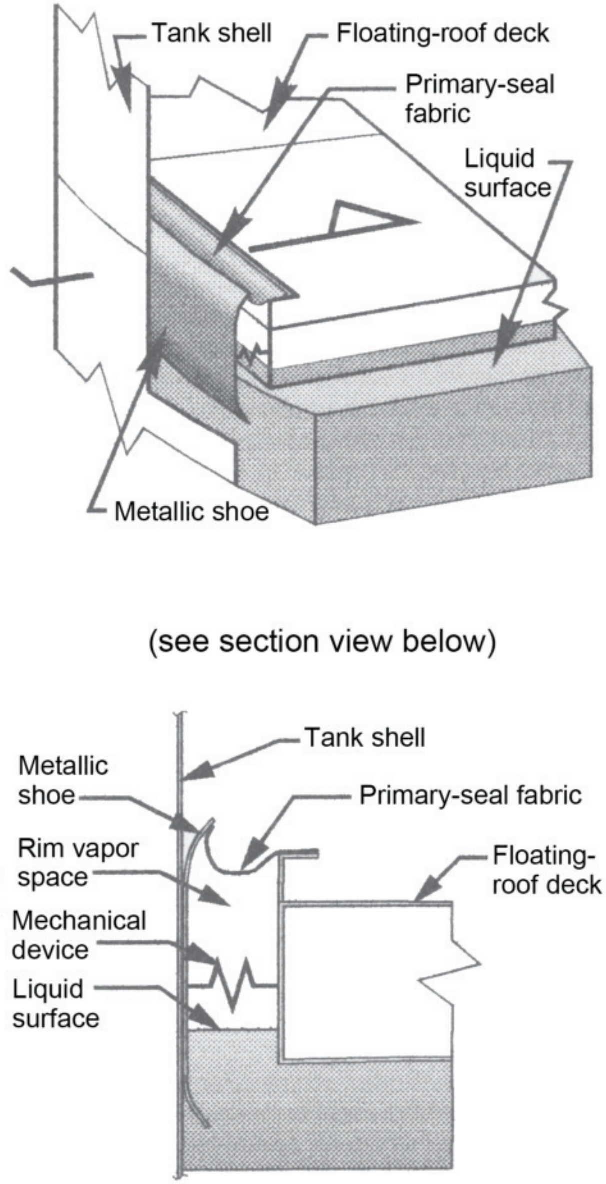

Figure 7—Mechanical-shoe Primary Seals[12]

This can be accomplished by jointing narrow pieces of fabric into the ring, by crimping the shoes at intervals, or by sliding joints between the sheets. The bottoms of the shoes extend below the liquid surface to confine the rim vapor space between the shoe and the rim of the floating roof.

The rim vapor space, which is bounded by the shoe, the rim of the floating deck, and the liquid surface, is sealed from the atmosphere by bolting or clamping a coated fabric called the primary-seal fabric that extends from the shoe to the rim. The specific type of fabric used varies with the tank manufacturer and the type of service.

Two locations are used for attaching the primary-seal fabric. With the most commonly used method, the fabric is attached to the top of the shoe and the rim of the floating deck. With the reduced-rim-vapor-space method, the fabric is attached to the shoe and the rim of the floating deck near the surface of the stored stock liquid. Rim vents (see 6.1.4) can be used to relieve excess pressure or vacuum in the rim vapor space.

Mechanical-shoe seals are usually designed to accommodate a local variation of ±5 in. in a nominal 8-in.-wide rim space. Different design details are available for tanks with large diameters or with rim spaces wider than 8 in. The shoe sealing ring and mechanism ordinarily provide sufficient flexibility to accommodate nominal irregularities in the tank shell. Mechanical-shoe seals can easily be fitted with wear plates for longer service life in riveted tanks.

In normal use (that is, when the floating roof is kept continuously floating), mechanical-shoe seals have a good service life. In general, the primary-seal fabric begins to show signs of aging before the metallic parts show wear. Where mechanical-shoe seals are used with a corrosive product or with unusual operating practices, such as when the underside of the floating roof is continuously exposed to air, corrosion can be severe. In such service, the use of corrosion-resistant metals or special coatings can be advantageous.

Since the integrity of the enclosed rim vapor space is important with respect to controlling evaporative loss, proper maintenance should be conducted to repair holes or other defects.

6.1.3.5 Secondary Seals

Generally, secondary seals can be divided into two categories: rim-mounted and shoe-mounted (see Figure 8). Rim-mounted secondary seals may attach directly to a rim angle or be mounted to an extended vertical rim plate. They are more effective in reducing losses than shoe-mounted secondary seals because they cover the entire rim vapor space. Shoe-mounted secondary seals, which are used only with mechanical-shoe primary seals, are effective in reducing losses from gaps between the shoe and tank shell, but do not reduce losses caused by defects in the primary-seal fabric.

Secondary seals can be made from a series of metallic sheets joined together to form a ring with a nonmetallic tip that slides on the inside surface of the tank shell. The joints may be bolted, riveted, or sliding and may incorporate a gasket material between the sheets. Secondary seals can also be made from fabric or elastomeric materials, sometimes reinforced with metallic or nonmetallic stiffeners or guided by external attachments. Some nonmetallic secondary seals are designed to reverse as the floating roof's direction of travel reverses, as shown by the dotted line in Figure 8. For secondary seals to be effective, they have to maintain contact with the tank shell.

Since the secondary seal is positioned above the primary seal, the effective operating capacity can be reduced in order for the secondary seal to remain in contact with the tank shell or to prevent contact with a fixed roof, if one is present.

6.1.3.6 Weather Shields

When external floating roofs that have a resilient-filled primary seal are not equipped with a secondary seal, most are furnished with weather shields, as shown in Figure 6. Weather shields are usually of a leaf-type construction and have numerous radial joints to allow for movement of the floating roof and irregularities in the tank shell. Weather shields may be of metallic, elastomeric, or composite construction. They are normally attached to the rim of the floating deck with either a mechanical or a pliable-hinge connection. Weather shields generally provide the primary seal with longer life by protecting the primary-seal fabric from deterioration due to exposure to weather, debris, and sunlight.

6.1.4 Deck Fittings

6.1.4.1 General

Numerous fittings pass through or are attached to a floating-roof deck to allow for operational functions or to accommodate structural support members. Deck fittings can be a source of evaporative loss when they require openings through the deck. Other accessories are used that do not penetrate the deck and are thus not sources of evaporative loss. The most common tank accessories that require openings in the deck are described below.

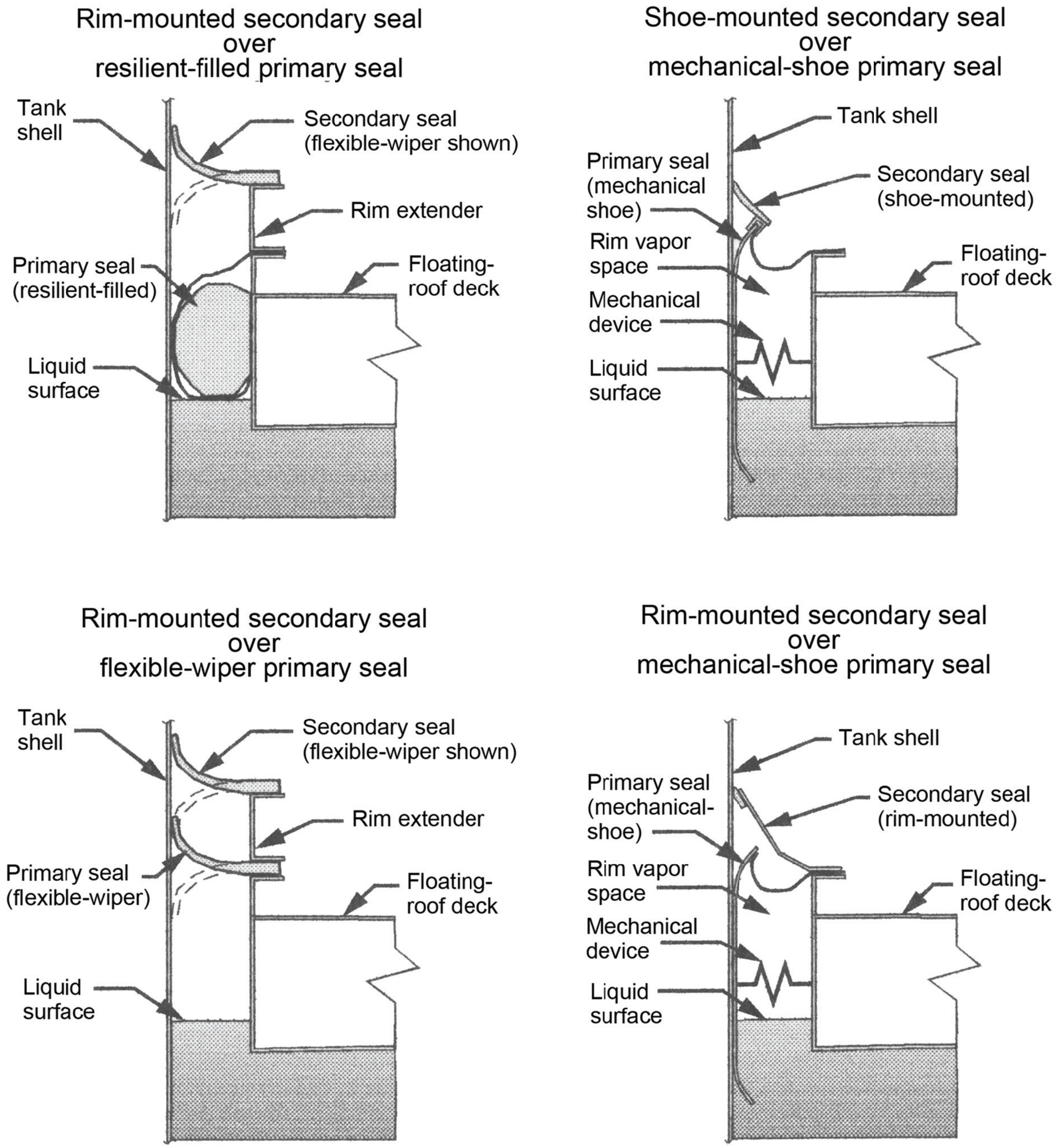

Figure 8—Secondary Seals[12]

6.1.4.2 Access Hatches

Figure 9 shows a typical access hatch, which consists of an opening in the deck with a peripheral vertical well attached to the deck and a removable cover. An access hatch is sized to provide for passage of workers and materials through the deck for construction and maintenance. The cover can rest directly on the well or a gasket can be used between the cover and the well to reduce evaporative loss. When a gasket is positioned under a cover or lid to seal it to the well, it is referred to as a well gasket. Bolting the cover to the well further reduces evaporative loss. With noncontact decks, the well extends into the stock liquid to seal off the vapor space below the deck.

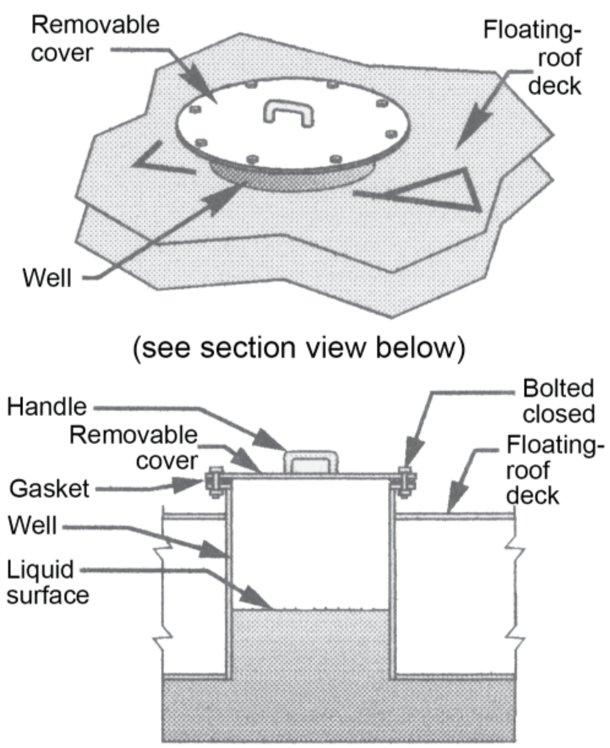

Figure 9—Access Hatch[12]

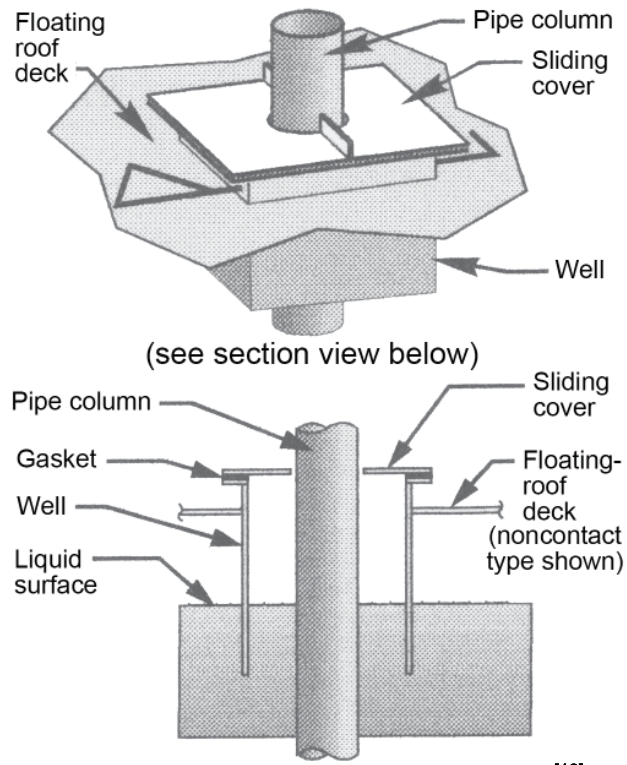

Figure 10—Fixed-roof Support Column[12]

6.1.4.3 Fixed-roof Support Columns

The most common fixed-roof designs are supported from inside the tank by means of vertical columns, which necessarily penetrate the floating deck. Some fixed roofs are entirely self-supporting and, therefore, have no support columns. EFRTs do not have fixed roofs, and thus have no fixed-roof support columns.

Fixed-roof support columns are made of pipe, with a circular cross section, or are built up from structural shapes with irregular cross sections. The number of columns varies with tank diameter and other factors, from a minimum of 0 to over 80 for very large diameter tanks.

The columns pass through deck openings with peripheral vertical wells (see Figure 10). With noncontact decks, the well extends into the stock liquid. A closure exists between the top of the well and the column, which has to accommodate the movements of the deck relative to the column as the stock level changes. There are several proprietary designs for this closure, including sliding covers and fabric sleeves. When a sliding cover is used, a well gasket can be used under the cover to reduce evaporative loss.

6.1.4.4 Gauge Floats

Figure 11 shows a typical gauge float and well. Gauge floats are a part of a device, sometimes referred to as an automatic gauging system that is used to indicate the level of stock within the tank. This system usually consists of a float contained within a well that passes through the floating-roof deck. The float is connected to an indicator on the exterior of the tank by a cable or tape that passes through a guide system. The well is closed by a cover that contains a hole through which the cable or tape passes. Evaporative loss can be reduced by gasketing and/or bolting the cover to the well, in a similar manner as for an access hatch. The hole in the cover is typically not gasketed, in that the cable or tape has to be allowed to pass freely in order to function properly.

6.1.4.5 Gauge Hatch/Sample Ports

Figure 12 shows typical gauge hatch/sample ports. Gauge hatch/sample ports provide access for hand gauging the level of stock in the tank and for taking thief samples of the tank contents. A gauge hatch/sample port consists of a pipe sleeve through the floating-roof deck and a self-closing cover. Gauge hatch/sample ports are usually located under the gauger's platform, which is mounted on the top of the tank shell. The cover may have a cord attached so that it can be opened from the gauger's platform. A gasketed cover will reduce evaporative losses.

On internal floating roofs, the sample port may have a fabric seal or diaphragm rather than a cover. The fabric seal is slit radially to allow entry of the sample thief, and the port may be funnel-shaped at the top to aid in guiding the sample thief into the opening in the deck. With noncontact decks, the pipe sleeve extends into the stock liquid to seal off the vapor space below the deck.

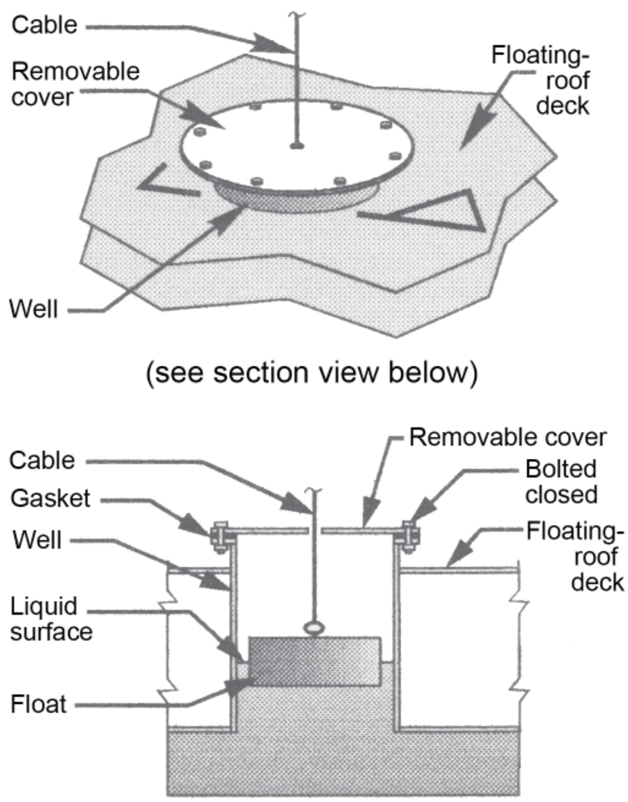

Figure 11—Gauge Float (Automatic Gauge)[12]

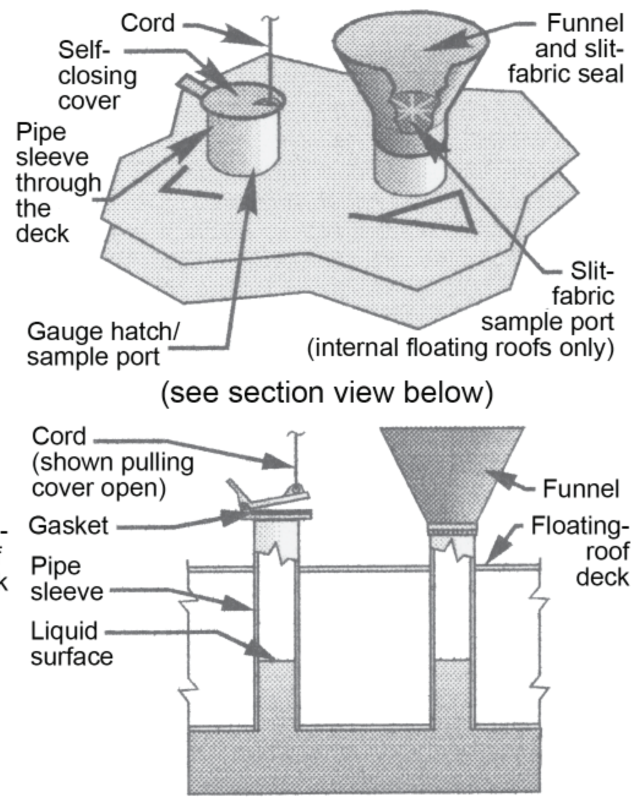

Figure 12—Gauge Hatch Sample Ports[12]

6.1.4.6 Vacuum Breakers

Figure 13 shows a typical vacuum breaker. A vacuum breaker is used to equalize the pressure in the vapor space beneath the floating roof when the roof is either landed on its legs or floated off its legs. This is accomplished by opening a deck fitting, usually consisting of a well formed of pipe or framing on which rests a cover.

A guided leg is attached to the underside of the vacuum-breaker cover which comes in contact with the tank bottom when the tank is being emptied, just prior to the point at which the deck support legs contact the tank bottom. When the vacuum-breaker leg contacts the tank bottom, it mechanically opens the vacuum breaker by lifting the cover off the well. When the leg is not in contact with the bottom, the opening is closed by the cover resting on the well. Some vacuum breakers have adjustable legs to permit changing the floating roof level at which the leg contacts the bottom. Since the purpose of the vacuum breaker is to allow the free exchange of air or vapor, the well does not extend below the bottom of the floating-roof deck. A well gasket can be used to reduce the evaporative loss when the cover is seated on the well.

6.1.4.7 Deck Drains

Deck drains, or open drains, are distinguished from closed drainage systems in that they permit water drainage from the surface of the floating-roof deck directly into the product. Deck drains consist of an open pipe that extends a short distance below the bottom of the floating-roof deck into the liquid product. Since these drainpipes are filled with product to the product level in the tank, evaporative loss occurs from the top of the drainpipes.

Closed drainage systems, on the other hand, carry rainwater from the surface of the floating-roof deck to the outside of the tank through a flexible or articulated piping system or through a flexible hose system located below the floating roof in the product space. Since product does not enter this closed drainage system, there is no associated evaporative loss.

Two types of deck drains are currently in common use in open drainage systems: flush drains and overflow drains (see Figure 14). Flush drains have a drain opening that is flush with the top surface of the deck. One-in. (1-in.) diameter flush drains are typically used on noncontact internal floating roofs. Overflow drains consist of a drain opening that is elevated above the top surface of the deck. Overflow drains limit the maximum amount of water that can accumulate on the floating roof and are thus used to provide emergency drainage of rainwater from external floating roofs. They are normally used in conjunction with a closed drainage system.

Some open deck drains are equipped with an insert, slit fabric, or other mechanical means to reduce the evaporative loss. Care shall be taken in the design and use of the insert to avoid impairment of the fitting's drainage ability.

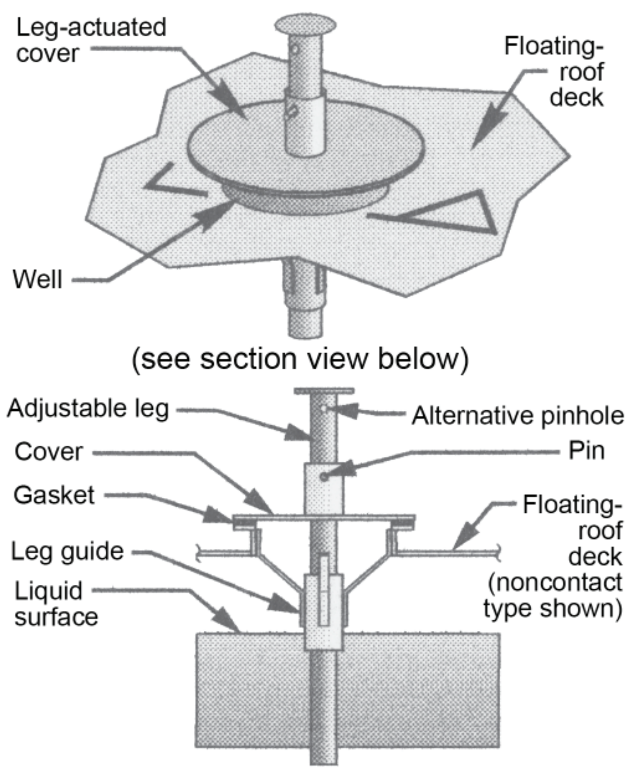

Figure 13—Vacuum Breaker[12]

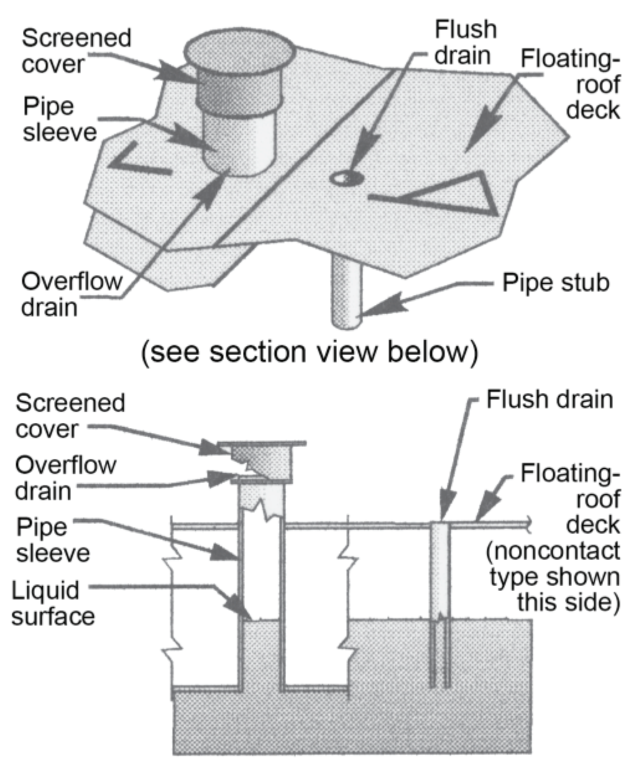

Figure 14—Deck Drains[12]

6.1.4.8 Deck Legs

Figure 15 shows a typical deck leg. To prevent damage to fittings located beneath the floating roof and to allow clearance for tank cleaning or repair, deck legs are provided to hold the floating roof at a predetermined distance above the tank bottom when the tank is emptied. The larger the diameter of the tank the greater the number of legs required. Deck legs generally consist of an adjustable pipe leg that passes through a slightly larger diameter vertical pipe sleeve. Evaporative loss occurs in the annulus between the leg and its sleeve.

The leg sleeve is attached to the deck, extending both above and below it. With noncontact decks, the sleeve extends into the stock liquid to seal off the vapor space below the deck. Pins are passed through holes in the sleeve and leg to permit height adjustment. The length of the sleeve above the floating roof varies, depending on its location on the roof. The sleeve height tends to be lower on internal floating roofs than on external floating roofs, in order to maximize the level to which the tank can be filled before the legs would contact the fixed roof. When EFRTs are converted to IFRTs by being retrofit with an aluminum dome fixed roof, the aluminum dome is often mounted on sidewalls above the top of the tank shell in order to avoid interference with the taller EFRT-type deck legs.

Some deck leg designs incorporate a seal to close the annulus between the leg and its sleeve to reduce evaporative loss. Boots or socks, which enclose the portion of the deck leg that extends above the floating deck, may also be used to reduce evaporative loss.

Fixed legs may be used that attach to the deck without any open penetrations, and thus have no associated evaporative loss.

On IFRTs, hanger systems may be used, which also avoid the need for an open penetration of the deck. Some internal floating-roof designs may use certain deck fittings, such as deck legs, that more closely resemble the construction typical of API 650, Appendix C-type decks[3]. Judgment should be used in determining the appropriate loss factor for a specific deck fitting.

6.1.4.9 Rim Vents

Figure 16 shows a typical rim vent. Rim vents are normally supplied only on tanks equipped with a mechanical-shoe primary seal. The rim vent is connected to the rim vapor space by a pipe and releases any excess pressure or vacuum that is present. The rim vapor space is bounded by the rim of the floating deck, the primary-seal shoe, the liquid surface, and the primary-seal fabric, as shown in Figure 16. Rim vents usually consist of weighted pallets that rest on gasketed surfaces.

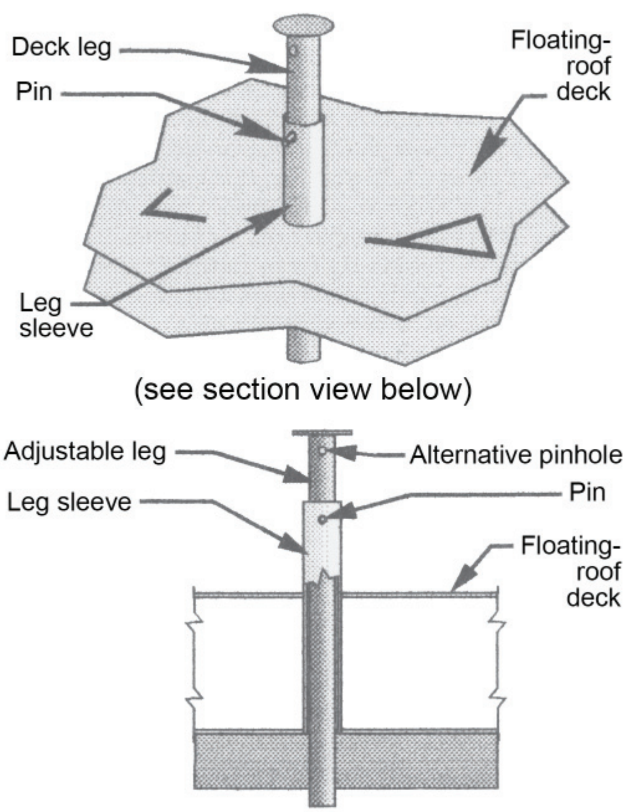

Figure 15—Deck Leg[12]

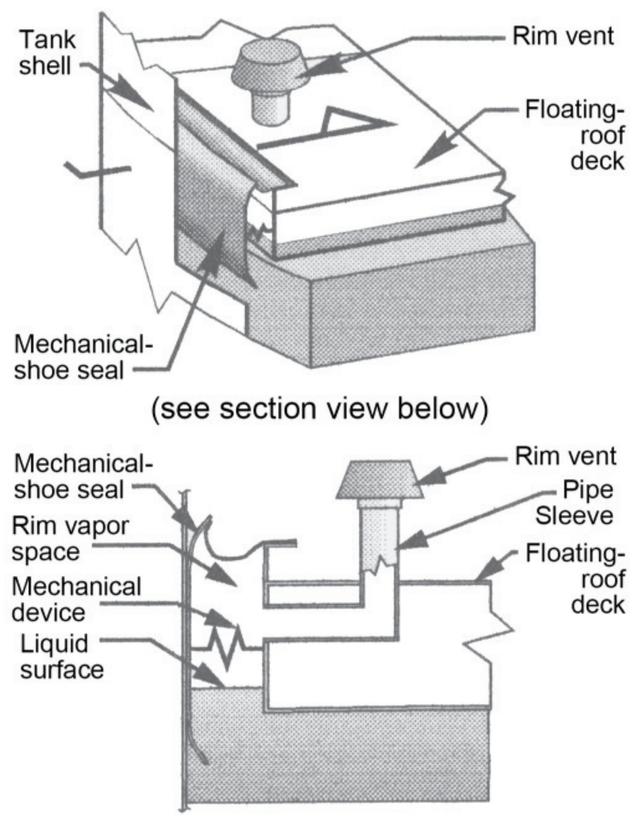

Figure 16—Rim Vent[12]

6.1.4.10 Ladders

Some tanks are equipped with vertical internal ladders, extending from the top of the shell to the tank bottom, as shown in Figure 17. The deck opening through which the ladder passes is constructed with design details and considerations similar to those previously discussed for column wells. Vertical internal ladders are typically only used on IFRTs.

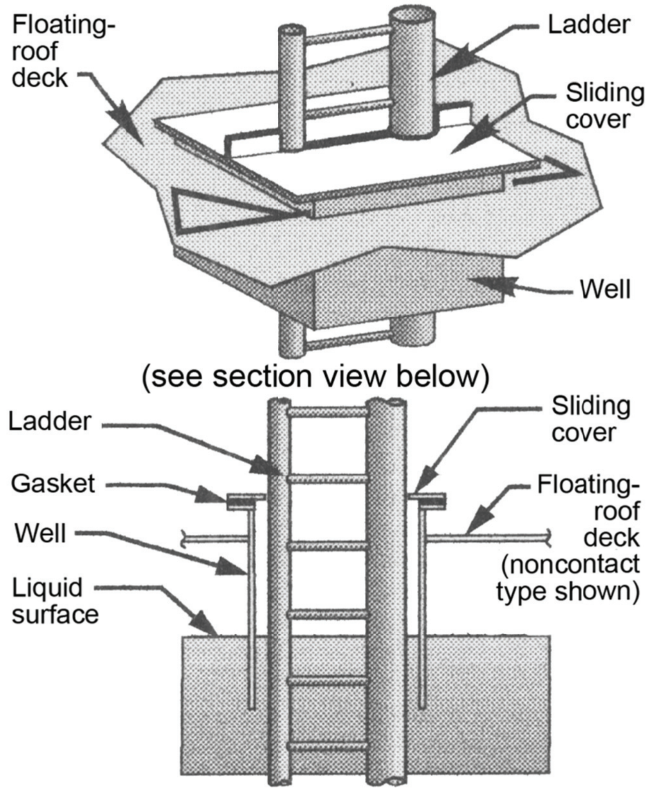

Figure 17—Vertical Ladder[12]

6.1.4.11 Unslotted (Unperforated) Guidepoles

Guidepoles are sometimes referred to as gaugepoles, gaugepipes, or stilling wells. The primary mechanical function of a guidepole is to prevent the floating roof from rotating as it rests on the stored liquid. The guidepole can also be used as an access to hand gauge the tank and take bottom samples. Because product can only enter an unslotted guidepole from the bottom, the stock within the guidepole does not exchange freely with the bulk contents of the tank. The composition and level of the liquid in the unslotted guidepole may therefore not be representative of the product in the tank.

Guidepoles are mounted from the tank at points above and below the range of travel of the floating roof and pass through an opening, or well, in the floating-roof deck (see Figure 18). One type of lid that covers this opening incorporates both a fixed cover and a sliding cover. The fixed cover is joined to the top of the well and has an oblong opening oriented in the radial direction of the tank. The sliding cover rests on top of the fixed cover and has a circular opening through which the guidepole passes. The sliding cover is allowed to slide horizontally in a radial direction with respect to the tank shell in order to accommodate differences between the plumbness of the guidepole and the tank. A well gasket can be used between the fixed cover and the sliding cover to reduce evaporative loss.

The guidepole fitting can also be equipped with a gasket referred to as a pole wiper, located between the guidepole and the sliding cover, to further reduce evaporative loss. Tests were conducted with the pole wiper at the same elevation as and 6 in. above the sliding cover. The data do not support differentiating between pole wiper elevations[11].

Another evaporative-loss device used on guidepoles is a pole sleeve that attaches to the underside of the sliding cover and extends downward into the product. The pole sleeve may be a length of pipe, the inside diameter of which is nominally larger than the outside diameter of the guidepole. By extending downward from the sliding cover into the product, this sleeve surrounds the guidepole, isolating it from the vapor space of the well.

The pole wiper and pole sleeve represent new technologies that have not yet been in widespread use. These emission control devices can have the potential to introduce unforeseen hazards and operating problems. The installation of a pole sleeve on an existing tank may require that the tank be degassed and cleaned, which can lead to additional emissions and safety concerns.

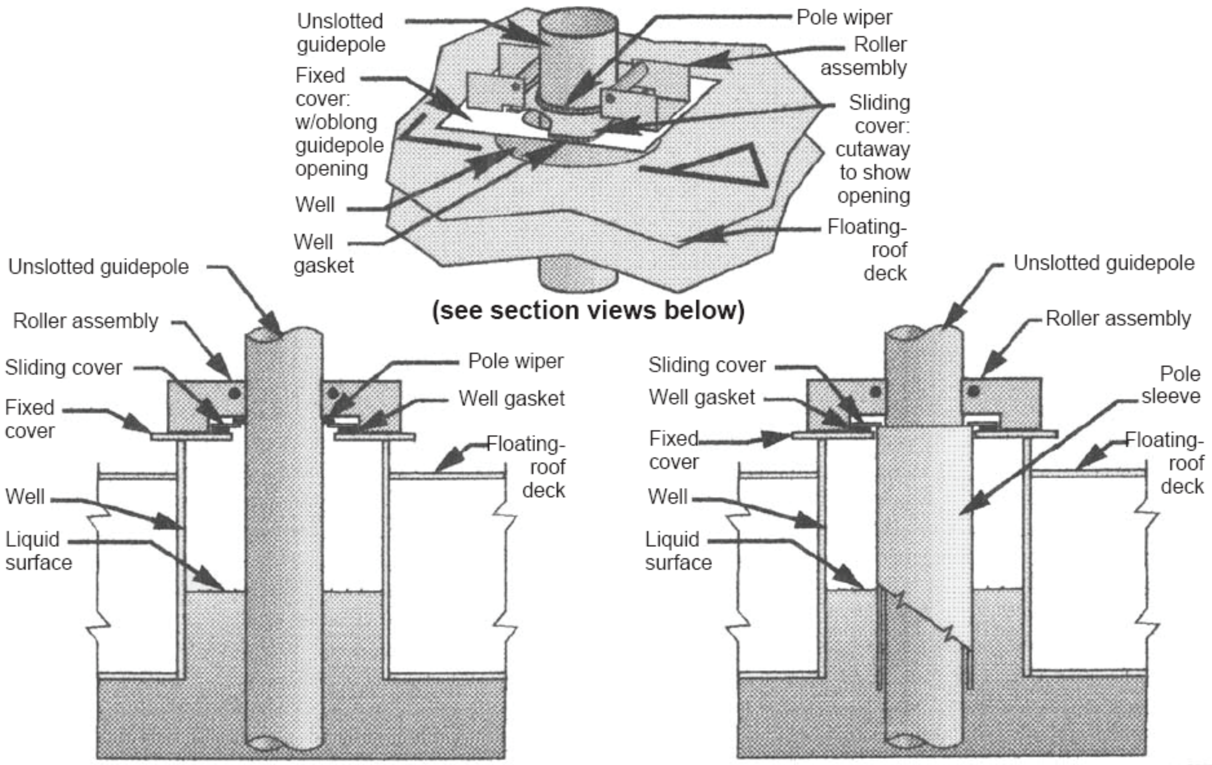

Figure 18—Unslotted (Unperforated) Guidepole[12]

6.1.4.12 Slotted (Perforated) Guidepoles

Figure 19 shows a typical slotted (perforated) guidepole. A guidepole is generally located adjacent to a platform at the top of the tank and offers an opening through which personnel may access the liquid below the floating roof. This access can be for the purpose of measuring the depth of the stored product or for obtaining product samples. When used as a sampling or gauging port, the guidepole typically has a series of perforations (slots or holes) along its length to allow product to flow freely through it. This mixing of the product in the pole is intended to ensure that the samples taken from within it are fairly representative of the contents of the tank. When perforations are limited to the portion of the guidepole below the lowest operating level of the floating roof, then the guidepole is considered to be unslotted.

The same controls described for unslotted guidepoles are also used with slotted guidepoles, although for certain configurations the limited available test data do not support differentiation for the presence or absence of a well gasket[11].

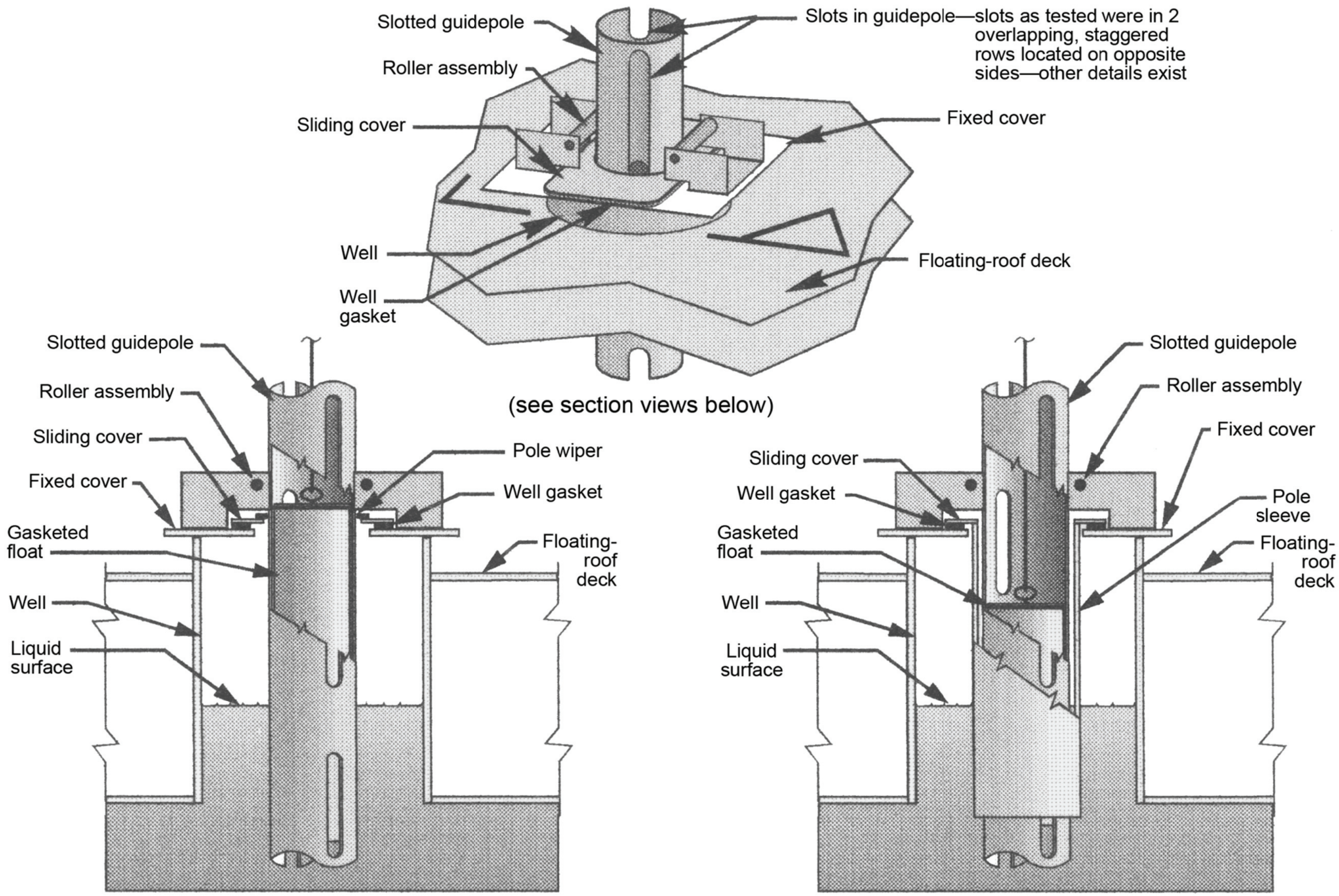

Figure 19—Slotted (Perforated) Guidepole[12]

In addition to the control devices discussed for unslotted guidepoles, a float is sometimes placed inside a perforated guidepole to reduce evaporative loss through these perforations. The float may be equipped with a wiper seal to close the annulus between the float and the inside surface of the guidepole.

In the absence of a pole sleeve, the float should be designed to reduce the flow of vapors through the perforations into the guidepole from the well vapor space. The float designs that have been tested without a pole sleeve included a wiper seal on the float that was mounted 1 in. above the sliding cover. Additional tests showed that no further reductions in emissions were achieved by positioning the float wiper at the same elevation as the sliding cover.

Tests conducted with both a float and a pole sleeve included positioning the float wiper at the same elevation as, 1 in. above, and 5 in. below, the sliding cover. The data do not support differentiating between float wiper elevations when a float is used with a pole sleeve[11].

6.1.4.13 Ladder/Guidepole Combination

The ladder/guidepole combination is a ladder which uses a slotted pipe for at least one of the vertical legs of the ladder. As with a standard ladder, a ladder/guidepole combination is typically used only in IFRTs. The slotted-pipe ladder leg may be used for gauging and/or obtaining samples of the stored liquid. A ladder sleeve is illustrated in Figure 20.

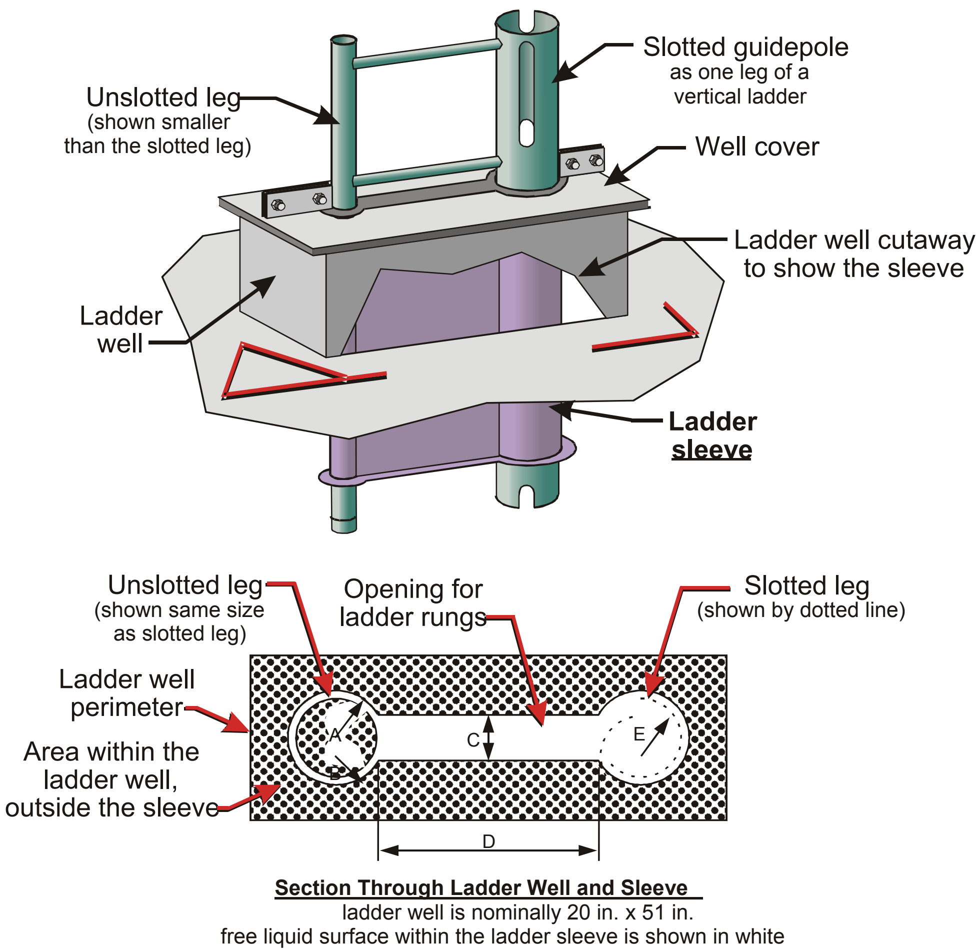

Figure 20—Ladder/Guidepole Combination[12]

The well for this ladder/guidepole combination is typically the same size as the well for a standard ladder. The rectangular well shown in Figure 20 is given nominal dimensions of 20 in. by 51 in., in order to match the surface area in the 36-inch diameter well configuration assumed in the development of emission factors for a standard ladder. In the uncontrolled condition, then, this fitting would have the same emission factor as for an ungasketed ladder well. When equipped with a sleeve around the ladder, however, the liquid surface area surrounding the ladder is significantly reduced.

When equipped with a ladder sleeve, the liquid surface area contributing vapors to potentially escape through the guidepole and past the ladder is limited to the liquid surface area within the sleeve, rather than the entire liquid surface area within the ladder well. The only remaining path for escape of vapors from outside the sleeve will be around the outer edge of the well cover.

6.1.5 Deck Seams

6.1.5.1 General

Floating decks are typically constructed by joining sheets or panels of deck material in the field. This may be accomplished by a mechanical means, such as bolting, or by welding. Decks with bolted seams are typically made of aluminum, whereas, welded decks are typically made of steel plates. Deck seam evaporative losses are only associated with IFRTs that have decks with bolted seams.

6.1.5.2 Noncontact Decks with Bolted Seams

This deck type consists of sheet aluminum bolted to an aluminum grid framework and is supported above the stock liquid surface by flotation devices such as sealed tubular aluminum pontoons. The bolted seam along the edges of the sheets forms a substantially tight barrier below which the stock vapor is contained in the space created by the means of deck flotation. The length of deck seam is determined by the width of the sheeting material used. The sheets often are continuous across the deck, except where interrupted by deck fittings.

6.1.5.3 Contact Decks with Bolted Seams

The most common design of this deck type consists of aluminum sandwich panels, with a honeycombed aluminum core, which float directly on the liquid surface. The panels are bolted to one another along their edges to form the deck. The length of deck seam is determined by the width and length of the panels used.

Another design consists of panels made up of rigid foam enclosed in a fiberglass-reinforced polyester skin or aluminum sheeting. These panels may also be bolted to form the deck, in a similar manner to that described above, except different materials are used.

6.1.5.4 Welded Contact Decks

This deck type consists of components that are welded together along their edges to form a deck. Welded construction is considered to result in a deck that has no associated evaporative loss at the seams. All decks designed in accordance with API 650, Appendix C[3] are of welded construction, and thus neither EFRTs nor domed EFRTs are considered to have deck seam losses. The steel-pan type of internal floating roof is also of welded construction. Any deck constructed of components which have the field joints welded along their entire lengths is considered a welded deck.

6.1.5.5 Other Deck Designs

Floating deck designs other than the most common designs discussed above are also available. One example is a contact deck with panels joined by adhesion and a continuous fiberglass-reinforced laminate. The panels are made of rigid foam enclosed in a fiberglass-reinforced polyester skin. No information is currently available on the evaporative-loss characteristics of this type of adhesively joined deck.

6.2 Types of Floating-Roof Tanks

6.2.1 External Floating-Roof Tanks

EFRTs do not have a fixed roof at the top of the shell, and the floating deck is therefore exposed to environmental loadings such as rainfall. The floating deck is typically constructed of welded steel plate. Minimum requirements for the design of external floating roofs are given in API 650, Appendix C[3]. Figures 1 and 2 show an EFRT with a pontoon floating roof and a double-deck floating roof, respectively.

While most of the various rim-seal designs are in usage on external floating roofs, the primary seal types in most common usage are the mechanical-shoe and resilient-filled. When floating roofs that have a resilient-filled primary seal are not equipped with a secondary seal, most are furnished with weather shields, as shown in Figure 6. Weather shields are usually of a leaf-type construction and have numerous radial joints to allow for movement of the floating roof and irregularities in the tank shell. Weather shields may be of metallic, elastomeric, or composite construction. They are normally attached to the floating roof with either a mechanical or a pliable-hinge connection. Weather shields generally provide the primary seal with a longer life by protecting the primary seal fabric from deterioration due to exposure to weather, debris, and sunlight.

Deck fittings on external floating roofs are typically of steel construction and are generally of heavier construction than those used on internal floating roofs. These fittings tend to have relatively tall housings or curbs. This is to minimize the potential for accumulated rainwater to empty from the deck into the stored liquid through the fitting penetration.

Manufacturers supply various versions of these basic types of external floating roofs, which are tailored to emphasize particular features, such as full liquid contact, load-carrying capacity, roof stability, or pontoon arrangement.

6.2.2 Internal Floating-Roof Tanks

IFRTs have a fixed roof (see Figure 3) at the top of the shell and a lightweight deck floating on the surface of the stock liquid. While the fixed roof shown in Figure 3 is a column-supported steel cone roof, an aluminum dome or any other type of roof that is permanently attached to the top of the tank may be used as the fixed roof for an IFRT. An IFRT is distinguished from a domed EFRT on the basis of the type of floating roof, rather than on the basis of the type of fixed roof. Minimum requirements for the design of internal floating roofs are given in API 650, Appendix H[3].

The use of an internal floating deck reduces the hydrocarbon vapor concentration in the vapor space between the floating deck and the fixed roof from that which would occur in a fixed-roof tank. Without sufficient ventilation, this can result in the occurrence of flammable vapor-air mixtures within the tank vapor space. To minimize the occurrence of flammable vapor-air mixtures in the tank vapor space, vents are installed at the top of the tank shell or in the fixed roof to permit circulation of air through the vapor space between the fixed roof and the floating deck. API 650, Appendix H, specifies the use of such vents and outlines design details for the storage of petroleum liquids. Such tanks are referred to as freely vented IFRTs and are those for which the loss-estimating equations in Section 4 are applicable.

Closed IFRTs refer to those that are vented only through a pressure/vacuum relief vent. Such tanks are sometimes used in chemical liquid service and in petroleum service where API 650 is not used. These tanks are typically designed with auxiliary safety devices specified by the user. The loss-estimating equations in this publication do not apply to closed IFRTs. However, API TR 2569[7] addresses this issue.

The basic types of primary rim seal in most common usage on internal floating roofs are the flexible-wiper and the resilient-filled. Mechanical-shoe seals have also been developed for internal floating roofs in recent years.

Deck fittings for internal floating roofs, whether of aluminum or steel construction, are typically of a different configuration than is generally used for external floating-roof decks. Rather than having tall housings to avoid rainwater entry, internal floating-roof deck fittings tend to have lower profile housings to minimize the potential for the deck fitting to contact the fixed roof when the tank is filled.

Manufacturers supply various versions of these basic types of internal floating roofs, which are tailored to emphasize particular features, such as full liquid contact, deck seam design, or pontoon arrangement.

6.2.3 Domed External Floating-Roof Tanks

Domed EFRTs have the heavier type of floating deck that is used in EFRTs, as well as a fixed roof at the top of the shell (see Figure 4). This is typically the result of retrofitting an EFRT with a fixed roof. This effectively converts the EFRT to an IFRT, while retaining the heavier external-type of floating-roof design. A domed EFRT is subject to the same venting requirements as an IFRT, in accordance with API 650 Appendix H[3]. As with an IFRT, the function of the fixed roof with respect to evaporative loss is not to act as a vapor barrier, but rather to block the wind.

While domed EFRTs are typically the result of converting an existing EFRT, a new tank can be built as a domed EFRT by supplying a floating roof built in accordance with API 650, Appendix C[3], and including a fixed roof at the top of the shell.

The type of fixed roof that is most commonly used as a retrofit cover for EFRTs is the self-supporting aluminum dome roof, which is of bolted construction. Minimum requirements for the design of aluminum dome roofs, both for new construction and retrofit applications, are given in API 650, Appendix G[3]. Other types of fixed roofs may be used as well, including steel cone roofs. While the domed EFRT designation can suggest a self-supporting fixed roof, and thus no support columns penetrating the floating roof, a steel cone roof typically requires support columns which have to be accounted for in the estimation of emissions.

The domed EFRT designation is dependent on the floating roof being of the external floating roof type. In the event that the floating deck is replaced with the lighter API 650, Appendix H-type of internal floating roof, the tank would then be designated an IFRT, regardless of whether the fixed roof is an aluminum dome or a steel cone roof. Again, an IFRT is distinguished from a domed EFRT on the basis of the type of floating roof, rather than on the basis of the type of fixed roof.

7 Loss Mechanisms

7.1 General

Evaporation is the natural process in which a liquid is converted to a vapor. Through evaporation, all liquids establish an equilibrium concentration of vapors above the liquid surface. Every liquid stock has a finite vapor pressure that depends on the surface temperature and composition of the liquid and causes the liquid to evaporate.

Under static conditions, an equilibrium vapor concentration is established, after which no further evaporation occurs. However, fixed-roof tanks are exposed to dynamic conditions that disturb this equilibrium, causing additional evaporation. These dynamic conditions are responsible for continued evaporation, resulting in stock loss and atmospheric emissions.

Evaporation loss from floating-roof tanks occurs when the evaporated vapor moves above the floating roof or liquid is left on the tank shell or columns above the floating roof.

Evaporative losses from EFRTs are primarily standing loss and are influenced significantly by ambient wind at the tank site. Sources of standing loss include the rim-seal system and fitting penetrations through the floating-roof deck. Relatively minor losses result from evaporation of liquid that clings to the tank shell as stock is withdrawn from the tank.

For freely vented IFRTs, the primary dynamic factor that promotes evaporation was thought to be the air movement through the vapor space between the floating deck and fixed roof, either as a result of external wind or ambient temperature changes. Diffusion within the tank was also thought to be a contributing factor. To determine the effect that varying air movement through the tank has on evaporative loss, tests[29] in the test tank were conducted over a wide range of air flow rates. The flow rates used in the test program equate to ambient wind speeds of up to approximately 35 mph, based on estimations from wind tunnel test data[38], [39]. The air flow rates tested were judged to simulate the full range of air movement occurring within freely vented IFRTs.

When the results from each test were statistically analyzed to determine the effect of varying the air-flow rate over the tested range, it was found that there were was no statistically significant change in the amount of evaporative loss as the air-flow rate was varied. As a result, air-flow rate and thus ambient wind speed and ambient temperature changes are not significant parameters in the evaporative-loss equation for freely vented IFRTs.

As with EFRTs, evaporative loss from IFRTs is primarily standing loss. In addition to the rim-seal area and deck-fitting penetrations, sources of standing loss from IFRTs include bolted seams in the floating deck.

7.2 Standing Loss

7.2.1 Rim-Seal Loss

The mechanisms of vapor loss from the rim seal are complex. However, wind has been found to be the dominant factor in inducing rim-seal vapor losses from EFRTs. Wind tunnel tests[35], [40], [41] have shown that the air that flows up and over the top of an EFRT produces a low-pressure zone above the floating roof on the upwind side of the tank. This results in air from the downwind side of the floating roof moving around the circumference of the floating roof above the rim seal. A steady wind thus establishes pressure differentials across the floating roof, with higher pressures on the downwind side and lower pressures on the upwind side. (Characterization of the wind-induced pressure differentials provided a means of converting air flow rates through the test tank into equivalent wind speeds for EFRTs, as discussed in Annex B.)

The differential pressure and air flow patterns established across an external floating roof are responsible for wind-induced losses in two basic ways. In one case, the pressure differentials cause air to enter any continuous rim vapor space beneath the rim seal on the downwind side of the floating roof. This air then flows circumferentially through the rim vapor space, flushing an air-hydrocarbon mixture out past the rim seal on the upwind (low-pressure) side of the floating roof. This action reduces the hydrocarbon concentration in the rim vapor space, so more liquid evaporates to reestablish more nearly equilibrium conditions. The magnitude of this wind-induced loss depends on the tightness of the rim-seal system and the presence of any gaps between the rim seal and the tank shell.

If no continuous rim vapor space exists between the rim seal and the liquid, the air flow pattern described above does not apply. In this case, the wind flowing above the rim seal produces turbulence in the air that is present in any gaps between the rim seal and the tank shell. This turbulence causes fresh air to mix with the hydrocarbon vapor within the gap, resulting in a reduction in the hydrocarbon concentration within the gap and causing more liquid to evaporate to reestablish more nearly equilibrium conditions. The magnitude of this wind-induced loss depends on the area of the rim-seal gap and the depth of the vertical contact area between the rim seal and tank shell. This mechanism can also contribute to losses from rim-seal systems that have a continuous rim vapor space. In general, lower wind-induced losses occur from rim seals with small gaps and from those with a large vertical contact area between the rim seal and the tank shell.

To a small extent, the wind-induced evaporative losses can be a function of the height of the floating roof in the tank. However, this loss variation is considered insignificant.

Other potential loss mechanisms include the expansion of gas in the rim vapor space attributable to changes in temperature, pressure, or both (that is, breathing) and the varying solubility of gases, such as air, in the rim-space liquid as a function of temperature and pressure.

Breathing in the rim vapor space can occur as the pressure or temperature (or both) of the rim vapor changes. As the vapor temperature increases or the barometric pressure decreases, an air-hydrocarbon mixture can be expelled from the rim vapor space. As the vapor temperature decreases or the barometric pressure increases, fresh air can be drawn into the rim vapor space. This causes further evaporation and can also result in vapor being expelled from the rim vapor space. The degree to which the vapor is contained in or expelled from the rim vapor space during temperature and pressure changes is a function of the tightness of the rim-seal system and the pressure and vacuum settings of any rim vents on the floating roof.

Changes in the temperature of the liquid in the rim space or the barometric pressure can cause air to dissolve in or be evolved from the liquid. As the liquid temperature increases or the barometric pressure decreases (or both), the air solubility generally decreases and air evolves from the liquid in the rim space. As air leaves the liquid, it carries with it some hydrocarbon vapor.

Other possible loss mechanisms include permeation of the sealing fabric by vapor and wicking of the liquid in the rim space up the tank shell into contact with the air above the rim seal.

The standing rim-seal loss factors presented for wind-dependent rim-seal losses from EFRTs were developed by averaging tests in which some or all of these loss mechanisms occurred.

For EFRTs, wind-generated air movement across the floating roof was the dominant factor affecting rim-seal loss. In comparison, for freely vented IFRTs in which the air movement is significantly reduced from ambient wind speed, no clearly dominant loss mechanism could be discerned. Nevertheless, the test program was designed so that the combined effects of all of the mechanisms would be measured. Therefore, although no conclusion can be drawn as to the dominant rim-seal area loss mechanism for IFRTs, all of the loss mechanisms are accounted for in the rim-seal loss equation and rim-seal loss factors given in 4.2.2.2.

Vapor permeability was the only potential rim-seal area loss mechanism that could be investigated independently. Seal fabrics are generally reported to have very low permeability to typical hydrocarbon vapors, so this source of loss is not considered significant. However, if a seal material is used that is highly permeable to the vapor from the stored stock, the rim-seal loss could be significantly higher than that estimated from the rim-seal loss factors in 4.2.2.2.

7.2.2 Deck-Fitting Loss

Fittings that penetrate the floating-roof deck are potential sources of loss because they can require openings that allow stock vapors to flow from the stored liquid to the atmosphere above the floating roof. Although such openings are routinely sealed, the design details of deck fittings generally preclude the use of a completely vapor-tight seal. As a result, some of the mechanisms discussed in 7.2.1 for rim-seal losses can cause losses from deck-fitting penetrations. These mechanisms include vertical mixing, resulting from diffusion or air turbulence, of vapor through any gaps between the deck-fitting seal and the fitting; expansion of any vapor spaces directly below the fitting seal, resulting from temperature and pressure changes; varying solubility of gases in the liquid directly below the fitting seal; wicking of liquid up the deck fitting; and permeation of any fitting seal or gasket by vapor.

The extent to which any one of these mechanisms contributes to the total deck-fitting loss is not known. The relative importance of the various mechanisms probably depends on the type of deck fitting and the design of the fitting seal. Nevertheless, the deck-fitting loss factors in 4.2.2.3 account for the combined effects of all of these mechanisms.

7.2.3 Deck-Seam Loss

Floating decks are typically made by joining several sections of deck material together, resulting in seams and joints in the deck. This may be accomplished by a mechanical means, such as bolting, or by welding. To the extent that these seams are not completely vapor tight, they become a source of evaporative loss. Deck-seam evaporative losses are only associated with IFRTs that have decks with bolted seams. Generally the same loss mechanisms discussed in 7.2.2 for deck fittings may apply to deck seams.

As in the case of deck fittings, the relative importance of each of the loss mechanisms is not known. Different mechanisms probably predominate, depending on whether or not the deck is in contact with the stored liquid. Nevertheless, the deck-seam loss factors in 4.2.2.4 account for the measured effect of all contributing loss mechanisms.

7.3 Working Loss

As the floating roof descends during stock withdrawal, some of the stock liquid clings to the inside surface of the tank shell (and fixed-roof support columns, if any) and is exposed to the atmosphere. To the extent that this clingage evaporates before the exposed shell area is again covered by the ascending floating roof during a subsequent filling, evaporative loss results.

The rim-seal, deck-fitting, and deck-seam evaporative losses are components of the standing loss, which addresses evaporative loss originating at the surface of the stored liquid. Withdrawal loss, however, pertains only to wetted portions of the tank that become exposed as the floating roof descends during withdrawal of the stored liquid.

8 Development of Estimation Methods

8.1 General

The topic of this standard was first addressed by API Bulletin 2517, *Evaporation Loss from External Floating-Roof Tanks*, and API Bulletin 2519, *Evaporation Loss from Internal Floating-Roof Tanks*. These publications were combined in 1997 in *API Manual of Petroleum Measurement Standards* (*MPMS*), Ch. 19.2, *Evaporative Loss from Floating-roof Tanks*.

8.2 Standing Loss

8.2.1 Standing Loss Data

Of the test-tank data[13] to [21] for EFRTs, 106 datasets had information relevant to an evaluation of the effects of tank construction and type of rim-seal system, wind speed, stock vapor pressure, and product type on the standing loss. Of these datasets, 44 could be used directly in the development of the rim-seal loss factors. Although the test tank was welded, some of the tests performed covered the gap-area ranges observed for rim seals in riveted tanks. The types of external floating-roof rim-seal systems that were used in these tests are listed below. These systems represent the vast majority of those currently in use.

a) Mechanical-shoe seal.

   1) Primary only.

   2) Shoe-mounted secondary.

   3) Rim-mounted secondary.

b) Liquid-mounted resilient-filled seal.

   1) Primary only.

   2) Weather shield.

   3) Rim-mounted secondary.

c) Vapor-mounted resilient-filled seal.

   1) Primary only.

   2) Rim-mounted secondary.

During the external floating-roof tests conducted in the test tank, the air flow rate was varied to simulate equivalent wind speeds of 2 mph to 15 mph. The stock true vapor pressure was varied from 0.75 psia to 9.25 psia. The stock liquid used in most tests was a mixture of normal octane and propane.

To evaluate the losses from various types of external floating-roof deck fittings, data[30], [31] from 52 bench-scale wind tunnel tests were evaluated in the first series of tests (1984 to 1985). During these tests, the stock true vapor pressure ranged from 1.3 psia to 8.4 psia, and the air flow rate was varied to simulate wind speeds of 5 mph to 14 mph. Most of the tests were conducted with normal hexane, but mixtures of normal octane and propane were also used. In addition, survey information on the number of various types of deck fittings typically used as a function of tank diameter was compiled and evaluated.

To determine the effect of EFRT diameter on standing loss, data[22], [23], [42] from a total of 16 field tanks were evaluated. Losses from three of these tanks[22], [23], which ranged in diameter from 35 ft to 152 ft, were precisely measured; and extensive supporting data on tank construction, rim-seal system, and ambient conditions were collected. The other 13 field-tank tests[42] used slightly less precise instrumentation and included somewhat less complete data on the field tanks, which ranged in diameter from 55 ft to 153 ft.

To relate test-tank rim-seal conditions to actual field-tank rim-seal conditions of EFRTs, data[28] from more than 400 measurements of field-tank rim-seal gap areas were analyzed. This analysis determined the frequency of occurrence of various ranges of rim-seal gap areas in operating external floating-roof field tanks.

Additional data[6] that were analyzed included tank temperature data to determine the effects of paint color on stock liquid temperature relative to ambient temperatures. Several loss-measurement tests[24], [25], [26] were conducted with gasoline and crude oil in the test tank. Data from these tests were used to develop the product factors. In addition, vapor samples from both gasoline and crude oil stocks were analyzed; and these showed a large range of hydrocarbon components, including methane and ethane.

The second series of tests[11], [32], [33], [34] on external floating-roof deck fittings (1991 to 1995) evaluated data from over 200 bench-scale tests in the wind tunnel. The air-flow rate was varied during these tests to simulate wind speeds of 4.3 mph, 8.5 mph, and 11.9 mph. These tests were conducted with normal hexane.

To relate the speed of air moving across the deck of an external floating roof to ambient wind speed at the tank site, data[35] were evaluated from wind tunnel studies of scale model tanks. Three tank diameters were modeled (48 ft, 100 ft, and 200 ft) at three different floating-roof heights. Wind speed data from 28 locations on these floating roofs were evaluated. These data[36] were related to field-tank data from two EFRTs that were instrumented and continuously monitored for a period of about one year. In addition, data[36] on the liquid heights of numerous field tanks were evaluated.

To determine loss rates for these deck fittings when used in domed EFRTs, an additional 31 tests[11], [32], [33], [34] were evaluated at a wind speed of 0 mph.

Of the internal floating-roof tests[29] conducted in the test tank, seventy-two tests had information relevant to an evaluation of the effects of deck and rim-seal system type, stock vapor pressure, and product type on standing loss. The types of internal floating-roof decks and rim-seal systems that were used in these tests are listed below. These systems represent the vast majority of those currently in use.

a) Bolted, noncontact aluminum deck.

    1) Vapor-mounted, flexible-wiper primary seal.

    2) Flexible-wiper secondary seal.

b) Welded, contact steel deck.

    1) Liquid-mounted, resilient, foam-filled primary seal.

    2) Flexible-wiper secondary seal.

c) Bolted, contact aluminum deck.

    1) Vapor-mounted, resilient, foam-filled primary seal.

    2) Resilient, foam-filled secondary seal.

During the internal floating-roof tests conducted in the test tank, the air-flow rate was varied from an equivalent wind speed of approximately 3 mph to 35 mph. The stock true vapor pressure was varied from approximately 0.25 psia to 7.0 psia. The molecular weight of the vapor ranged from approximately 46 lb/lb-mol to 112 lb/lb-mol. The stock liquid used in most tests was a mixture of normal octane and propane, but pure normal hexane and pure normal octane were also tested.

To evaluate the losses from various types of internal floating-roof deck fittings, data from 14 bench-scale tests[29] were evaluated. During these tests the stock true vapor pressure ranged from approximately 2 psia to 7 psia. Most of the tests were conducted on normal hexane, but mixtures of normal octane and propane were also tested.

To determine the effects of tank diameter on standing loss, data from several different sources were used. Rim-seal losses from the 20ft-diameter test tank[29] and a 100-ft-diameter field tank[22] were compared. Survey information on the number of various types of deck fittings typically used as a function of tank diameter was compiled and evaluated. Measurements and estimations were made to relate the typical length of deck seams to tank diameter.

To relate the specific rim-seal conditions evaluated in the test tank to an average seal condition, representative of a typical operating field tank, data[28] from measurements of field-tank seal gap areas were used. These data were previously compiled and analyzed as part of API's EFRT test program. The data provide information on the frequency of occurrence of various ranges of seal gap areas in external floating-roof field tanks. In the absence of seal gap data specific to IFRTs, these data were assumed to be applicable to internal floating-roof field tanks.

8.2.2 Standing Loss Estimate Development

8.2.2.1 General

The important parameters that affect standing loss were identified and separately evaluated to determine their independent effects on the total loss. These parameters include: the type and condition of the rim-seal system (K_{ra}, K_{rb}, n, F_r); wind speed (V); tank diameter (D); the type, number, and general design of the deck fittings (K_{fa}, K_{fb}, m, N_f, F_f); fitting wind-speed correction factor (K_v); deck seam construction (K_d, S_d, F_d); stock vapor pressure (P); and type of stock (K_c). The methods used to develop the functional loss relationships involving these parameters are outlined in 8.2.2.2 through 8.2.2.7. The annexes are referenced for more detailed discussions of some of the parameters.

8.2.2.2 Rim-Seal Loss Factors

As discussed in Annex B, a regression analysis was used to develop equations to convert the air-flow rate in the test tank to the equivalent wind speed across an external floating-roof field tank. An analysis[43] of the test-tank data indicated that straight-line plots are obtained when the logarithm of the net losses, after subtracting the zero wind speed value, is plotted against the logarithm of the wind speeds. Therefore, loss, L, is related to wind speed, V, by an equation of the following general form:

$$L = K_a + K_b V^n$$

where K_a, K_b, n = constants for a given rim-seal system and condition.

For IFRTs and domed EFRTs, $V = 0$, and the above equation becomes:

$$L = K_a$$

By regression analysis[43] of the external floating-roof test-tank data, values of K_a, K_b and n were estimated for each rim-seal system, as discussed in Annex A. By considering the vapor pressure, vapor molecular weight, and test-tank diameter, the rim-seal loss factors K_{ra}, K_{rb} and n were determined.

It should be noted that 5.2.1 recommends the use of wind-speed data from local weather stations, including local airport weather stations, if tank-site wind-speed data are not available. During two of the field-tank testing programs[22], [23], National Weather Service wind-speed data were collected from the nearest airport and compared with wind speeds measured at the tanks. Tank wind speeds were expected to exceed the National Weather Service data, since the former measurements were made at greater distances above ground level. In all cases, however, tank wind speeds were lower than the National Weather Service data. For the four tank sites checked, tank wind speeds averaged about 50 % of the wind speeds obtained from local airports. Airports are generally large flat areas; tank farms are characterized by local roughness caused by tanks, dikes, buildings, and other obstructions. These tank farm features contribute to turbulence that could conceivably decrease the local effective horizontal wind component, but the data were too limited to develop general conclusions. However, the data indicate that use of wind-speed data from local airports will generally provide conservative loss estimates. Estimated losses based on airport wind-speed data will generally be higher than those estimated using wind-speed data from the tank site.

8.2.2.3 Tank Diameter

The dependence of evaporative loss on tank diameter, D, was determined by comparing measured field-tank losses[22], [23], [42] with predicted losses based on the test-tank data. As discussed in Annex C, test-tank data for external floating roofs were selected that most closely matched the conditions for the field-tank rim-seal systems. The data from these tests were used to predict expected field-tank losses as a function of the tank diameter raised to a variable exponent. The predicted losses were then plotted against varying values of the exponent. The exponents that resulted in the predicted losses being equivalent to the measured losses were read directly from these graphs. For the three field tests of EFRTs used as the primary database, within the accuracy of the measured results, an exponent of 1 was observed. Although a similar analysis of the other 13 field-tank tests[42] showed significantly more variability, it too supported an exponent of 1.

For IFRTs in which air movement is significantly reduced, a theoretical analysis[39] clearly indicated that rim-seal losses are directly proportional to the length of the rim seal and, therefore, that losses are directly proportional to the tank diameter. To further substantiate this result for IFRTs, measured losses from the 20-ft-diameter test tank[29] and a 100-ft-diameter field tank[22] were analyzed to compare directly the rim-seal area losses. This comparison confirmed that rim-seal losses are directly proportional to tank diameter.

8.2.2.4 Deck-Fitting Loss Factors

As described in Annex D, losses from various types and designs of deck fittings were directly measured[30], [31], [32], [33], [34] on a bench-scale test apparatus that used a wind tunnel to simulate the ambient wind speed at an EFRT site, and a zero mile per hour wind speed condition to simulate IFRT and domed EFRTs. Using the bench-test apparatus, losses were determined by measuring the loss of stock liquid weight over time. These data were analyzed to obtain the deck-fitting loss factors K_{fa}, K_{fb}, and m, for each fitting type.

For those fittings where an accessory penetrated a well cover (e.g. guidepole, support column, automatic gauge float, etc.), the tests were conducted with a gap of approximately $^1/_8$ in. between the accessory and the edge of the opening in the cover, unless the fitting description included a wiper gasket to seal that gap.

The loss factors are applicable to average ambient wind speeds from 0 mph to 15 mph, which are factored to the corresponding wind speed across the deck of the floating roof by applying the fitting wind-speed correction factor K_v[36] (and as discussed in Annex H).

Survey information from manufacturers was compiled to determine typical values for the number of each type of deck fitting generally installed, N_f, as a function of tank diameter.

To arrive at a total deck-fitting loss factor, F_f, for a given tank, deck-fitting loss factors K_{fa}, K_{fb}, and m can be combined either with information on the specific number of each deck-fitting type included in the tank under consideration or with typical N_f values.

8.2.2.5 Deck-seam Loss Factors

Losses from two general types of floating decks (decks with bolted seams and welded decks) were measured[29] in the test tank by sealing off all other sources of loss. The decks were of commercial design, in conditions representative of properly maintained decks. No losses were attributed to the welded deck, assuming generally recognized welding standards. Two bolted decks with different deck seam construction details were tested; one was a contact deck and the other was a noncontact deck. The losses measured from the two bolted decks were of the same order of magnitude when estimated on a loss per length of seam basis. The results were averaged to develop a general deck-seam loss factor, relative to seam length, K_d, for decks with bolted seams.

Typical deck-seam length factors, S_d, were estimated based on survey information of commonly used deck construction designs.

The approach used to analyze the bolted deck loss data is consistent with assuming that the deck losses are directly proportional to the length of the deck seams. (That is, the losses occur continuously or from discrete, localized points distributed along the entire length of the deck seam.) This assumption leads to the deck seam losses being proportional to the square of the deck diameter, since deck seam length increases as a function of the area of the deck. Because the deck diameter is only slightly smaller than the tank diameter, D, the deck area was assumed to be approximately proportional to tank diameter squared, D^2. To the extent that losses from some specific proprietary deck designs can originate from joints or seam details that are not proportional to deck seam length, this assumption can result in an over-estimate of the increase in deck losses with increasing tank size. Since an analysis of specific proprietary equipment is beyond the scope of this publication, this conservative assumption (potentially over-estimating deck-seam loss) was judged to be the most reasonable basis for determining one general loss factor for all bolted deck seams. See also Annex I.

8.2.2.6 Vapor Pressure Function

As detailed in Annex E, test-tank data[16] in which the only variable was stock true vapor pressure were analyzed to determine how the standing loss varies with vapor pressure P. Two proposed[44] functional relationships were tested by correlation analysis techniques. The functions were found to correlate about equally well with the data. However, one function becomes infinite as P approaches atmospheric pressure P_A, and the other does not. Therefore, the latter function for P^* (as defined in 4.2.3.2) was selected to determine the effect of stock true vapor pressure on standing loss.

8.2.2.7 Product Factor

A product factor K_C is included in the equation for standing loss to account for the effects of different types of stock liquid on evaporative loss. These effects (such as weathering) are in addition to those accounted for by consideration of differences in stock true vapor pressure and vapor molecular weight. Since the loss equation was developed primarily from tests of mixtures of normal octane and propane, the product factor quantifies the relative loss from a given stock type compared with the loss from mixtures of normal octane and propane. The product factor is effectively a crude oil loss estimate reduction factor because the product factor is 1.0 for all stocks other than crude oil.

Tests[24], [24], [26] were performed in the test tank to compare mixtures of normal octane and propane with both a midcontinent crude oil and gasoline. As a first approximation, it was assumed that the only differences would be the vapor pressure P and the molecular weight of the emitted vapors M_V. However, after the data were normalized for these factors, the losses from crude oil were observed to be consistently less than those from the mixtures of normal octane and propane at all wind speeds, whereas, the losses from gasoline were approximately equal to those from the mixtures of normal octane and propane.

As outlined in Annex F, an analysis of the crude oil and gasoline data resulted in a product factor of 0.4 for crude oil and a product factor of 1.0 for gasoline. In a separate study, test-tank loss data for single-component liquids were compared to loss data for the normal octane and propane mixtures, resulting in a product factor of 1.0 for single-component stocks.

8.2.2.8 Liquid Surface Temperature

The liquid surface temperature is used to determine the stock true vapor pressure. The true vapor pressure is used to determine the vapor pressure function (to which standing loss is directly proportional). The liquid surface temperature may be determined using the following methods, in order of decreasing accuracy:

a) The liquid surface temperature may be measured.

b) The liquid bulk temperature may be measured, and the liquid surface temperature estimated using Equation (14) from the liquid bulk temperature, average ambient temperature, and insolation.

c) The liquid bulk temperature may be estimated using Equation (18) from the average ambient temperature and tank surface solar absorptance; then the liquid surface temperature can be estimated from the liquid bulk temperature using method (b).

The liquid bulk temperature T_B is preferably obtained from actual measurements. The time required for the liquid bulk to achieve thermal equilibrium with ambient conditions is typically longer than the time product dwells in the tank. Equations to estimate liquid bulk temperature, however, are based on the assumption that the product is in thermal equilibrium. Therefore, it is highly preferable to use measured values for the liquid bulk temperature rather than calculated values. If measured values are unavailable and the product is in thermal equilibrium, T_B may be estimated using API *MPMS* Ch. 19.4, 3rd Edition, Appendix I or the following equation:

$$T_B = T_{AA} + (6\alpha - 1) \tag{18}$$

8.3 Working Loss

8.3.1 Working Loss Data

Tests[26] [27] were conducted to determine the amount of stock that clings to the exposed tank wall as stock is withdrawn from a tank. In these tests, a lightly rusted steel test plate was alternately raised out of and lowered into a liquid. Sections of a floating-roof rim seal were placed above the liquid surface so that they provided a wiping action against the steel test plate as it was withdrawn. Measurements were made of the change in liquid level after many withdrawal cycles. These data were analyzed to estimate clingage factors C_L for different stocks and tank-shell conditions. This analysis is discussed in more detail in Annex G.

8.3.2 Working Loss Estimate Development

In IFRTs with column-supported fixed roofs, the support columns provide additional surface area for stock clingage. Therefore, the working loss equation given in 4.3 includes a term that represents the sum of the tank shell and fixed-roof support column surface areas.

Annex A
(informative)

Development of Rim-Seal Loss Factors

A.1 Development Methodology

The rim-seal loss factors and equation introduced in the 2nd Edition of API 2517[47] did not allow for a rim-seal loss factor value other than 0 at a wind speed of 0 mph and were not considered to be valid at wind speeds below 2 mph. The equation had a wind-dependent rim-seal loss factor and a wind-dependent rim-seal loss exponent. The form of equation has been modified to add a zero-wind-speed rim-seal loss factor, K_{ra}, as shown in Equation (A.1):

$$K_r = K_{ra} + K_{rb} V^n \tag{A.1}$$

where

K_r is the rim-seal loss factor, in pound-moles per foot per year (lb-mol/ft-yr);

K_{ra} is the zero–wind-speed rim-seal loss factor, in pound-moles per foot per year (lb-mol/ft-yr);

K_{rb} is the wind-dependent rim-seal loss factor, in pound-moles per (miles per hour)^n per foot per year [lb-mol/(mph)^n-ft-yr];

V is the average ambient wind speed at the tank site, in miles per hour (mph);

n is the wind-dependent rim-seal loss exponent (dimensionless).

Test data from previous external floating-roof research[48], which are summarized in the 1981 documentation file for Appendix B of the 2nd Edition of API 2517, were evaluated in the context of Equation (11). Loss factor values were determined for the following cases, representing specific types of tank construction and types of primary rim seals.

a) Welded tanks with:

   1) mechanical-shoe primary seals,

   2) resilient-filled primary seals mounted with the rim seal in contact with the liquid (liquid mounted), and

   3) resilient-filled primary seals mounted so that a vapor space exists between the rim seal and the liquid surface (vapor mounted).

b) Riveted tanks with mechanical-shoe primary seals.

For each of these four tank-construction/primary-rim seal cases, three-rim-seal system configurations were included:

   a) primary seal only,

   b) primary seal plus shoe-mounted secondary seal (or a weather shield for a resilient-filled primary seal),

   c) primary seal plus rim-mounted secondary seal.

Two distinct computational procedures[43] were used, depending on the availability of information. In the first case, data were available for the specific combination of primary and secondary rim seal of interest for all gap sizes included in the analysis. In the second case, data were unavailable for the specific combination of primary and secondary seal of interest, so secondary seal emission reductions were estimated from analogous configurations. Procedures used for each case are outlined below.

For cases with data available for the combination of primary and secondary seal of interest, estimating equation coefficients (K_{ra}, K_{rb}, and n) were obtained using a three-step process. The first two steps generated coefficients for specific gap sizes, while the third step averaged across the gap sizes of interest. However, prior to the first step, the raw data from the documentation file[48] were modified by replacing emission rates for replicate tests at the same wind speed with the average emission rate for all replicates at that wind speed. The three steps used to obtain the final coefficient estimates are outlined below.

In the first step, values of S_{ra} (a coefficient analogous to the zero-wind-speed loss factor, K_{ra}, but in units of pounds per day) were determined for each series of tests. Previous internal floating-roof research[2] included testing at the 0-mph wind speed condition, but did not include any testing of mechanical-shoe seals. All common rim-seal systems were tested in previous external floating-roof research[48], but only at wind speeds ranging from 2.2 mph to 13.1 mph. To estimate values for the zero-wind-speed coefficient, S_{ra}, the data from the external floating-roof testing were regressed to 0 mph by an iterative process.

A starting trial value for S_{ra} was obtained by an exponential curve fit routine. Using that estimate of S_{ra}, net emission rates (E_{net}) were calculated for each tested wind speed by subtracting S_{ra} from the average of the measured emission rates at each tested wind speed. If the value of E_{net} obtained was less than zero, that test was eliminated from the analysis. A standard least squares regression routine was then used to fit a linear equation with the log transform of the net emission rate [$\log(E_{\text{net}})$] as the dependent variable and the log transform of the wind speed [$\log(V)$] as the independent variable. The estimate of S_{ra} was then changed iteratively, and the process was repeated. The trial value that yielded the best fit linear equation was assumed to be the best estimate of S_{ra}.

In the second step, the linear equation of the log-transformed data from Step 1 corresponding to the selected estimate of S_{ra} was expressed in the following form, where E_{net} and S_{rb} have units of pounds per day rather than pound-moles per foot per year:

$$\log(E_{\text{net}}) = \log(S_{rb}) + n\log(V) \tag{A.2}$$

Least squares regression was used to obtain estimates of n and $\log(S_{rb})$, which was then exponentiated to obtain an estimate of S_{rb} (analogous to K_{rb}, the wind-dependent loss factor).

In the third step, estimates of the percentage of tanks represented by each gap size used in Step 1 and Step 2 were used to generate a weighted average estimating equation for each rim-seal configuration (see the discussion in A.2 and A.3). For each gap size considered, the equations generated in Step 1 and Step 2 were used to estimate emission rates in pounds per day at wind speeds of 0 mph, 4 mph, and 10 mph. Percentage weights were then applied, based on assumed frequency of gap sizes in the field, in order to obtain average emission rates in pounds per day at each of these wind speeds. The value obtained for a wind speed of 0 mph was used as the estimate of S_{ra}. To obtain the estimates of n and S_{rb}, net emission rates were calculated by subtracting the estimate of S_{ra} from the weighted average emission rates at 4 mph and 10 mph. The net emission rates estimated at these two wind speeds were log transformed, and a linear equation was fit to the resulting two points to obtain estimates of n and $\log(S_{rb})$, which was exponentiated to obtain an estimate of S_{rb}. Finally, S_{ra} and S_{rb} were converted to K_{ra} and K_{rb}.

For six of the primary/secondary combinations of interest, no test data were available. However, test data were generally available for all primary seals of interest with no secondary seal and all secondary seals of interest applied in combination with at least one of the primary seals. Consequently, loss factors for the primary/secondary combinations without test data were developed by applying the reduction, or control efficiency, achieved by the secondary seal of interest applied in combination with a different type primary seal to the uncontrolled emissions from the primary seal of interest.

Two sets of rim-seal loss factors were developed for the different combinations of tank construction and rim-seal system. These two sets of rim-seal loss factors represent average-fitting and consistently tight-fitting rim-seal conditions. Their development is outlined in A.2 and A.3.

A.2 Development and Applicability of Average Rim-Seal Loss Factors

In many cases, but not all, losses were observed to increase as the tightness of fit of the rim seal against the tank shell decreased. This seal fit was characterized by the total area of the gap between the rim seal and the tank shell per foot of tank diameter. However, this measure of rim-seal tightness is not the only rim-seal condition that affects loss. Other conditions, such as relative location of the rim-seal gap, also affect loss, but these could not be quantified. Because of the effects of such randomly varying rim-seal conditions in field tanks, an explicit correlation between loss and area of the rim-seal gap will not exist. Therefore, to develop average rim-seal loss factors for each type of tank construction and rim-seal system described in A.1, the test-tank data selected for analysis included a wide range of rim-seal conditions marked by varying rim-seal gap areas and relative rim-seal gap locations.

In general, three categories of rim-seal gap areas were defined:

a) tight seals, with no gaps greater than $^{1}/_{8}$ in.;

b) small gap areas, which are commonly encountered in operating tanks;

c) large gap areas, which occur only infrequently.

For each type of tank construction and rim-seal system, all of the applicable loss data in each category were averaged together to determine representative factors for each category. To determine average factors for each type of tank construction and rim-seal system representative of a typical operating tank, the loss factors for each category were averaged. Categories were averaged by weighting according to the frequency with which each category occurs in operating tanks.

Field-tank gap measurement data[28] collected by an air regulatory agency were used to determine the frequency with which operating tanks exhibit specific rim-seal gap areas. Data from more than four hundred tank inspections were analyzed by tank construction and rim-seal system. These data were interpreted as an indication of the percentage of time that a typical operating tank will exhibit a specific gap area. Since operating tanks generally have gap areas that vary as the roof height changes, no one gap area is representative of an average tank. A typical tank is assumed to have a range of gap areas that corresponds to the distribution of gap areas determined from the tank inspection data.

The average rim-seal loss factors (see Table 1) are judged to be applicable to all typical operating tanks. These loss factors are based on distributions of rim-seal gap areas measured in operating tanks between 1976 and 1977. The difference in rim-seal loss factors between riveted and welded tanks with the same rim-seal system reflects the fact that the average rim-seal gap area in riveted tanks is greater than that in welded tanks. If future design or maintenance practice causes a significant change in gap area distributions, these average loss factors could be modified accordingly.

The average rim-seal loss factors developed are applicable to average ambient wind speeds from 0 mph to 15 mph.

A.3 Development and Applicability of Tight Rim-Seal Loss Factors

From the tank inspection data, rim-seal systems are tight (this is, have no gaps greater than $^{1}/_{8}$ in.) a significant percentage of the time (depending on tank construction and rim-seal system). Loss data from tests representing only a tight primary-seal condition were averaged to determine the rim-seal loss factors for tight primary-seal systems given in Table 1. Because the presence of small gaps in the primary seal below a tight secondary seal does not significantly influence loss, the rim-seal loss factors for tight secondary-seal systems given in Table 1 are based on data from both tight systems and those with small gaps in the primary seal under a tight secondary seal.

The tight rim-seal loss factors are applicable to welded tanks with rim-seal systems that remain consistently tight throughout the range of operating roof heights. No information is available on the extent to which it is possible to maintain consistently tight-fitting seals.

The tight rim-seal loss factors developed are applicable to average ambient wind speeds from 0 mph to 15 mph.

A.4 Database for Rim-Seal Loss Factors

Eighteen test-tank datasets[13] to [18] were used to develop the average and tight rim-seal loss factors for mechanical-shoe primary seals in welded tanks. In this case, the loss rate from primary seals did not vary with rim-seal gap area from tight-fitting seals to those with the rim-seal gap areas found approximately 90 % of the time. Twenty test-tank datasets[13] to [18] were used to develop the average and tight rim-seal loss factors for mechanical-shoe primary seals in riveted tanks. In addition to variable gap areas and relative gap locations, a wide range of variability in the tightness of the primary-seal fabric is represented by the selected tests of mechanical-shoe primary seals for both welded and riveted tanks.

Six test-tank datasets[19] were used to develop the loss factors for liquid-mounted resilient-filled primary seals, and eighteen test-tank datasets[20], [21] were used to develop the loss factors for vapor-mounted resilient-filled seals. The vapor-mounted rim-seal tests were conducted with a vertical vapor space of approximately 8 in. between the bottom of the rim seal and the stock liquid, representing the upper end of the range of rim vapor space sizes typical of vapor-mounted seals. Loss rates should decrease as this vapor space becomes smaller, approaching those from liquid-mounted seals. However, the effect of rim vapor space size on loss rates could not be quantified with currently available data.

A complete summary of the test conditions for the more than 100 test-tank datasets considered in the analysis of rim-seal loss factors is included in the documentation files for the 2nd Edition of API 2517[48] (Appendix B) and the 3rd Edition of API 2519[51] (Section B.3). The 1981 documentation file for API 2517[48], 2nd Edition, also includes graphs of loss rate versus wind speed for all the tests used to develop the rim-seal loss factors for each category. A summary of the field-tank inspection data is also included in the 1981 documentation file for API 2517[48], 2nd Edition.

Annex B
(informative)

Development of Rim-Seal Relationship Between Airflow Rate and Wind Speed

A test tank with a diameter of 20 ft was used to determine relative evaporative-loss levels. This test tank was fitted with an external floating roof (minus all roof fittings) and several different rim-seal systems. However, unlike an EFRT in the field, the test tank was covered to allow direct loss measurements. Air was blown into the test tank through a duct and exited through another duct 180° from the inlet. This permitted direct measurements of flow rate and concentration from which losses could be calculated. The airflow rate was varied to simulate varying wind speeds above an EFRT. To relate losses from the test tank to those expected from field tanks, it was necessary to develop a relationship between the test-tank airflow rate and the corresponding wind speed at a tank site.

The approach taken was to relate the measured[45] airflow-induced pressure differentials around the perimeter of the test tank's floating roof to wind-induced pressure differentials that had been measured in wind-tunnel tests[40], [41] and on an actual field tank[20], [21]. A review of these results showed that the patterns of pressure differentials obtained in the test tank were similar to those obtained in both the wind-tunnel and field tests. It was, therefore, concluded that wind effects on losses from EFRTs were adequately simulated in the test tank.

A series of tests was conducted in which the pressures at various positions around the perimeter of the floating roof were measured as a function of airflow rate. Using these data, a regression analysis was performed to relate the measured test-tank airflow rate to the corresponding wind speed at a tank site, as outlined below.

Wind speed is related to pressure differentials by the following equation:

$$V = \left[\frac{(P_1 - P_j)2g}{(C_{p1} - C_{pj})\gamma} \right]^{0.5} \tag{B.1}$$

where

- V is the wind speed;
- $P_1 - P_j$ is the differential pressure between Positions 1 and j around the perimeter of the floating roof;
- g is the acceleration due to gravity;
- $C_{p1} - C_{pj}$ is the difference in pressure coefficients between Positions 1 and j;
- γ is the specific weight of air.

A value of 1 for $C_{p1} - C_{pj}$ was determined from wind-tunnel and field tests[20], [21], [41].

Pressures, P_j, at varying circumferential positions, j, around the perimeter of the floating roof, relative to a reference pressure at the leeward position on the floating roof, P_1, were found to be related to the airflow rate, G, by the following equation:

$$P_1 - P_j = A_j G^b \tag{B.2}$$

where

- A_j is the position-dependent constant;

G is the airflow rate;

b is the airflow rate exponent.

Values for A_j and b were calculated by linear regression of $\log (P_1 - P_j)$ versus $\log G$.

Because the data analysis supported a value of 2 for b, Equation (B.1) and Equation (B.2) were combined to result in the following relationship between the test-tank airflow rate, G, and the corresponding wind speed, V, at a tank site:

$$V = B_j G \tag{B.3}$$

where B_j is the constant evaluated for the case where Position j is on the windward side of the roof.

Equation (B.3) was used to calculate the wind speed that corresponds to the test-tank airflow rate.

The wind-tunnel tests indicated that the pressure differentials did not vary significantly with the height of the roof in the tank. Since wind-induced losses are proportional to wind speed, and, thus, to the pressure differentials, these losses should not vary significantly with roof height.

The mathematical analysis and all supporting data used to develop the relationship between airflow rate and wind speed are in the documentation file for the 2nd Edition of API 2517[48] (Appendix A).

Annex C
(informative)

Development of Diameter Function

The API correlation for estimating evaporative losses from floating-roof tanks in the 1st Edition of API 2517[46] indicated that losses are proportional to diameter raised to the 1.5 power. However, more recent aerodynamic studies[49] of wind effects on tank losses concluded that the diameter exponent should be 1 (that is, that losses are directly proportional to tank diameter).

To determine an empirical value for the diameter exponent, test programs were conducted to measure evaporative losses from field tanks that varied from 35 ft to 152 ft in diameter. The 1977 to 1979 API field-test program is summarized (see bibliographic reference [50]).

Losses from the field tanks were determined by the density change method. Increases in stock bulk density were examined in two tanks tested by API[22] and one tank tested independently[23]. The increases in stock density were related to the decrease in stock volume (evaporative loss)[22], [24], [25], [26].

Field-tank rim-seal conditions were analyzed and compared with the test-tank database, as described in 8.2.2.3. Loss predictions for the field tanks were developed from the test-tank data. These predictions, which incorporated the properties of the stock and climatic conditions at the field tanks, were used to evaluate the influence of tank diameter on evaporative loss.

Field-tank losses were calculated as a function of a variable exponent of tank diameter. These calculated values were plotted to determine the relationship between loss and diameter exponent, as shown in Figure C.1. Measured losses from the field tests were then compared with the predicted losses. Based on this comparison, a diameter exponent of 1 was established for the loss equation.

Data from a floating-roof tank test program sponsored by the Western Oil and Gas Association (WOGA) in 1976[42] were evaluated in a similar manner. The WOGA tests involved 13 tanks in gasoline or volatile stock service, for which losses were measured with similar techniques. The WOGA program was the first in which sophisticated density-measurement instrumentation was used. Data scatter in this developmental program was higher than in the test programs discussed above. Wind speeds at the tank sites were not measured, and less information about the rim-seal conditions was obtained. Nevertheless, the average diameter exponent developed from the WOGA results supports the conclusion that the diameter exponent in the loss equation is 1.

The mathematical analysis and all supporting data used to develop the diameter exponent are in the documentation file for the 2nd Edition of API 2517[48] (Appendix D).

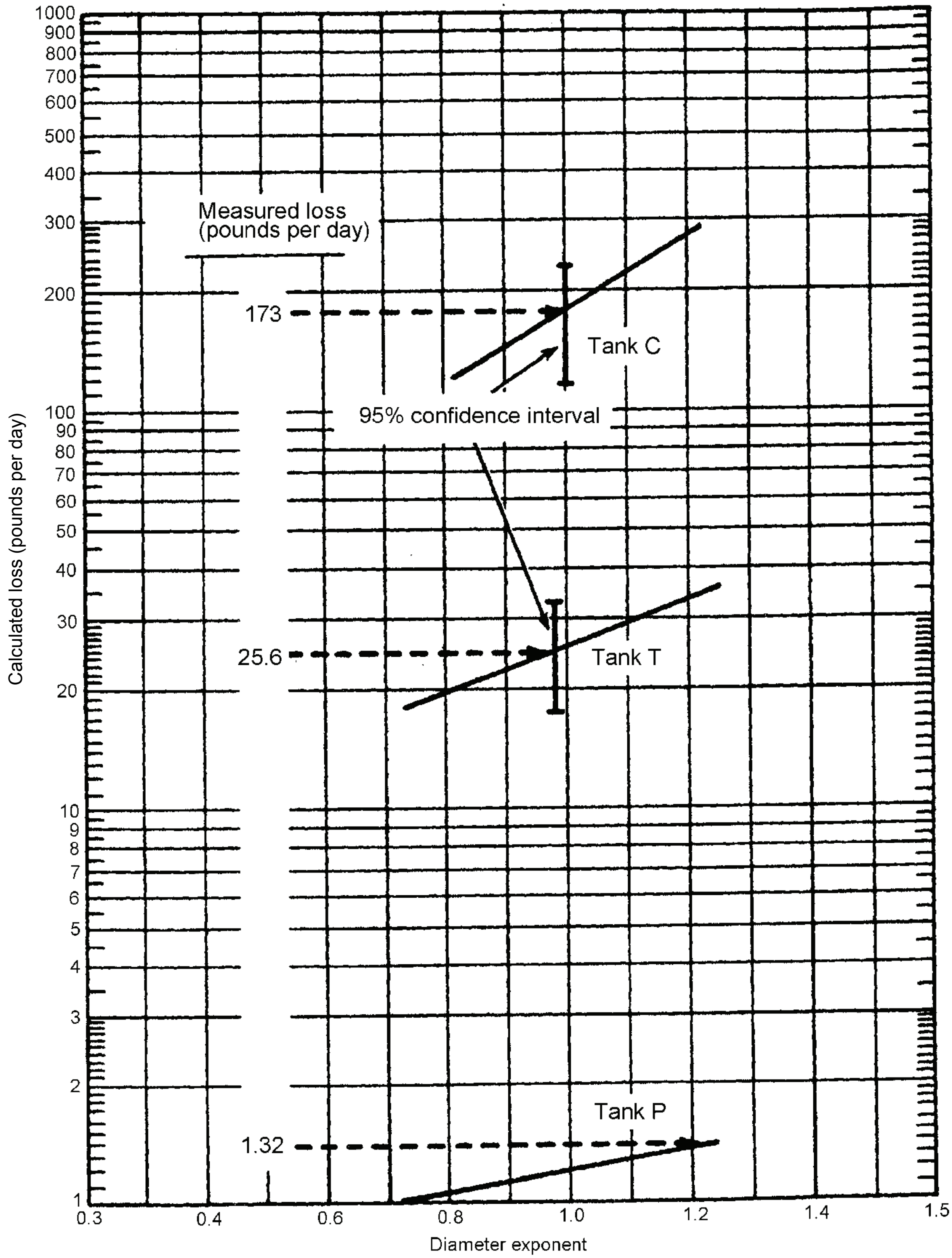

Figure C.1—Calculated Losses as a Function of Diameter Exponent

Annex D
(informative)

Development of Deck-Fitting Loss Factors

D.1 Development Methodology

The evaporative loss from the deck fittings on a floating roof is the sum of the losses from each type of deck fitting. The loss factor for each type of deck fitting can be estimated as follows:

$$K_f = K_{fa} + K_{fb} V^m \quad \text{(D.1)}$$

where

K_f is the deck-fitting loss factor, in pound-moles per year (lb-mol/yr);

K_{fa} is the zero-wind-speed deck-fitting loss factor, in pound-moles per year (lb-mol/yr);

K_{fb} is the wind-dependent deck-fitting loss factor, in pound-moles per (miles per hour)^m per year [lb-mol/(mph)^m-yr];

V is the average wind speed in the wind tunnel, in miles per hour (mph);

m is the wind-dependent deck-fitting loss exponent (dimensionless).

The estimating equation coefficients (K_{fa}, K_{fb}, and m) were obtained[11] by fitting the curve described by Equation (D.1) to the test data[32], [33], [34] for each deck fitting. The curve-fitting methodology is outlined below.

Values for the zero-wind–speed loss factor, K_{fa}, were determined from test results for specific deck fittings. Net emission rates (E_{net}) were calculated at each of the positive wind speeds tested by subtracting K_{fa} from the measured emission rate. A standard least squares regression routine was then used to fit a linear equation with the log transform of the net emission rate [$\log(E_{\text{net}})$] as the dependent variable and the log transform of the wind speed [$\log(V)$] as the independent variable.

The linear equation of the log-transformed data was expressed in the following form, where E_{net} has units of pounds-moles per year:

$$\log(E_{\text{net}}) = \log(K_{fb}) + m \log(V) \quad \text{(D.2)}$$

The least squares regression generated estimates of m and $\log(K_{fb})$, which was then exponentiated to obtain an estimate of K_{fb}.

The various slotted guidepole configurations were each tested at multiple orientations of the slots to the direction of the wind. The data analyses gave equal weighting to 0°, 45°, and 90° orientations of the slots with respect to the wind direction.

D.2 Database for Deck-Fitting Loss Factors

Experimental data[30], [32], [33], [34], [51] from three API testing programs were used to determine deck-fitting loss factors. Some loss factor data at 0 mph were obtained from a 1982 testing program[29] from which loss factors were developed for the 3rd Edition of API 2519[2]. A limited selection of internal floating-roof deck fittings was included in this testing program.

The other two testing programs[30], [32], [33], [34] used a wind tunnel to generate positive wind speeds across a deck fitting. Four deck fittings could be tested simultaneously in this facility. Each deck fitting was mounted on an independent product reservoir that rested on a digital platform scale. The top of each deck fitting extended into the wind tunnel. Air passed over the deck fitting at a known velocity to simulate the wind on an actual external floating roof. Evaporation loss was measured by a weight-change method, using a computer-controlled data acquisition system that would automatically record the weight of each test fixture, the product temperature, the air temperature, and the wind speed at specified time intervals.

During earlier wind-tunnel testing programs[30], the wind tunnel was operated at wind speeds of 0 mph, 5 mph, and 14 mph. The later testing program[32], [33], [34] measured evaporative losses at three positive wind speeds (4.3 mph, 8.5 mph, and 11.9 mph) in the wind tunnel, and conducted separate 0 mph tests in a facility using similar test fixtures and weight-change methodology, but having only low levels of air movement that were required to prevent the build-up of hydrocarbons vapors.

The wind speeds measured in the wind tunnel were assumed to represent the wind speed at a particular deck fitting on the floating roof, which is typically lower than the ambient wind speed at the tank site. The correction from average ambient wind speed to wind speed on the floating-roof deck is represented by the wind speed coefficient, K_v, defined in 4.2.2.3.

Both single-component hydrocarbons (n-hexane) and mixtures of propane and n-octane were tested during the earlier wind tunnel testing program. The data did not show a weathering effect for mixtures. Only n-hexane was used in the later wind tunnel testing program.

D.3 Deck Fittings Tested

The deck fittings tested in the latest testing program[32], [33], [34] were chosen as being representative of the most common deck fittings on existing EFRTs. Where possible, data from this testing program were used, in which the following deck fittings were tested.

a) An 8-in.-diameter, Schedule 40 slotted guidepole in a 21-in.-diameter well. Thirteen different control scenarios were tested having various combinations of well gaskets, floats, float wipers, pole wipers, and pole sleeves.

b) An 8-in.-diameter, Schedule 40 unslotted guidepole in a 21-in.-diameter well. Five different control scenarios were tested having various combinations of well gaskets, pole wipers, and pole sleeves.

c) A 24-in.-diameter access hatch with an unbolted cover, with and without a well gasket.

d) A gauge float in a 20-in.-diameter well with an unbolted cover, with and without a well gasket.

e) An 8-in.-diameter gauge hatch/sample port with and without a lid gasket.

f) A vacuum breaker in a 10-in.-diameter well, with and without a well gasket.

g) A 3-in.-diameter deck drain, with and without an insert covering 90 % of the drain opening.

h) A 3-in.-diameter, Schedule 40 pipe deck leg in a 4-in.-diameter, Schedule 40 pipe sleeve. Testing was conducted with both 30-in. and 48-in. long sleeves having no gasket or sock (boot). Two additional test series were run with the 30-in. long sleeve; one in which it was equipped with a gasket and another in which it was equipped with a sock.

D.4 Analysis of the Deck-Fitting Loss Data

The computer-controlled data acquisition system recorded the test data from the wind tunnel. The test results were documented in the form of plots of product loss vs. net time. Least-square regressions were performed on all the test data to determine the slope of the product loss data plots for each deck fitting at the beginning of each test. Whenever possible, the loss data were fitted to a first-order polynomial, and the loss rate was determined by evaluating the first derivative of the polynomial. In several of the tests, however, the loss rate changed significantly as the test progressed. In these cases, the test data were fitted to a second-order polynomial and the initial loss rate was determined by evaluating the first derivative of the polynomial at the beginning of the test. The second-order fit was used for all tests in which the liquid level changed significantly during the test. Only the initial loss rate was used to calculate the deck-fitting loss factor for a test.

For each deck-fitting test, the deck-fitting loss factor, K_f, was determined from the initial loss rate (in pound-moles per year) and the product vapor pressure.

These normalized test data represent the bulk of the data used to determine the deck-fitting loss factors. However, some additional data were obtained from the test data used to write API 2517[1] and API 2519[2]. These testing programs[29], [30] used similar testing methods, but only selected deck-fitting scenarios were tested. Loss factors for other specific deck fittings were then extrapolated from the loss factors of the tested fittings.

With this information, a table of deck-fitting loss factors of the type used in Equation (D.1) was developed.

The loss factors developed are applicable to average wind speeds from 0 mph to 15 mph, which is the same range applicable to the rim-seal loss factors described in Annex A.

The mathematical analysis and all supporting data used to develop the deck-fitting loss factors are in the documentation files for API 2517[52] and API 2519[51].

D.5 Algorithm for Uncontrolled IFRT/CFRT Deck Fittings

An algorithm was developed for estimating loss factors for uncontrolled deck fittings at the 0 mph wind speed condition. The premise for this algorithm is that the deck-fitting loss factor may be satisfactorily determined as a function of the height of the vapor space and the area of the liquid surface within the deck fitting, as long as sufficient pathways for vapor loss are present. For a given height of vapor space, the loss factor may be expressed solely as a function of the liquid surface area, in the following form:

$$K_{fai} = C_f \left(A_{fi} \right)^p \tag{D.3}$$

where

K_{fai} is the zero-wind-speed loss factor for a particular type of deck fitting, in pound-moles per year (lb-mol/yr);

C_f is the a correlation coefficient, in pound-moles per (square inch)^p per year [lb-mol/(in.^{2})^p-yr];

A_{fi} is the liquid surface area within a particular type of deck fitting, in square inches (in.^{2});

p is the a correlation exponent, (dimensionless).

Deck fittings for external-type floating roofs were tested with the top of the deck fitting well or leg sleeve positioned 18 in. above the liquid surface in the 1993 and 1995 API studies. The 1982 study of deck fittings for internal-type floating roofs included test assemblies with varying heights of vapor space in the deck-fitting well or leg sleeve, depending upon the type of deck fitting being tested. It appears, from a review of these test results, that all uncontrolled deck fittings with a vapor space height equal to 12 in. or greater can be characterized by a single algorithm, for the 0 mph wind speed condition.

The deck fittings selected for inclusion in the data regression, then, were those uncontrolled configurations with open pathways for vapor loss that had a height of vapor space equal to at least 12 in. The deck fittings selected, and the loss factor for each, are summarized in Table D.1. The loss factor in each case was determined from the results of testing that particular deck-fitting configuration. The liquid surface area is the area inside the deck-fitting well or leg sleeve, less any area occupied by an obstruction in the deck-fitting well or leg sleeve (such as a fixed-roof support column, unslotted guidepole, guidepole float, or deck support leg).

Equation (D.3) was fit to the data by using a standard least-squares regression routine on a log-log scale, which required that the equation first be transformed from an exponential to a linear form. Taking the log of each side of the equation yields the following:

$$\log (K_{fai}) = \log(C_f (A_{fi})^p) \tag{D.4}$$

This may be expressed as:

$$\log(K_{fai}) = \log(C_f) + p\log(A_{fi}) \tag{D.5}$$

A least-squares regression was used to fit the linear curve of Equation (D.5) to the log-transformed emission factor and liquid surface area data. The slope of the resulting line was taken as the exponent p, and the y-intercept was taken as the value of $\log(C_f)$. The coefficient C_f was then obtained from Equation (D.6).

$$C_f = 10^{[\log(C_f)]} \tag{D.6}$$

The regression of the log-transformed data yielded a value for the correlation coefficient C_f of 0.27 and a value for the correlation exponent p of 0.86, resulting in the following equation:

$$K_{fai} = 0.27(A_{fi})^{0.86} \tag{D.7}$$

The suitability of the model represented by Equation (D.7) was evaluated by the R-squared coefficient of determination, which is a measure of the fit of the linear regression to the data. The R-squared coefficient represents the proportion of variation in the data that is explained by the model. The regression of the log-transformed data had an R-squared correlation of 0.92, which indicates that the model explains 92 % of the variation in the data. In other words, the model fit the data extraordinarily well.

Table D.1—Summary of Deck Fittings Selected for Data Regression, and Associated Loss Factors for Each

API Test No. and Year of Report	Deck-fitting Description	Control Status	Liquid Surface Area A_f (in.^{2})	Vapor Space Height in the Well	Loss Factor, K_{fa} (lb-mol/yr)
13 (1982)	Access hatch	⅛ in. gap all around lid	398	12 in.	54.2
8 (1982)	Column, built-up	½ in. gap all around column	391	12 in.	52.3
4 (1982)	Slotted guidepole (8 in.)	uncontrolled	389	12 in.	45.3
1 (1993)	Slotted guidepole (8 in.)	uncontrolled	346	18 in.	45.5
25 (1993)	Slotted guidepole (8 in.)	uncontrolled	346	18 in.	40.6
3 (1993)	Slotted guidepole (8 in.)	float, no pole sleeve or wiper	288	18 in.	35.9
26 (1993)	Slotted guidepole (8 in.)	float, no pole sleeve or wiper	288	18 in.	25.6
18 (1993)	Unslotted guidepole (8 in.)	uncontrolled	288	18 in.	31.2
2 (1993)	Slotted guidepole (8 in.)	pole sleeve and gasket, no float	58	18 in.	16.4
31 (1995)	Slotted guidepole (8 in.)	pole sleeve and gasket, no float	58	18 in.	4.9
5 (1993)	Deck leg, pontoon (3 in.)	uncontrolled	10	18 in.	2.0

D.6 Emission Factors for a Ladder/Guidepole Combination

The net liquid surface area within a well or sleeve is the total cross-sectional area less the area occupied by the ladder. Ladder sleeve dimensions vary with the size of the ladder components and the manufacturer of the sleeve, but one design uses the dimensions shown in Figure 20, which would result in a total net liquid surface area within the sleeve of 229 in.^{2}, as tabulated below. This compares to a net liquid surface area of 950 in.^{2} for a 36 in. diameter (or a 20 in. by 51 in. rectangular) well.

	in.	in.	Area (in.^{2})
Net area around unslotted leg	A = 5.1875[a]	B = 4.3125[a]	26.1
Area of slot for ladder rungs	C = 5[a]	D = 23.625[a]	118.1
Area for slotted leg	E = 5.1875[a]		84.5
Total net area (in.^{2})			229
[a] See Figure 20 for dimensions A, B, C, D and E.			

The resulting emission factor for the ladder sleeve, from the algorithm for uncontrolled deck fittings [Equation (D.7)], is estimated as:

$$K_{fai} = 0.27(229)^{0.86}$$

$$K_{fai} = 29 \text{ lb-mole/yr}$$

The reduction in the emission factor, as illustrated in the graph shown in Figure D.1 below, is from nearly 100 lb-mol/yr to just under 30 lb-mol/yr.

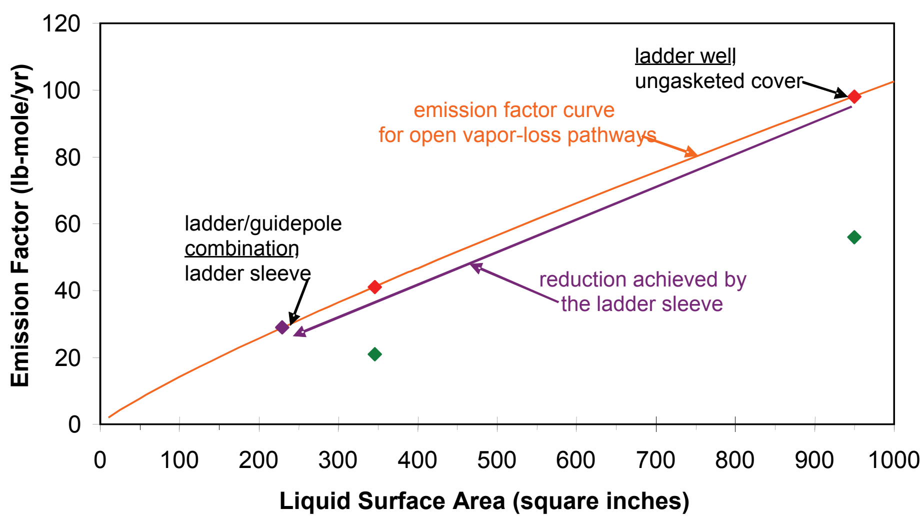

Figure D.1—IFRT Deck Fitting Emission Factors – Effect of Ladder Sleeve on Emission Reduction

The reduction in emissions illustrated for the ladder/guidepole combination is based strictly on the reduction in contributing liquid surface area, and does not take any credit for the further reduction that can be achieved by the use of wiper gaskets around the ladder. This, then, would be a conservative estimate of the emissions that escape past an IFRT ladder/guidepole combination equipped with a ladder sleeve. However, in addition to the emissions associated with the ladder/guidepole combination itself, there would be a contribution to emissions from the well area outside the ladder sleeve.

The well area outside the ladder sleeve is isolated from the emissions paths at the ladder by the ladder sleeve, but there would still be potential for emissions from this area to escape past the edge of the deck cover – in the same manner as for an unbolted access hatch lid. This additional contribution to emissions, then, can be modeled as an access hatch.

Overall emission factors for ladder sleeves can then be compiled, as shown in Table D.2:

Table D.2—Emission Factors for IFRT Ladder Sleeves

Control Status		Emission Factor
Ladder sleeve (and ungasketed cover)	29 + 36 =	65 lb-mole/yr
Ladder sleeve (and gasketed cover)	29 + 31 =	60 lb-mole/yr

The ladder/guidepole combination further reduces emissions by eliminating the need for a separate deck fitting for gauging or sampling. An IFRT with a standard ladder (i.e. one that does not have one leg serving as a slotted guidepole) would need either a separate slotted guidepole or a separate sample well. Table D.3 compares the emission factor for a ladder/guidepole combination, equipped with a ladder sleeve, to the sum of the emission factors for a standard ladder and a separate deck fitting for gauging or sampling.

The case of the ladder and a separate slotted guidepole assumes a gasketed sliding cover for the ladder well and a deck cover gasket, pole wiper, and pole float for the guidepole. The case of the ladder and a separate sample well assumes a gasketed sliding cover for the ladder well and a slit fabric seal for the sample well.

Table D.3—IFRT Emission Factor Comparison for a Ladder/Guidepole Combination

Deck Fittings		Emission Factor
Ladder + Slotted Guidepole	56 + 21 =	77 lb-mole/yr
Ladder + Sample Well	56 + 12 =	68 lb-mole/yr
Ladder/Guidepole combination with ladder sleeve and gasketed cover	29 + 31 =	60 lb-mole/yr

It is evident that a ladder/guidepole combination, equipped with a ladder sleeve, would have lower emissions than a standard ladder with a separate deck fitting for gauging or sampling, each equipped with gasketed covers.

Annex E
(informative)

Development of Vapor Pressure Function

In the 1st Edition of API 2517[46], the evaporative-loss correlation included a vapor pressure function in the form of the following empirical relationship:

$$P' = \left[\frac{P}{14.7 - P}\right]^{0.7} = \left[\frac{P/14.7}{1-(P/14.7)}\right]^{0.7} \tag{E.1}$$

where P is the true vapor pressure, in pounds per square inch absolute (psia).

This function has the undesirable property that when the stock true vapor pressure approaches 14.7 psia, the evaporative-loss rate becomes infinite. Therefore, a new vapor pressure function was derived that approaches a finite value as the true vapor pressure approaches atmospheric pressure.

The following vapor pressure relationship was derived[44] based on theoretical considerations:

$$P^* = \frac{P/P_a}{\left\{1+\left[1-(P/P_a)\right]^{0.5}\right\}^2} \tag{E.2}$$

where

P is the true vapor pressure, in pounds per square inch absolute (psia);

P_a is the atmospheric pressure, in pounds per square inch absolute (psia).

This vapor pressure function results in a finite evaporative-loss rate as the true vapor pressure approaches atmospheric pressure. Therefore, this function is a more appropriate one to use in predicting evaporative loss.

To determine the effects of the P^* relationship, a series of tests[16] were performed in which only the stock true vapor pressure was varied. During this series of tests, the stock was a mixture of propane and n-octane in which the propane content was varied to change the product vapor pressure from 0.75 psia to 9.25 psia. Test results were plotted as loss rate versus wind speed for each test and clearly showed increasing loss rate with increasing vapor pressure.

To choose the more appropriate vapor pressure function, the test results were normalized with respect to each vapor pressure function. Curves for the loss functions vs. wind speed were developed.

The evaporative-loss equation can be written as follows:

$$E = K_s M_v D \overline{P} V^n \tag{E.3}$$

where $\overline{P}$ = some function of vapor pressure.

To normalize for vapor pressure (and molecular weight), the equation can be rewritten as follows:

$$\frac{E}{M_v \overline{P}} = KV^n \tag{E.4}$$

where K is the constant equal to $K_s\, D$.

To evaluate a given vapor pressure function, the function can be substituted into Equation (E.4) by plotting $\log(E/M_v \overline{P})$ versus $\log\ V$, the data can be analyzed with a linear regression technique to determine the values of K and n that yield the best-fitting curve. The correlation coefficient calculated for each curve can then be used to evaluate how well the vapor pressure function accounts for changes in loss with varying vapor pressure.

Such an analysis was done for both vapor pressure functions, P' and P^*. It was found that both functions were approximately equally good predictors within the range 2.50 psia to 9.25 psia. No tests were made at higher vapor pressures. One test was made below this range, at 0.75 psia; neither function predicted the results of this test as accurately as it predicted the results of the other tests.

It was concluded that the theoretically derived vapor pressure function, P^* [Equation (E.2)], is the most appropriate function to use in the evaporative-loss equation, since it approaches a finite value as P approaches P_a. This function is judged to be applicable for non-boiling stocks down to a true vapor pressure of approximately 1.5 psia.

The mathematical analysis and all supporting data used to select the vapor pressure function are in the documentation files for the 2nd Edition of API 2517[48] (Appendix C) and the 3rd Edition of API 2519[51] (Section B.1).

Annex F
(informative)

Development of Product Factors

F.1 General

The test-tank data used to determine relative losses were obtained with mixtures of propane and n-octane, using direct measurement of vapor losses. To apply these results to refined products, such as gasolines, and to crude oil stocks, it was necessary to relate direct measurements from gasoline and crude oil to the mixtures of propane and n-octane under the same rim-seal configuration and wind-speed conditions. It was expected that after the measurements were normalized for differences in true vapor pressure and vapor molecular weight, these different stocks would have the same loss. However, differences in losses were observed even after this normalization. Therefore, a product factor K_C was needed in the loss equation to account for this observed difference in losses from one stock to another.

F.2 Theoretical Considerations

Crude oil losses were significantly lower than the losses from the mixtures of propane and n-octane under the same conditions of rim-seal configuration and wind speed. This difference was attributed to mass transfer effects that would occur when the evaporation was taking place under nonequilibrium conditions. If the rate at which evaporation occurs exceeds the rate at which the evaporating light ends migrate from the liquid bulk to the liquid surface, the evaporation is occurring under a nonequilibrium condition. The migration rate of the light ends depends strongly on the viscosity of the liquid; that is, as stock viscosity increases, migration rate decreases, promoting nonequilibrium conditions. Therefore, under the same conditions, as a stock's viscosity increases compared with that of mixtures of propane and n-octane, the loss will be less.

F.3 Product Factor

Evaporative-loss data for crude oil and mixtures of propane and n-octane at varying wind speeds and three different rim-seal configurations were compared to quantify a crude oil product factor[26]. The data were first analyzed as described in Annex B and the documentation files for the 2nd Edition of API 2517[48] (Appendix E) and the 3rd Edition of API 2519[51] (Section B.2). After the data were normalized for vapor pressure and vapor molecular weight, the average ratios of losses from crude oil to losses from mixtures of propane and n-octane were calculated. For rim-seal systems tested with only a primary seal, the average ratio was approximately 0.3. For rim-seal systems that included a rim-mounted secondary seal, the ratio was approximately 0.6, although the absolute magnitude of the crude oil losses was lower.

The increase in the product factor when a secondary seal was present is consistent with a reduced loss rate (that is, more nearly equilibrium conditions) caused by the secondary seal. However, more data are necessary to confirm that these factors are generally applicable. By averaging all the data together, an average product factor of 0.4 was determined. Because of the limited database, it was judged that 0.4 is the most appropriate product factor for all tanks used to store crude oil, regardless of the tank rim-seal system.

The product factor is judged to be conservative for crude oils in general, since a relatively light crude oil was tested and heavier crude oils would have lower product factors.

The 1st Edition of API 2518[6] on losses from fixed-roof tanks included a product factor of 0.58 for crude oil losses compared with gasoline losses. Although the data on which this factor is based are not directly comparable with data for floating-roof tanks, they tend to support the product factor discussed above. Also, a theoretical determination[26] of the expected product factor for crude oil resulted in an estimate of 0.5, which also supports the test results.

F.4 Gasoline Factor

Evaporative-loss data for gasoline were also compared with the loss data for mixtures of propane and n-octane[24]. These data were available only for a single rim-seal condition at a single wind speed. By a similar analysis, a ratio of losses from gasoline to losses from mixtures of propane and n-octane of approximately 0.9 was calculated. However, because of the similarity in viscosity between gasoline and mixtures of propane and n-octane and the limited loss data available for comparison, a product factor of 1.0 was judged to be reasonable and conservative for predicting gasoline losses. (That is, such calculated losses will be higher than losses calculated using a factor of 0.9.)

The mathematical analysis and all supporting data used to develop the product factors are in the documentation files for the 2nd Edition of API 2517[48] (Appendix E) and the 3rd Edition of API 2519[51] (Section B.2).

Annex G
(informative)

Development of Clingage Factors

G.1 General

A number of shell-wetting tests were performed to estimate the amount of stock remaining on the tank shell as the floating roof descends while the tank is emptied. In these tests, a steel test plate was immersed in stock and then slowly withdrawn past sections of rim seal to simulate roof travel inside a tank.

A container was filled with a known volume of the test liquid. The test plate was slowly pulled out of the liquid between a pair of resilient-foam-filled seals 2 ft in length at a rate roughly equivalent to that at which a tank would be emptied. The plate was then reimmersed after most of the liquid had evaporated, and the remaining volume of liquid was determined. Enough tests were made to determine an accurate volume change, from which the clingage factor C_L in bbl/1000 ft^2 was calculated.

A separate series of tests was conducted to determine the evaporation that would have occurred without movement of the test plate, so that the results could be adjusted to represent only the withdrawal loss due to stock clingage to the test plate.

G.2 Gasoline Tests

Four shell-wetting tests[27] were conducted with n-octane stock, which has clingage characteristics representative of those of gasoline. A lightly rusted steel plate was used, and the seal position was varied. The resulting clingage factors ranged from 0.0010 bbl/1000 ft^2 to 0.0019 bbl/1000 ft^2, with an average of approximately 0.0015 bbl/1000 ft^2. The test results are considered conservative, since rim-seal pressure was not introduced to produce a wiping action on the steel plate.

G.3 Crude Oil Tests

Five shell-wetting tests[26] were conducted with a medium-volatility crude oil. Again, a lightly rusted steel plate was used, and the seal position was varied. The resulting clingage factors ranged from 0.0032 bbl/1000 ft^2 to 0.0072 bbl/1000 ft^2, with an average of approximately 0.0060 bbl/1000 ft^2.

G.4 Other Shell Conditions

Clingage factors for dense rust were determined by multiplying the values for light rust by a factor of 5. This factor is based on data referred to in the 1st Edition of API 2517[46]. This publication also referred to data that indicated that gunite-lined tanks have a clingage factor 100 times greater than the factor for lightly rusted steel. The resulting clingage factors are summarized in Table 7.

Annex H
(informative)

Development of Fitting Wind-Speed Correction Factor

H.1 Mathematical Development of Fitting Wind-Speed Correction Factor

Evaporative loss from EFRTs has been shown to be wind dependent. The floating roof of an EFRT is partially shielded from the effects of ambient wind by the shell of the tank. A fitting wind-speed correction factor, K_v, has been added to the deck-fitting loss equation to account for the reduction in wind speed across the floating roof as compared to the ambient wind speed. This addition results in the following form of the deck-fitting loss estimating equation:

$$K_f = K_{fa} + K_{fb}\,(K_v V)^m \qquad \text{(H.1)}$$

where

K_f is the deck-fitting loss factor, in pound-moles per year (lb-mol/yr);

K_{fa} is the zero-wind-speed deck-fitting loss factor, in pound-moles per year (lb-mol/yr);

K_{fb} is the wind-dependent deck-fitting loss factor, in pound-moles per (miles per hour)^m per year [lb-mol/(mph)^m-yr];

K_v is the fitting wind-speed correction factor, (dimensionless);

V is the average ambient wind speed at the tank site, in miles per hour (mph);

m is the wind-dependent deck-fitting loss exponent (dimensionless).

A value for the fitting wind-speed correction factor, K_v, was developed from wind tunnel testing, an industry survey of typical floating-roof positions (that is, variations over time of the product level in actual storage tanks) and an evaluation of field measurements of wind speed on a floating roof.

H.2 Database for Fitting Wind-Speed Correction Factor

A wind-tunnel testing program[35] modeled EFRTs of 48 ft, 100 ft, and 200 ft in diameter, with the floating roof positioned at three different heights in each tank. Average horizontal wind speeds were calculated for each floating-roof height range at 28 locations across each floating-roof deck. The floating-roof heights chosen were grouped to result in three ranges of floating-roof height as follows:

$$0.35 \le R/H \le 0.75$$

$$0.80 \le R/H \le 0.90$$

$$R/H = 1.0$$

(The ratio R/H is the ratio of the floating-roof height to the tank-shell height.)

A survey[36] of product levels in EFRTs was conducted in order to develop a frequency distribution for the position of the floating roof. Forty tanks were evaluated based on twelve consecutive monthly records of liquid level.

Field data[36] were also used in the development of a fitting wind-speed correction factor. Measurements of wind speed were taken at two EFRTs at a petroleum refinery over an eleven-month period. Site wind speed was measured at a platform located at the top of the shell of one of the tanks. Wind speed across the floating roof of each tank was measured at two locations on the deck, one near the perimeter and one near the center of the deck. Both horizontal and vertical wind speed were measured. Approximately 30 readings were taken per day. Five months worth of data from one of these tanks were evaluated which, after adjusting for interruptions in the field measurements, resulted in a database derived from 142 days of measurements.

H.3 Analysis of the Fitting Wind-Speed Correction Factor Data

The wind-tunnel testing program[35] concluded that a single factor could reasonably be used to account for the reduction in wind speeds for all areas of the floating roof, at all roof heights and tank diameters. This factor was determined by calculating separate correction factors for each of the roof height ranges and then calculating a weighted average of these three factors based on an assumed distribution of time that the floating roof would spend in each height range. The distribution was based on a complete cycle of a floating roof, where the tank begins empty, rises through each height range, and then empties back through each range. This assumption results in the following distribution.

R/H Range	Frequency
$0.35 \le R/H \le 0.75$	40 %
$0.80 \le R/H \le 0.90$	40 %
$R/H = 1.0$	20 %

The wind-tunnel testing program determined that the wind speed on the floating roof is about 0.4 times the ambient site wind speed in the first two height ranges, but increases to about 0.7 times the ambient at the third roof height. Although the third roof height (R/H = 1.0) is not a position that occurs in the normal operation of storage tanks, it was conservatively included in the calculation of the weighted average correction factor. A value of 0.52 was calculated for the single fitting wind-speed correction factor.

The frequency distribution assumed in the wind-tunnel testing program was compared to that resulting from a survey[36] of EFRT liquid levels. The comparison is shown in the following table.

R/H Range	Assumed Frequency	Survey Frequency
$0.35 \le R/H \le 0.75$	40 %	77.7 %
$0.80 \le R/H \le 0.90$	40 %	15.6 %
$R/H = 1.0$	20 %	6.7 %

While the weighted average single factor had assumed the floating roof to be at the top of the tank shell 20 % of the time, in the survey it was found to be in the top 10 % of the shell height only 6.7 % of the time. The distribution assumed in the wind-tunnel test study was, therefore, conservative compared to the distribution determined from the survey.

The weighted average single factor was also compared to field data[36]. Daily average wind speeds were determined from the approximately 30 readings per day at each of the two locations on the floating roof, as well as at the platform. The wind speeds were summed for each measurement location and the ratio of floating roof to ambient wind speed was calculated for the two deck locations. The resulting ratios were 0.45 for the outer area of the deck and 0.53 for the inner area. The resulting average, 0.49, corresponded well with the value of 0.52 calculated for the weighted average single factor from the wind-tunnel test program.

H.4 Adjustment of the Fitting Wind-speed Correction Factor for Turbulence

The data analysis for the development of a weighted average single factor considered only the horizontal component of the wind speed, in that the deck-fitting loss factor development was based on horizontal wind flow in a wind tunnel. Although the affect of turbulence on evaporative loss from deck fittings is unknown, an increase in turbulence can cause an increase in evaporative loss.

In that the field study measured both horizontal and vertical wind speed vectors, this data was used to add a vertical component to the fitting wind-speed correction factor. A vector addition was performed[37] on the horizontal and vertical components of the wind speed measured on the floating deck to determine a total deck wind-speed vector for each daily average at both inner and outer locations. The ratio of deck to ambient wind speed was calculated for each data point and measurement location. An average ratio was then determined for the inner and the outer locations. These two ratios were then averaged and an average fitting wind-speed correction factor of 0.69 was calculated.

The field data indicate that a vertical wind-speed component is present at the deck surface on an EFRT. In the absence of data to evaluate the effect of a vertical wind-speed component on evaporative loss, the result of the vector addition was used to determine a value of 0.7 for the fitting wind-speed correction factor.

Annex I
(informative)

Development of Deck-Seam Loss Factors

I.1 Mathematical Development

The evaporative-loss factor, F_d, for the deck seams on an internal floating roof can be estimated as follows:

$$F_d = kS_dA \quad \text{(I.1)}$$

where

F_d is the total deck-seam loss factor, in pound-moles per year (lb-mol/yr);

k is the loss rate per unit length of deck seam, in pound-moles per foot per year (lb-mol/ft-yr);

S_d is the deck-seam length factor, in feet per square foot (ft/ft^2);

A is the area of the floating-roof deck, in square feet (ft^2).

Substituting $\pi D^2/4$ for A, where D is the diameter of the tank, in feet (ft), yields:

$$F_d = kS_d\pi D^2/4 \quad \text{(I.2)}$$

Defining a deck-seam loss per unit seam length factor, K_d, as the product of the loss rate k and the constant ratio $\pi 4$ results in the following:

$$F_d = K_dS_dD^2 \quad \text{(I.3)}$$

where K_d = deck-seam loss per unit seam length factor, in pound-moles per foot per year (lb-mol/ft-yr).

The deck-seam length factor, S_d, is defined as the ratio of the total length of deck seams, L, to the area of the deck, A. For continuous sheet construction this ratio may be approximated as:

$$S_d = 1/w \quad \text{(I.4)}$$

where

w is the sheet width, in feet (ft), and for rectangular panel construction:

$$S_d = (l + w)/(l \times w) \quad \text{(I.5)}$$

where

l is the panel length, in feet (ft);

w is the panel width, in feet (ft).

The total deck-seam loss factor, then, is a function of the loss rate per unit length of deck seam and the total length of deck seams in the floating roof.

I.2 Database for Deck-Seam Loss Factors

Experimental data[29] were used to determine the deck-seam loss factor coefficient, k. Losses were measured in a 20-ft-diameter internal floating-roof test tank by monitoring both the airflow rate induced through the space between the floating-roof deck and the fixed roof and the hydrocarbon concentration in the inlet and outlet air.

Two deck constructions were tested in this facility. One was a noncontact deck with overlapping sheet construction, in which deck seams only occurred along the edges of the sheets. The other was a contact deck with abutting panel construction, having deck seams along each edge and perpendicular joints at the corners of the panels. Seams of welded decks were not tested in that it was assumed that no losses occur from properly welded seams.

I.3 Analysis of the Deck-Seam Loss Data

For each of the two types of deck construction tested, a loss rate was determined in units of pound-moles per day. Dividing this measured loss rate from the test tank by the total length of deck seams in the floating roof, a loss rate was developed in terms of pound-moles per day per foot of deck seam length. Since it was not possible to determine from the test results the relative effects on loss rate of the deck location (contact versus noncontact) as compared to the deck seam construction details and since the measured loss rates from the two tests were of the same order of magnitude, the results were averaged to develop a general deck-seam daily loss rate. The loss rate per unit length of deck seam, k, was then determined as the product of the daily loss rate multiplied by 365 days per year. Combining k with the constant ratio $\pi/4$ produced the deck-seam loss per unit seam length factor, K_d, in pound-moles per foot per year.

The mathematical analysis and all supporting data used to develop the deck-seam loss factors are in the documentation file for the 3rd Edition of API 2519[51] (Section B.5).

Annex J
(informative)

Documentation Records

The documentation records for this standard are located in the following documents listed in the bibliography:

Tank Type	**Reference**	**Subject**
EFRT	[48] Appendix A	Relationship between air flow rate and wind speed
EFRT	[48] Appendix B	Rim seal loss factors
IFRT	[51] Section B.3	
EFRT	[48] Appendix C	Vapor pressure function
IFRT	[51] Section B.1	
EFRT	[48] Appendix D	Diameter function
EFRT	[48] Appendix E	Product factor
IFRT	[51] Section B.2	
IFRT	[51] Section B.5	Deck seam loss factor
EFRT	[52]	Fitting loss factors
IFRT	[51] Section B.4	

Annex K
(informative)

SI Units

Guidelines to convert the inch pound units employed in this document to equivalent units of the International System of Units are given in API *MPMS* Ch. 15[4].

The unit of length is either the kilometer, designated km, or the meter, designated m.

The unit of mass is the kilogram, designated kg.

The unit of volume is the cubic meter, designated m^3.

The unit of time is the year, designated yr.

The unit of temperature is the degree Celsius, designated °C, or the kelvin, designated K.

The unit of heat energy is the joule, designated J.

The unit of pressure is the kilopascal, designated kPa.

Bibliography

[1] API Publication 2517, *Evaporative Loss from External Floating-Roof Tanks*, 3rd Edition, February 1989.

[2] API Publication 2519, *Evaporation Loss from Internal Floating-Roof Tanks*, 3rd Edition, June 1983.

[3] API Standard 650, *Welded Tanks for Oil Storage*, 11th Edition, June, 2007.

[4] API *MPMS* Chapter 15, *Guidelines for the Use of the International System of Units (SI) in the Petroleum and Allied Industries*, (formerly API Publication 2564), 3rd Edition, December, 2001.

[5] Laverman, R.J., Gallagher, T.A., and Cherniwchan, W.N., "Emission Reduction Options for Floating Roof Tank Fittings," Paper presented at Energy Week 1996, held in Houston, TX, January 29 to February 2, 1996.

[6] API Bulletin 2518, *Evaporation Loss From Fixed-Roof Tanks*, June 1962.

[7] API Technical Report 2569, *Evaporative Loss from Closed-Vent Internal Floating Roof Storage Tanks*, August 2008.

[8] API Technical Report 2567, *Evaporative Loss from Storage Tank Floating Roof Landings,* April 2005.

[9] API Technical Report 2568, *Evaporative Loss from the Cleaning of Storage Tanks*, November 2007.

[10] API Standard 2610, *Design, Construction, Operation, Maintenance, and Inspection of Terminal and Tank Facilities*, 1st Edition, Washington, DC, July 1994.

[11] Ferry, R.L., "Development of Deck-Fitting Loss Factors for Floating-Roof Tanks," Report prepared by The TGB Partnership, prepared for API, Committee on Evaporation Loss Measurement, Task Group 3, Washington, DC, 1996.

[12] Courtesy of Rob Ferry, The TGB Partnership, Hillsborough, NC.

[13] "Western Oil and Gas Association Metallic Sealing Ring Emission Test Program" (Interim Report, Research Contract R-0136), Chicago Bridge & Iron Company, Plainfield, IL, January 19, 1977.

[14] "Western Oil and Gas Association Metallic Sealing Ring Emission Test Program" (Final Report, Research Contract R-0136), Chicago Bridge & Iron Company, Plainfield, IL, March 25, 1977.

[15] "Western Oil and Gas Association Metallic Sealing Ring Emission Test Program" (Supplemental Report, Research Contract R-0136), Chicago Bridge & Iron Company, Plainfield, IL, June 30, 1977.

[16] "Hydrocarbon Emission Loss Measurements on a 20 Foot Diameter Floating-Roof Tank With a Type SR-1 Seal for a Product at Various Vapor Pressures" (Report 2, Research Contract R-0134), Chicago Bridge & Iron Company, Plainfield, IL, October 25, 1977.

[17] R.J. Laverman, "Floating Roof Seal Development, Emission Test Measurements on Proposed CBI Wiper Type Secondary Seal for SR-1 Seals" (Letter Report, Research Contract R-0134), Chicago Bridge & Iron Company, Plainfield, IL, February 23, 1977.

[18] W.N. Cherniwchan, "Hydrocarbon Emissions from a Leaky SR-1 Seal With a Mayflower Secondary Seal" (Report 1, Research Contract R-0177), Chicago Bridge & Iron Company, Plainfield, IL, September 20, 1977.

[19] "Hydrocarbon Emission Loss Measurements on a 20 Foot Diameter External Floating-Roof Tank Fitted With a CBI SR-5 Liquid Filled Seal" (Final Report, Research Contract R-0167), Chicago Bridge & Iron Company, Plainfield, IL, August 31, 1978.

[20] "SOHIO/CBI Floating-Roof Emission Test Program" (Interim Report, Research Contract R-0101), Chicago Bridge & Iron Company, Plainfield, IL, October 7, 1976.

[21] "SOHIO/CBI Floating-Roof Emission Test Program" (Final Report, Research Contract R-0101), Chicago Bridge & Iron Company, Plainfield, IL, November 18, 1976.

[22] Radian Corporation, "Field Testing Program to Determine Hydrocarbon Emissions from Floating-Roof Tanks," Report prepared for the Floating-Roof Tank Subcommittee, Committee on Evaporation Loss Measurement, American Petroleum Institute, Washington, DC, May 1979.

[23] "Measurement of Emissions from a Tubeseal Equipped Floating-Roof Tank," Pittsburgh-Des Moines Steel Company, Pittsburgh, PA, December 4, 1978 (including supplemental report issued January 16, 1979).

[24] Engineering Science, Inc., "Phase I, Test Program and Procedures," Report prepared for the Floating-Roof Tank Subcommittee, Committee on Evaporation Loss Measurement, American Petroleum Institute, Washington, DC, November 1977.

[25] Chicago Bridge & Iron Company, "Development of Laboratory Procedures for Use in the Field Testing Program to Determine Hydrocarbon Emissions from Floating-Roof Tanks," Report prepared for the Floating-Roof Tank Subcommittee, Committee on Evaporation Loss Measurement, American Petroleum Institute, Washington, DC, May 18, 1978.

[26] Chicago Bridge & Iron Company, "Hydrocarbon Emission Measurements of Crude Oil on the 20 Foot Diameter Floating-Roof Pilot Test Tank," Report prepared for the Floating-Roof Tank Subcommittee, Committee on Evaporation Loss Measurement, American Petroleum Institute, Washington, DC, August 15, 1978.

[27] "SOHIO/CBI Floating-Roof Emission Test Program" (Supplemental Report, Research Contract R-0101), Chicago Bridge & Iron Company, Plainfield, IL, February 15, 1977.

[28] Docket OAQ PS 78-2 Petroleum Liquid Storage Vessels Part 4-B-7, Memo: "Gap Criteria for External Floating-Roof Seals," from L. Hayes of TRW: EED to the NSS Docket, December 4, 1979.

[29] Chicago Bridge & Iron Co., "Testing Program to Measure Hydrocarbon Emissions from a Controlled Internal Floating-Roof Tank," Final Report, prepared for API, CBI Contract No. 05000, Washington, DC, March 1982.

[30] CBI Industries, Inc., "Testing Program to Measure Hydrocarbon Evaporation Loss from External Floating-Roof Fittings" (CBI Contract 41851), Final report prepared for the Committee on Evaporation Loss Measurement, American Petroleum Institute, Washington, DC, September 13, 1985.

[31] R.L. Russell, "Analysis of Chicago Bridge & Iron Co. External Floating-Roof Tank Fitting Loss Data," Report prepared for Task Group 2517, Committee on Evaporation Loss Measurement, American Petroleum Institute, Washington, DC, October 17, 1985.

[32] Owens, J.E., Laverman, R.J., Winters, P.J., Johnson, J.G., Gemelli, M.J., "Testing Program to Measure Evaporative Losses from Floating Roof Fittings," Final Report, prepared by Chicago Bridge & Iron Technical Services Co., prepared for API, Committee on Evaporation Loss Measurement, Task Group 3, Washington, DC, October 1, 1993.

[33] Owens, J.E., Laverman, R.J., Winters, "Testing Program to Measure Evaporative Losses from Floating Roof Fittings," Supplemental Report No. 1, prepared by Chicago Bridge & Iron Technical Services Co., prepared for API, Committee on Evaporation Loss Measurement, Task Group 3, Washington, DC, December 31, 1993.

[34] Laverman, R.J. and Schoerner, W.S., "Testing Program to Measure Evaporative Losses from Slotted Guidepole Fittings," Final Report, prepared by Chicago Bridge & Iron Technical Services Co., prepared for API, Committee on Evaporation Loss Measurement, Task Group 3, Washington, DC, November 10, 1995.

[35] Petersen, R.L. and Cochran, B.C., "Wind Tunnel Testing of External Floating Roof Storage Tanks," (CPP Reports 92-0869, 93-0934, and 93-1024), prepared by Cermak, Peterka Petersen, Inc., prepared for API, Committee on Evaporation Loss Measurement, Task Group 3, Washington, DC, 1993.

[36] Ferry, R.L., "Documentation of the Fitting Wind-Speed Correction Factor," Report prepared by The TGB Partnership, prepared for API, Committee on Evaporation Loss Measurement, Task Group 3, Washington, DC, March 25, 1995.

[37] Parker, A. and Neulicht, R., "Fitting Wind Speed Correction Factor for External Floating Roof Tanks," Letter report prepared by Midwest Research Institute, prepared for U.S. EPA, September 25, 1995.

[38] Helm, N.C. and Giese, P.D., "Wind Tunnel Tests of a 0.017-Scale Model to Determine Pressure, Flow, and Venting Characteristics of a Liquid Storage Tank," Fluidyne Engineering Corp., Fluidyne Report No. 1114, (CBI Research Contract R-0150), June 1977.

[39] Runchal, A.K., "Influence of Wind on Hydrocarbon Emissions from Internal Floating Roof Tanks," prepared by Analytical and Computational Research, Inc., prepared for API, Washington, DC, November 17, 1980.

[40] J.F. Marchman, "Wind Effects on Floating Surfaces in Large Open-Top Storage Tanks," Paper presented at the Third Conference on Wind Effects on Buildings and Structures, Tokyo, 1971.

[41] J.F. Marchman, "Surface Loading in Open-Top Tanks," *Journal of the Structural Division*, American Society of Civil Engineers, November 1970, Vol. 96, No. ST11, pp 2551 to 2556.

[42] Engineering Science, Inc., "Hydrocarbon Emissions from Floating-Roof Storage Tanks," Report prepared for the Western Oil and Gas Association, Los Angeles, January 1977.

[43] Ferry, R.L., "Documentation of Rim Seal Loss Factors for the Manual of Petroleum Measurement Standards, Chapter 19—Evaporative Loss Measurement, Section 2—Evaporative Loss from Floating-Roof Tanks," Report prepared by The TGB Partnership, prepared for API, Committee on Evaporation Loss Measurement, Task Group 3, Washington, DC, April 5, 1995.

[44] R.J. Laverman, "Emission Measurements on a Floating Roof Pilot Test Tank," 1979 Proceedings-Refining Department, Vol. 58, American Petroleum Institute, Washington, DC, 1979, pp 301 to 322.

[45] "Wind Speed Versus Air Flow Rate Calibration of 20 Foot Diameter Floating-Roof Test Tank" (Final Report, Research Contract R-0177), Chicago Bridge & Iron Company, Plainfield, IL, October 5, 1977.

[46] API Publication 2517, *Evaporation Loss from External Floating-Roof Tanks*, 1st Edition, 1962.

[47] API Publication 2517, *Evaporation Loss from External Floating-Roof Tanks*, 2nd Edition, February 1980.

[48] API, Documentation File for Revised API Publication 2517, Washington, DC, June 26, 1981.

[49] Runchal, A.K., "Hydrocarbon Vapor Emissions from Floating-Roof Tanks and the Role of Aerodynamic Modifications," Air Pollution Control Association Journal, Vol. 28, No. 5, May 1978, pp 498 to 501.

[50] J.G. Zabaga, "API Floating-Roof Tank Test Program," Paper presented at the 72nd Air Pollution Control Association Meeting, Cincinnati, OH, June 26, 1979.

[51] API Publication 2519D, Documentation File for API Publication 2519, 1st Edition, Washington, DC, March 1993.

[52] API Publication 2517D, Documentation File for API Publication 2517, 1st Edition, Washington, DC, March 1993.

THERE'S MORE WHERE THIS CAME FROM

REQUEST A QUOTATION
www.api.org/quote

API Monogram® Licensing Program
Sales: 877-562-5187
(Toll-free U.S. and Canada)
(+1) 202-682-8041
(Local and International)
Email: certification@api.org
Web: www.api.org/monogram

API Quality Registrar (APIQR®)
- ISO 9001
- ISO/TS 29001
- ISO 14001
- OHSAS 18001
- API Spec Q1®
- API Spec Q2®
- API Quality*Plus*®
- Dual Registration

Sales: 877-562-5187
(Toll-free U.S. and Canada)
(+1) 202-682-8041
(Local and International)
Email: certification@api.org
Web: www.api.org/apiqr

API Training Provider Certification Program (TPCP®)
Sales: 877-562-5187
(Toll-free U.S. and Canada)
(+1) 202-682-8041
(Local and International)
Email: tpcp@api.org
Web: www.api.org/tpcp

API Individual Certification Programs (ICP®)
Sales: 877-562-5187
(Toll-free U.S. and Canada)
(+1) 202-682-8041
(Local and International)
Email: icp@api.org
Web: www.api.org/icp

API Engine Oil Licensing and Certification System (EOLCS)
Sales: 877-562-5187
(Toll-free U.S. and Canada)
(+1) 202-682-8041
(Local and International)
Email: eolcs@api.org
Web: www.api.org/eolcs

Motor Oil Matters
Sales: 877-562-5187
(Toll-free U.S. and Canada)
(+1) 202-682-8041
(Local and International)
Email: motoroilmatters@api.org
Web: www.motoroilmatters.org

API Diesel Exhaust Fluid Certification Program
Sales: 877-562-5187
(Toll-free U.S. and Canada)
(+1) 202-682-8041
(Local and International)
Email: apidef@api.org
Web: www.apidef.org

API Perforator Design Registration Program
Sales: 877-562-5187
(Toll-free U.S. and Canada)
(+1) 202-682-8041
(Local and International)
Email: perfdesign@api.org
Web: www.api.org/perforators

API WorkSafe®
Sales: 877-562-5187
(Toll-free U.S. and Canada)
(+1) 202-682-8041
(Local and International)
Email: apiworksafe@api.org
Web: www.api.org/worksafe

API-U™
Sales: 877-562-5187
(Toll-free U.S. and Canada)
(+1) 202-682-8041
(Local and International)
Email: training@api.org
Web: www.api-u.org

API Data®
Sales: 877-562-5187
(Toll-free U.S. and Canada)
(+1) 202-682-8041
(Local and International)
Service: (+1) 202-682-8042
Email: data@api.org
Web: www.APIDataNow.org

API Publications
Phone: 1-800-854-7179
(Toll-free U.S. and Canada)
(+1) 303-397-7956
(Local and International)
Fax: (+1) 303-397-2740
Web: www.api.org/pubs
global.ihs.com

API Standards
Sales: 877-562-5187
(Toll-free U.S. and Canada)
(+1) 202-682-8041
(Local and International)
Email: standards@api.org
Web: www.api.org/standards

energy API®
AMERICAN PETROLEUM INSTITUTE

energy API®

AMERICAN PETROLEUM INSTITUTE

1220 L Street, NW
Washington, DC 20005-4070
USA

202-682-8000

Additional copies are available online at www.api.org/pubs

Phone Orders:	1-800-854-7179	(Toll-free in the U.S. and Canada)
	303-397-7956	(Local and International)
Fax Orders:	303-397-2740	

Information about API publications, programs and services is available on the web at www.api.org.

Product No. H190203